Evaluation of the Aerodynamic Characteristics of a 1/20-Scale A-10 Model at Mach Numbers from 0.30 to 0.75

Phillip L. Yeakley
ARO, Inc.

September 1979

Final Report for Period 5 – 7 June 1978

ARNOLD ENGINEERING DEVELOPMENT CENTER
ARNOLD AIR FORCE STATION, TENNESSEE
AIR FORCE SYSTEMS COMMAND
UNITED STATES AIR FORCE

NOTICES
When U. S. Government drawings, specifications, or other data are used for any purpose other than a definitely related Government procurement operation, the Government thereby incurs no responsibility nor any obligation whatsoever, and the fact that the Government may have formulated, furnished, or in any way supplied the said drawings, specifications, or other data, is not to be regarded by implication or otherwise, or in any manner licensing the holder or any other person or corporation, or conveying any rights or permission to manufacture, use, or sell any patented invention that may in any way be related thereto.
Qualified users may obtain copies of this report from the Defense Documentation Center.
References to named commerical products in this report are not to be considered in any sense as an indorsement of the product by the United States Air Force or the Government.

This report has been reviewed by the Information Office (OI) and is releasable to the National Technical Information Service (NTIS). At NTIS, it will be available to the general public, including foreign nations.

APPROVAL STATEMENT

This report has been reviewed and approved.

GREGORY COWLEY, 1st Lt, USAF
Test Director, PWT Division
Directorate of Test Operations

Approved for Publication:

FOR THE COMMANDER

JAMES D. SANDERS, Colonel, USAF
Deputy for Operations

REPORT DOCUMENTATION PAGE		READ INSTRUCTIONS BEFORE COMPLETING FORM
1 REPORT NUMBER AEDC-TR-78-66 AFATL-TR-78-103	2 GOVT ACCESSION NO.	3 RECIPIENT'S CATALOG NUMBER
4. TITLE (and Subtitle) EVALUATION OF THE AERODYNAMIC CHARACTERISTICS OF A 1/20-SCALE A-10 MODEL AT MACH NUMBERS FROM 0.30 TO 0.75		5 TYPE OF REPORT & PERIOD COVERED Final Report, 5 - 7 June 1978
		6. PERFORMING ORG. REPORT NUMBER
7. AUTHOR(s) Phillip L. Yeakley, ARO, Inc., a Sverdrup Corporation Company		8. CONTRACT OR GRANT NUMBER(s)
9 PERFORMING ORGANIZATION NAME AND ADDRESS Arnold Engineering Development Center Air Force Systems Command Arnold Air Force Station, Tennessee 37389		10. PROGRAM ELEMENT, PROJECT, TASK AREA & WORK UNIT NUMBERS Program Element 64225F System 329A Task 00
11 CONTROLLING OFFICE NAME AND ADDRESS Air Force Armament Laboratory/DLJC Eglin Air Force Base, Florida 32542		12. REPORT DATE September 1979
		13 NUMBER OF PAGES 88
14 MONITORING AGENCY NAME & ADDRESS(if different from Controlling Office)		15. SECURITY CLASS. (of this report) UNCLASSIFIED
		15a. DECLASSIFICATION DOWNGRADING SCHEDULE N/A

16 DISTRIBUTION STATEMENT (of this Report)

Approved for public release; distribution unlimited.

17. DISTRIBUTION STATEMENT (of the abstract entered in Block 20, if different from Report)

18 SUPPLEMENTARY NOTES

Available in DDC.

19 KEY WORDS (Continue on reverse side if necessary and identify by block number)

A-10 aircraft
aerodynamic characteristics
external-store effects
wind tunnel tests

20 ABSTRACT (Continue on reverse side if necessary and identify by block number)

A 1/20-scale model of the A-10 aircraft was tested in the AEDC Aerodynamic Wind Tunnel (4T) to (1) determine the aerodynamic and control characteristics of the basic aircraft, (2) evaluate the effect of external store configurations on the static stability and drag characteristics of the aircraft, and (3) investigate the effects of Reynolds number, boundary-layer transition grit, and aerodynamic hysteresis on the data. Data were obtained at angles of attack from -4 to 20 deg and at sideslip angles from

DD FORM 1 JAN 73 1473 EDITION OF 1 NOV 65 IS OBSOLETE

20. ABSTRACT (Continued)

-10 to 10 deg. The Mach number range was from 0.30 to 0.75, and the Reynolds number range was from 0.7 to 4.9 million per foot.

PREFACE

The work reported herein was conducted by the Arnold Engineering Development Center (AEDC), Air Force Systems Command (AFSC), at the request of the Air Force Armament Laboratory (AFATL/DLJC), Eglin Air Force Base, Florida. The AFATL project manager was Lt. Tom Speer. The results of the test were obtained by ARO, Inc., AEDC Division (a Sverdrup Corporation Company), operating contractor for the AEDC, AFSC, Arnold Air Force Station, Tennessee, under ARO Project Number P41C-21A. Data reduction was completed on July 15, 1978, and the manuscript was submitted for publication on September 26, 1978.

CONTENTS

ILLUSTRATIONS

TABLES

1.0 INTRODUCTION

A wind tunnel test was conducted using a 1/20-scale A-10 aircraft model to (1) determine the aerodynamic and control characteristics of the basic aircraft, (2) evaluate the effect of external store configurations on the static stability and drag characteristics of the aircraft, and (3) investigate the effects of Reynolds number, boundary-layer transition grit, and aerodynamic hysteresis on the data. The test was conducted in the AEDC Propulsion Wind Tunnel Facility (PWT) Aerodynamic Wind Tunnel (4T). The Pave Penny pod/pylon, which is considered by the Systems Program Office (SPO) to be integral to the basic A-10 aircraft, was not installed during this test. Data were obtained at Mach numbers from 0.30 to 0.75 and Reynolds numbers from 0.7 to 4.9 million per foot. The model angle of attack was varied from -4 to 20 deg, and the sideslip angle was varied from -10 to 10 deg. Results of the test have been documented in Ref. 1, and only selected data are presented and discussed in this report. This test was the first to use this A-10 model, and this report is intended to document the aerodynamic characteristics of the model.

2.0 APPARATUS

2.1 TEST FACILITY

The Aerodynamic Wind Tunnel (4T) is a closed-loop, continuous flow, variable density tunnel in which the Mach number can be varied from 0.1 to 1.3 and can be set at discrete Mach numbers of 1.6 and 2.0 by placing nozzle inserts over the permanent sonic nozzle. At all Mach numbers, the stagnation pressure can be varied from 300 to 3,700 psfa. The test section is 4 ft square and 12.5 ft long with perforated, variable porosity (0.5- to 10-percent open) walls. It is completely enclosed in a plenum chamber from which the air can be evacuated, allowing part of the tunnel airflow to be removed through the perforated walls of the test section. The model support system consists of a sector and sting attachment which

has a pitch angle capability of -8 to 28 deg with respect to the tunnel centerline and a roll capability of -180 to 180 deg about the sting centerline. A more complete description of the test facility can be found in Ref. 2.

2.2 TEST ARTICLES

Details and dimensions of the 1/20-scale basic A-10 model are shown in Fig. 1. The model geometry variables include aileron, elevator, and rudder deflections. Details of the A-10 armament pylons are presented in Fig. 2, and details of the triple ejector rack (TER), MK-82, and SUU-30 stores are presented in Fig. 3. Installation of the model in Tunnel 4T is shown in Fig. 4. The various store loading configurations discussed are presented schematically in Table 1. For selected runs, boundary-layer transition grit (No. 120 carborundum) was applied to the model in strips 0.1 in. wide and 0.3 in. aft of the leading edges of the wing and both vertical and horizontal stabilizers. The basic configuration consisted of the A-10 model with empty pylons at all 11 armament stations, control surfaces set to zero deflection, the Pave-Penny pod removed, and no boundary-layer transition grit.

2.3 INSTRUMENTATION

A six-component, internal strain-gage balance was used to measure the aerodynamic forces and moments on the model. Two pressure orifices located in the body cavity and connected to pressure transducers were used to determine the model base pressure.

Electrical signals from the balance, pressure transducers, and standard tunnel instrumentation were processed by the 4T Digital Data Acquisition System (DDAS) and the DEC System 10 digital computer for online data reduction.

3.0 TEST DESCRIPTION

3.1 TEST PROCEDURES AND CONDITIONS

Model force and moment data were obtained by varying the angle of attack or sideslip angle in a pitch-pause mode while holding the Mach number and total pressure constant. The angle of attack was varied from -4 to 20 deg, and the sideslip angle was varied from -10 to 10 deg. In addition, for the polars taken to investigate aerodynamic hysteresis, the model attitude was varied from -4 to 20 to 0 deg in pitch and from 0 to -12 to 12 to -12 deg in sideslip. The nominal test conditions are presented in Table 2.

3.2 DATA REDUCTION AND CORRECTIONS

The aerodynamic force and moment data were reduced to coefficient form in both the body and stability axis systems. Forebody coefficients were also computed by adjusting the model base pressure to the free-stream value, but these data are not included in the present report. All coefficient data presented in this report were determined from measured values with no correction for base pressure or nacelle internal drag. All moment data were referenced to the moment reference point (MRP), as listed in the nomenclature and shown in Fig. 1.

The aircraft model attitude was corrected for flow angularity in the pitch plane and for sting and balance deflections caused by measured loads. The components of model weight acting on the balance (normally termed static tares) were accounted for before the loads were reduced to coefficient form.

3.3 DATA UNCERTAINTY

The uncertainties of the balance measurements were combined with the appropriate tunnel parameter uncertainties using a Taylor series approximation for error propagation to estimate the aerodynamic coefficient uncertainties. These uncertainties are based on a 95-percent confidence level and are presented in Table 3. The precision in setting and maintaining a specific Mach number was ±0.005, and the uncertainties in the model angle of attack and roll angle were ±0.1 and ±0.4 deg, respectively.

4.0 TEST RESULTS

4.1 AERODYNAMIC AND CONTROL CHARACTERISTICS OF THE BASIC CONFIGURATION

The static longitudinal aerodynamic characteristics of the basic A-10 model configuration are presented in Fig. 5. These data were collected at Reynolds numbers corresponding to P_T = 1,200 psfa in Table 2. The variation of lift coefficient with angle of attack (Fig. 5a) was nearly linear for moderate angles of attack but displayed an indication of moderate wing stall (decrease in slope) for large values of angle of attack. The angle of attack at which the slope change occurred decreased as Mach number was increased, varying from 18 deg at Mach number 0.30 to 8 deg at Mach number 0.75. This effect can be seen more dramatically in the pitching-moment versus lift coefficient data presented in Fig. 5b. The pitching-moment data varied smoothly for lift coefficients up to a point corresponding to the change in lift curve slope. Beyond this point, a further increase in angle of attack resulted in a strong nose-down pitching moment. The data presented in Fig. 5 are summarized in Fig. 6 in terms of static longitudinal stability parameters and minimum drag coefficients. In the region of zero lift, the A-10 model was statically stable across the Mach number range. The lift curve slope was a maximum at Mach number 0.50, and the drag coefficient remained relatively constant through Mach number 0.65.

The lateral-directional characteristics of the model are presented in Fig. 7 for angles of attack of 0, 5, 10, 15, and 20 deg. The data indicate that the model was generally insensitive to Mach number variation within the range investigated, but was sensitive to model angle of attack. The variation of the coefficients with angle of attack was generally linear and well behaved at angles of attack through 10 deg. The yawing and rolling moment coefficients, however, became less linear and subject to aerodynamic hysteresis effects at the high angles of attack. These hysteresis effects are discussed more fully in Section 4.3. The data presented in Fig. 7 are summarized in Fig. 8 in terms of lateral-directional stability parameters versus Mach number. The model was directionally stable throughout the Mach number range. Except for the angle of attack of 20 deg, the directional stability of the model decreased as the angle of attack was increased. The data indicate a favorable dihedral effect for the conditions investigated.

The stability parameters presented in Figs. 6 and 8 were calculated using a linear least squares curve fitting technique applied to the data over the angle of attack or sideslip angle range from -4 to 4 deg. This procedure provides a reasonable approximation for model attitudes within this range but does not reflect the nonlinear characteristics at high angles of attack or sideslip.

Control effectiveness of the basic configuration was investigated for elevator deflections (DELE) of 0, 10, and 20 deg and for aileron deflections (DELA) and rudder deflections (DELR) of 0 and 10 deg. The data are presented in Fig. 9 and summarized in Fig. 10. Except for an elevator deflection of 20 deg at angles of attack greater than 16 deg, all control surfaces remained uniformly effective at all test conditions. The effectiveness of all control surfaces remained nearly constant as Mach number was increased.

4.2 EFFECT OF REYNOLDS NUMBER AND TRANSITION GRIT

The effect of Reynolds number on the aerodynamic data was investigated by testing the basic A-10 model at unit Reynolds numbers ranging from 0.7 to 4.9 x 10^6 1/ft at Mach numbers of 0.30, 0.50, and 0.75. The effect of transition grit was investigated at Reynolds numbers corresponding to P_T = 1,200 psfa only (this P_T gives the second lowest Reynolds number at each Mach number). The grit-free data are presented in Fig. 11 for M_∞ = 0.50 and unit Reynolds numbers of 1.1, 1.7, 2.8, and 3.7 x 10^6 1/ft. These data are representative of the Reynolds number effects obtained at all Mach numbers and are summarized together with Fig. 12 grit data in Fig. 13. As the unit Reynolds number was increased from 1.1 to 3.7 x 10^6 1/ft, the maximum lift coefficient increased and the minimum drag coefficients were generally insensitive to Reynolds number variation, whereas the rolling-moment coefficient tended to become more negative as the Reynolds number was increased. Although the trends in the data were generally as expected, the magnitude of these Reynolds number effects was larger than anticipated. From the variation of these parameters, it can generally be concluded that a sufficiently high Reynolds number was not reached for Reynolds number to be excluded as a factor in the data.

The grit used to fix transition was specified by AFATL and satisfies the criteria of Ref. 3. The data in Figs. 12 and 13 compare the cases of the variation of Reynolds number with grit off and the case of moderately low Reynolds number with grit on. The data show that there was little or no effect of grit on the side-force or yawing-moment coefficients but that agreement between the low and high Reynolds number pitching- and rolling-moment data was generally improved by adding grit to the low Reynolds number case. The data also show a small increase in the drag when grit was added. However, the maximum lift coefficient obtained with grit would be expected to agree with or exceed the value obtained at the maximum Reynolds number without grit. This expected trend of the

lift coefficient is not borne out by the data of Figs. 12 and 13, which indicate a reduction in $C_{L,MAX}$ rather than an increase. Thus, it can be concluded that the maximum lift coefficient data did not follow expected trends, and further investigation of the use of grit with this model is warranted.

4.3 AERODYNAMIC HYSTERESIS

Aerodynamic hysteresis occurs when the values of the aerodynamic forces and moments depend on the past history of the model attitude, making analysis and application of the data difficult. Aerodynamic hysteresis had been observed in pitch and yaw polars at high angles of attack during recent transonic wind tunnel tests of other aircraft configurations. Therefore, a survey was conducted to determine whether aerodynamic hysteresis occurred within the angle-of-attack and sideslip ranges of the current test.

Hysteresis effects were investigated by obtaining data while pitching or yawing the model in one direction and then obtaining data in the reverse direction. No significant hysteresis effects were observed in the data for pitch polars or yaw polars at $\alpha \leq 10$ deg. For yaw polars at angles of attack of 15 or 20 deg, apparent hysteresis effects were observed. The data presented in Fig. 14 are the worst case of aerodynamic hysteresis observed with this model; the arrows drawn on the figure indicate the direction of model movement. These apparent hysteresis effects are seen primarily in the moment coefficient data (C_m, C_n, and C_ℓ) and to a lesser extent in the force coefficient data (C_L, C_D, and C_Y). The source of this hysteresis phenomenon is not known, and the asymmetry of the data about $\beta = 0$ suggests that the hysteresis may not be aerodynamic in nature. However, it should be pointed out that the A-10 model, including cannon and antennas, is itself asymmetric, and the hysteresis observed could be of aerodynamic origin. Where possible all yaw polars were run with sideslip increasing in an effort to minimize the hysteresis.

4.4 EFFECT OF EXTERNAL STORE LOADING

The aerodynamic characteristics of the A-10 model with 38 store-loading configurations were investigated during this test. In general, the addition of stores resulted in a decreased lift slope, a more nose-down pitching moment, increased drag, decreased directional stability, and a more favorable effective dihedral. The data in Fig. 15 illustrate these characteristics of the data for selected store loads (see Table 1). It should be noted that while the general trend, as stated above, was for the added stores to produce a nose-down pitching moment, the addition of the empty TER produced a more nose-up pitching moment.

5.0 SUMMARY OF RESULTS

A transonic wind tunnel test was conducted to determine the static aerodynamic characteristics of the A-10 model with and without external stores, and to investigate the effect of control deflections, Reynolds number variation, boundary-layer transition grit, and aerodynamic hysteresis on the data. Data were obtained at angles of attack from -4 to 20 deg and sideslip angles from -10 to 10 deg. The Mach number range was from 0.30 to 0.75, and Reynolds number was varied from 0.7 to 4.9 million per foot. The results obtained are summarized as follows:

1. For the moment reference point chosen, the basic configuration was longitudinally stable near zero lift. The model was directionally stable at each angle of attack investigated. A favorable dihedral effect was observed at all test conditions.

2. In general, the control surfaces were uniformly effective over the range of model attitude and Mach numbers examined. The elevator exhibited some loss of effectiveness when deflected to 20 deg for angles of attack greater than 16 deg.

3. Variation in the test Reynolds number resulted in the expected trends in the data; however, the changes due to Reynolds number variation were larger than anticipated.

4. The addition of boundary-layer transition grit to the baseline A-10 configuration decreased the maximum lift coefficient and increased the minimum drag coefficient. The trends for maximum lift coefficient were not as expected, and further study of the use of grit on this model is warranted.

5. Aerodynamic hysteresis was observed for yaw polars at angles of attack of 15 or 20 deg. Hysteresis was observed in all aerodynamic coefficients, but primarily in the yawing-, rolling-, and pitching-moment coefficients.

6. In general, the addition of stores resulted in a decreased lift slope, a more nose-down pitching moment, increased drag, decreased directional stability, and a more favorable dihedral effect.

REFERENCES

1. Yeakley, Phillip L. "Documentation of a Performance, Stability and Control Test on the 1/20-Scale Model A-10 Aircraft at Mach Numbers from 0.30 to 0.75." AEDC-TSR-78-P14, July 14, 1978.

2. Test Facilities Handbook (Tenth Edition). "Propulsion Wind Tunnel Facility, Vol. 4." Arnold Engineering Development Center, May 1974.

3. Braslow, A. L., Hicks, M., and Harris, R. V., Jr. "Use of Boundary-Layer Transition Trips on Wind-Tunnel Models." NASA TN D-3579, September 1966.

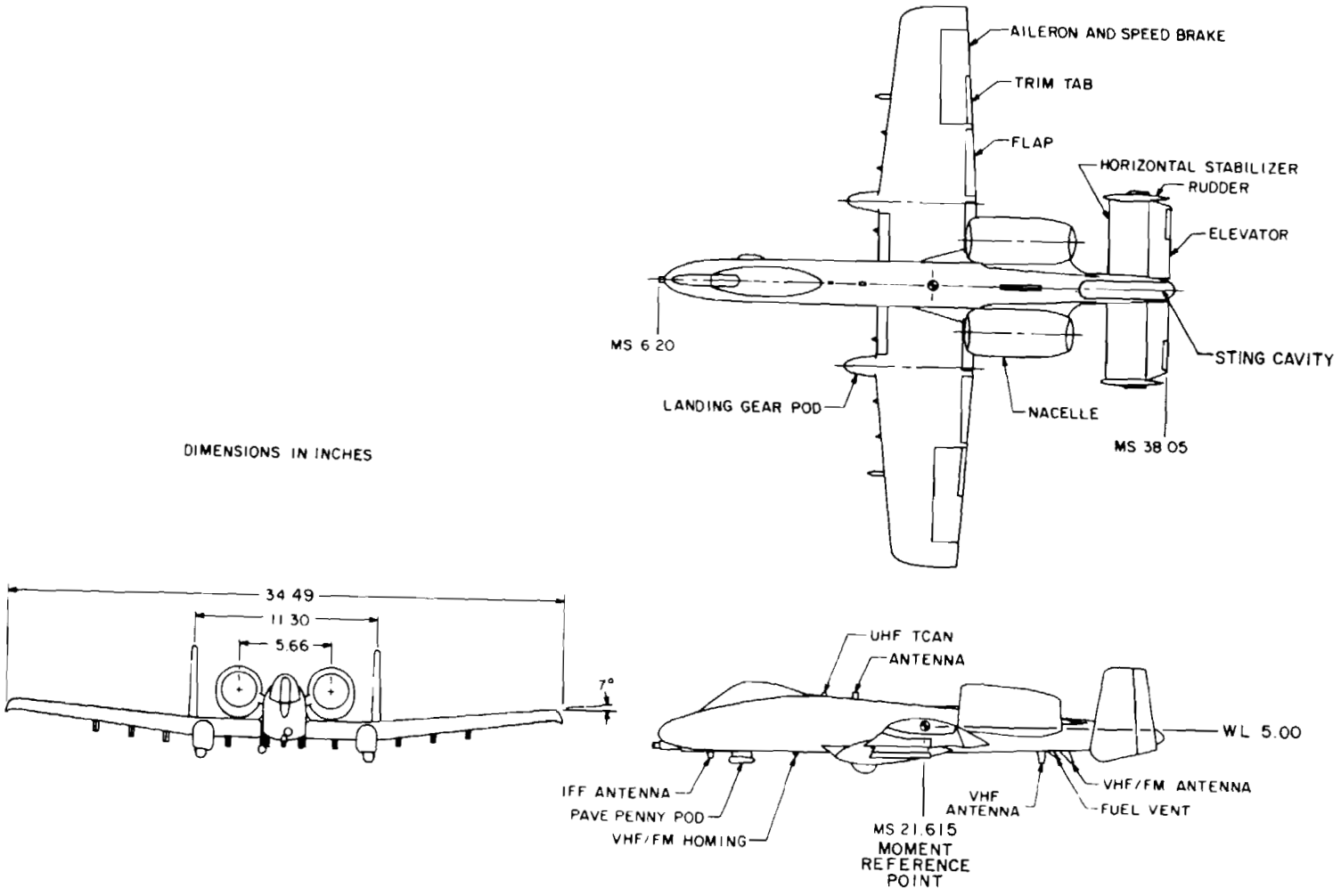

Figure 1. Details and dimensions of the A-10 model.

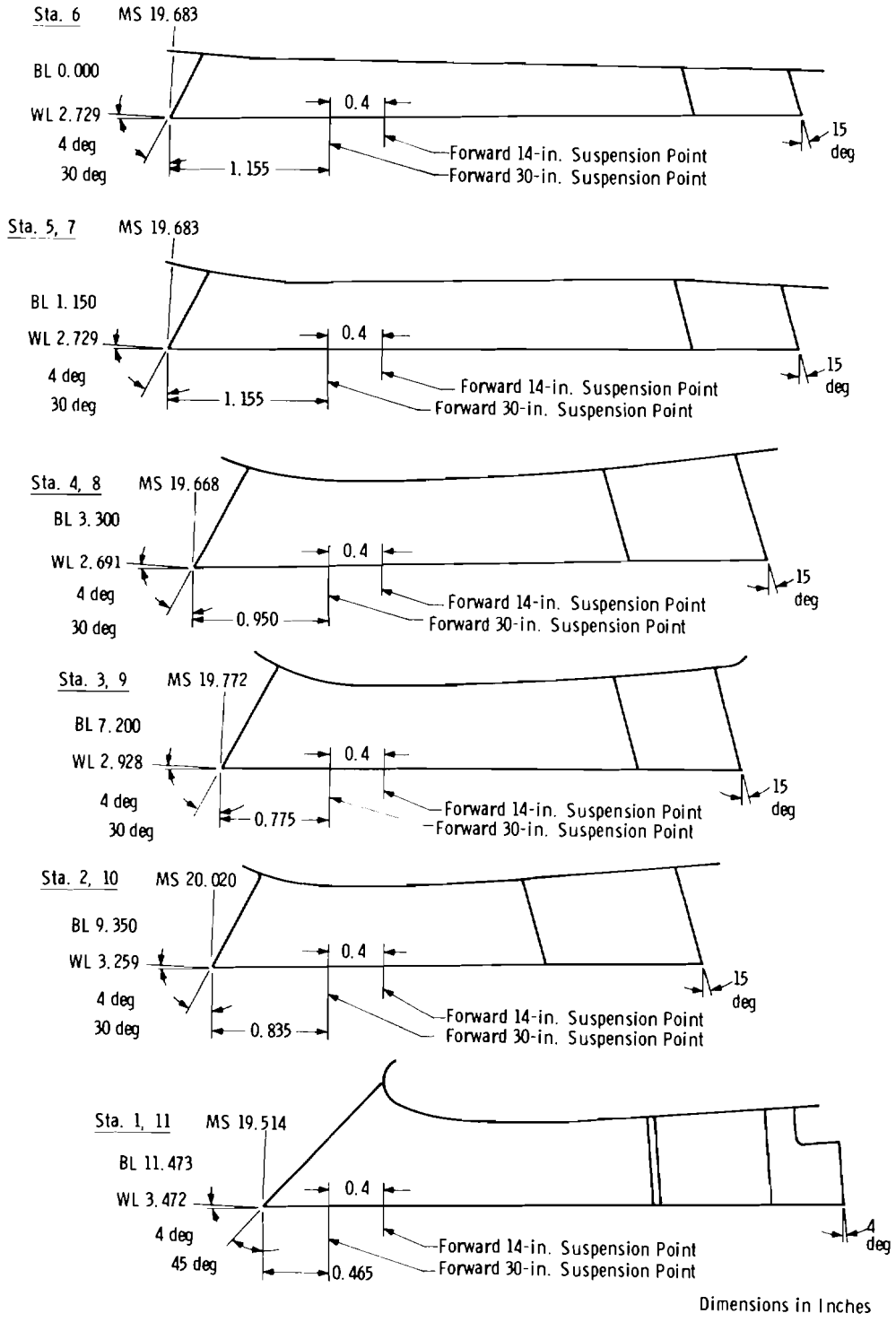

Figure 2. Details of the A-10 armament pylons.

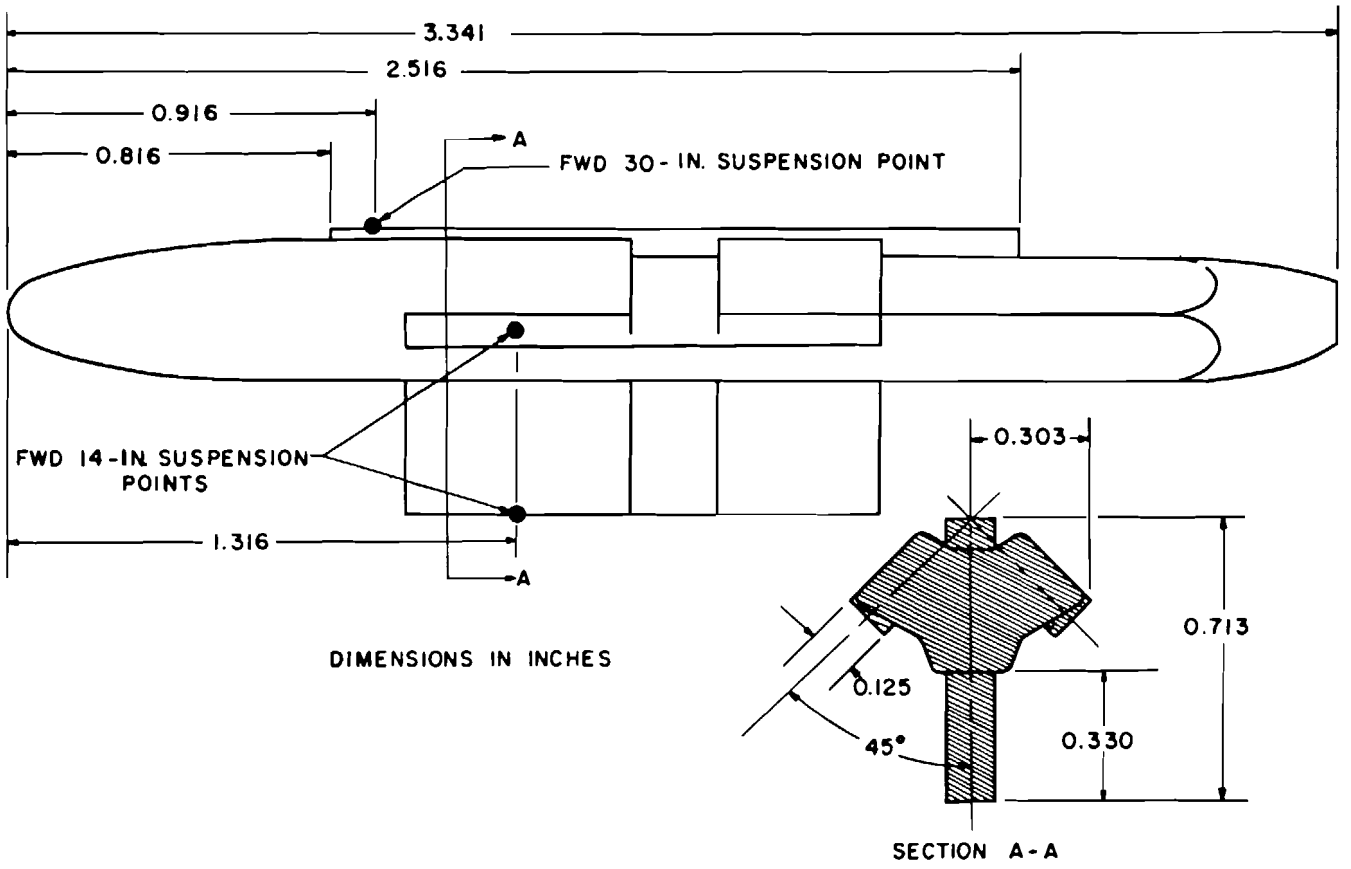

a. Triple ejector rack (TER)

Figure 3. Details of the store rack and stores.

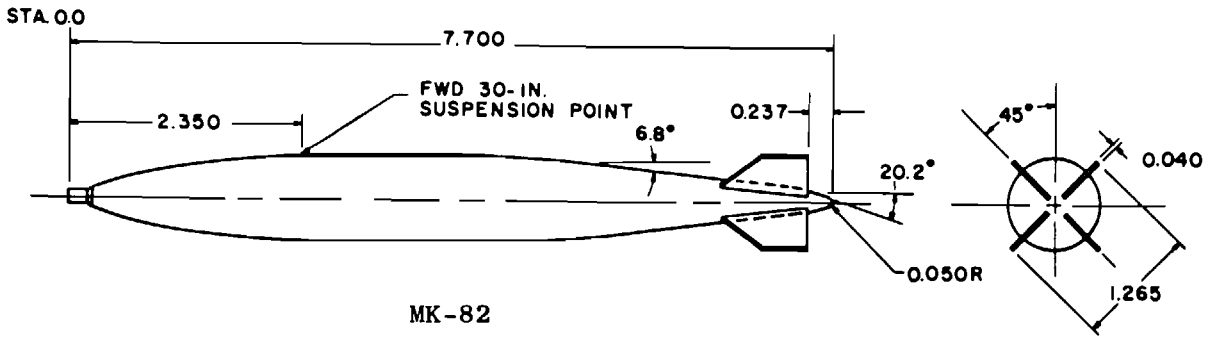

MK-82

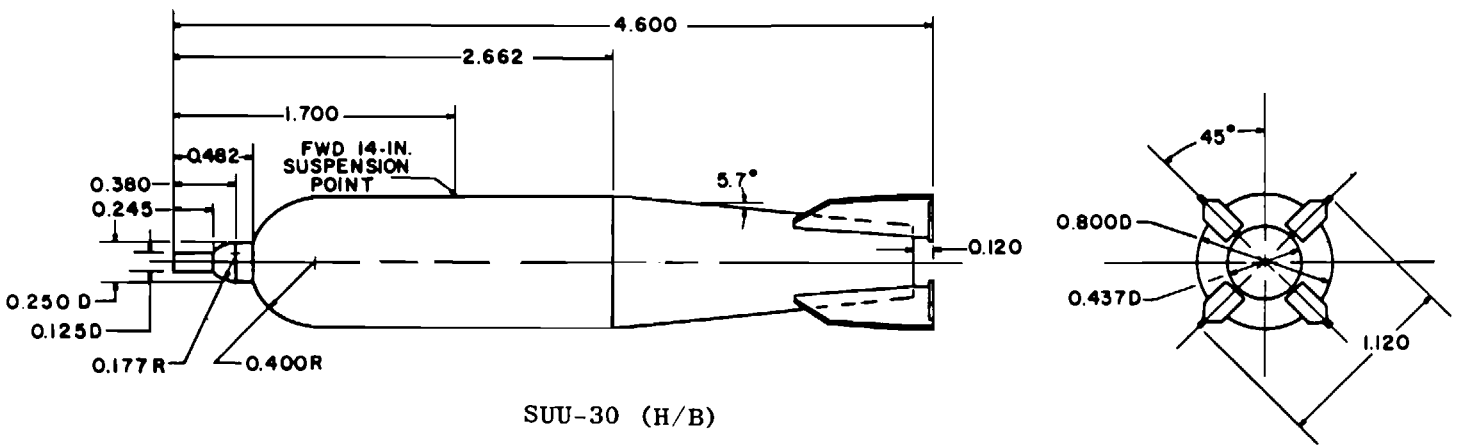

SUU-30 (H/B)

b. Store models

Figure 3. Concluded.

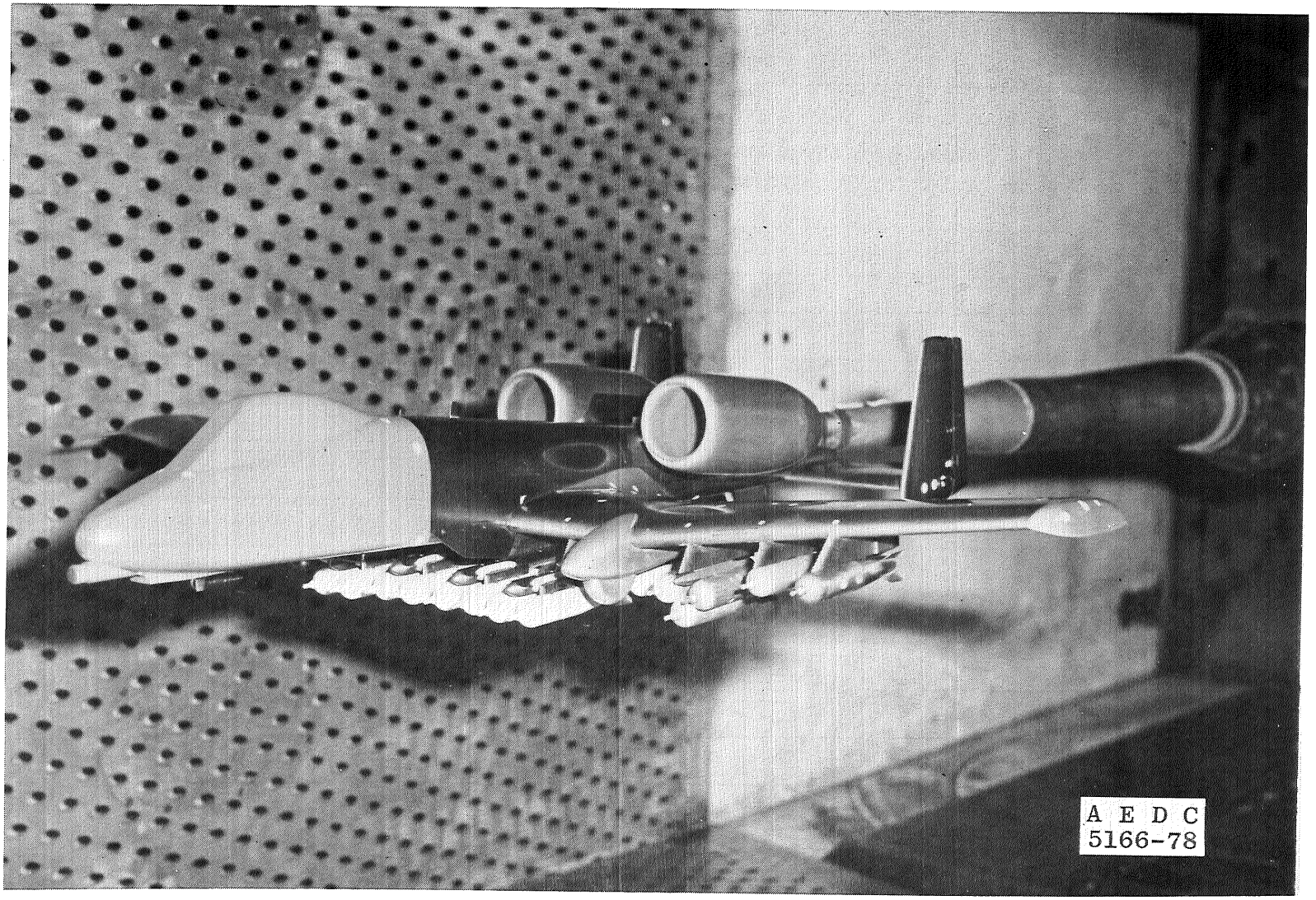

Figure 4. A-10 model with stores in Tunnel 4T.

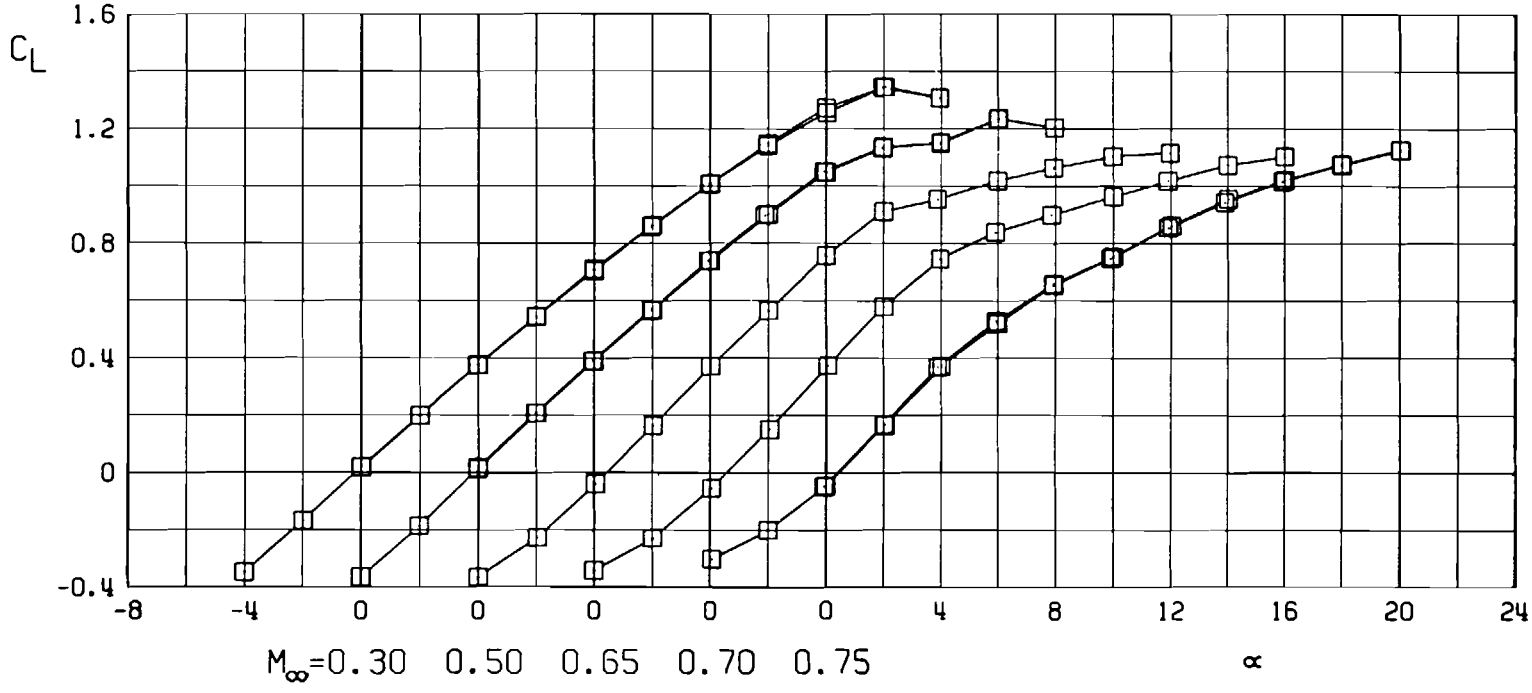

a. Lift characteristics

Figure 5. Longitudinal characteristics of the A-10 model.

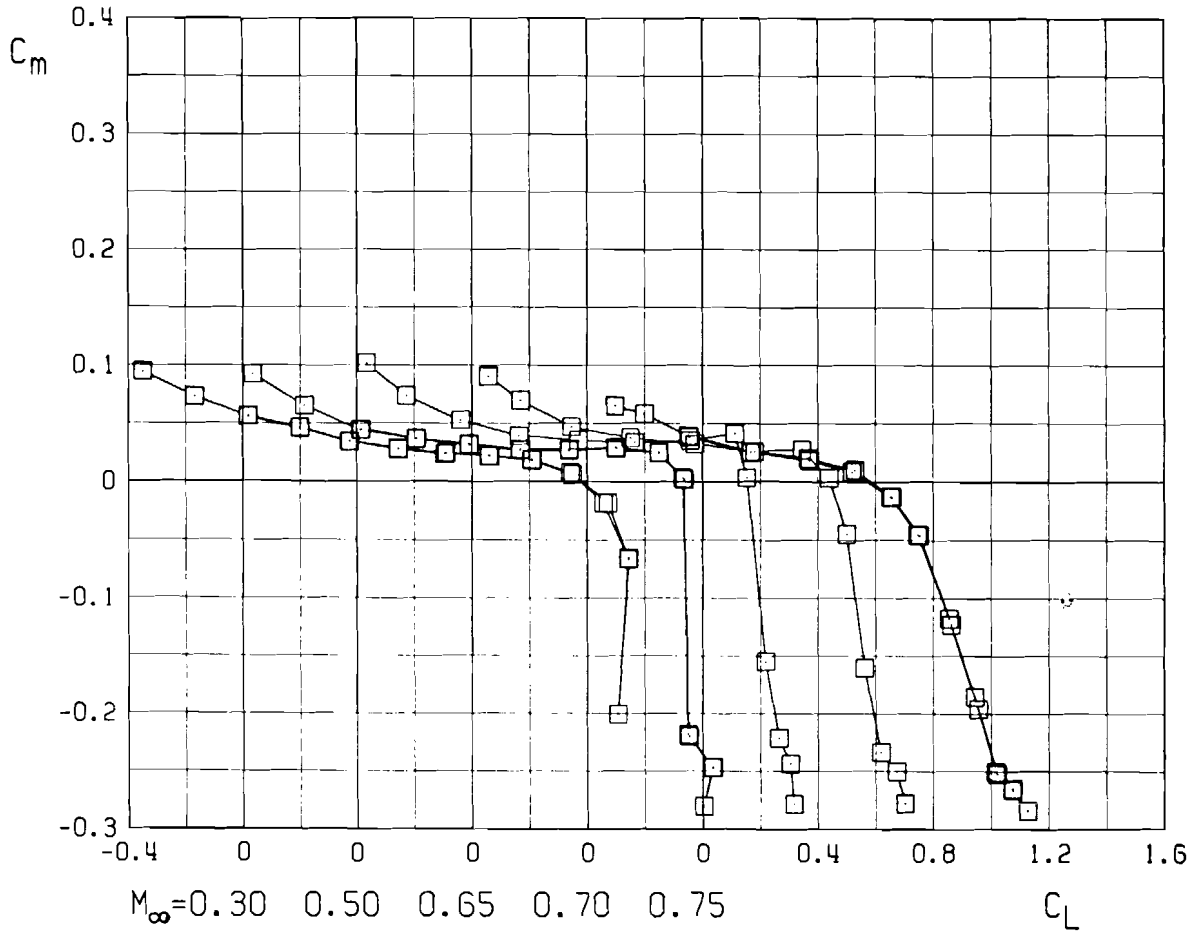

b. Pitching-moment characteristics
Figure 5. Continued.

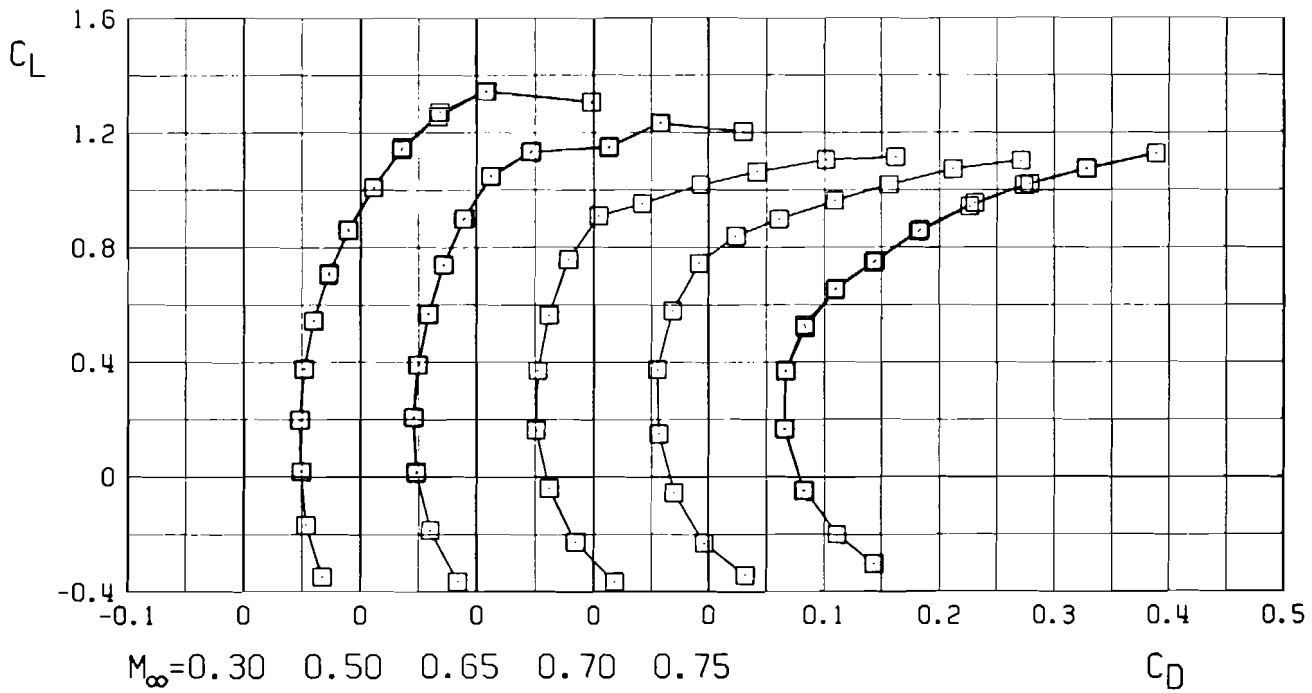

c. Drag characteristics

Figure 5. Concluded.

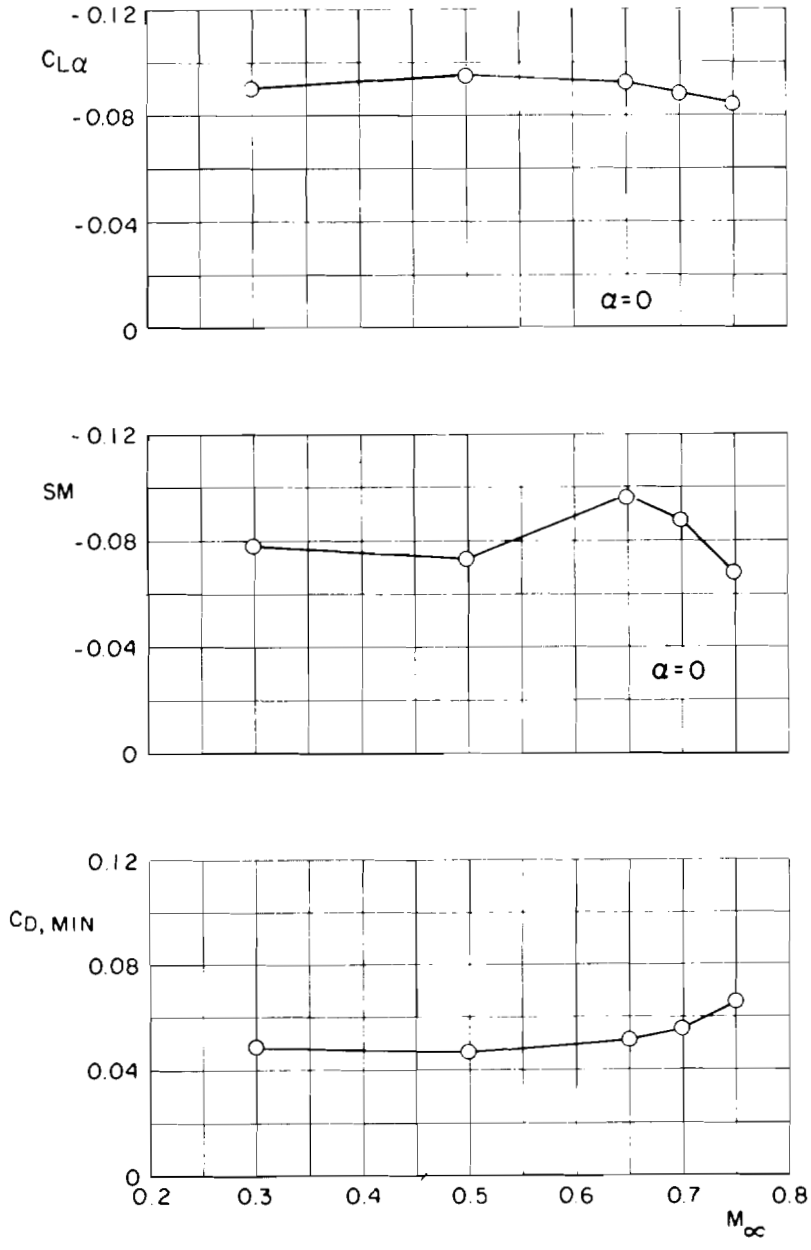

Figure 6. Summary of longitudinal characteristics.

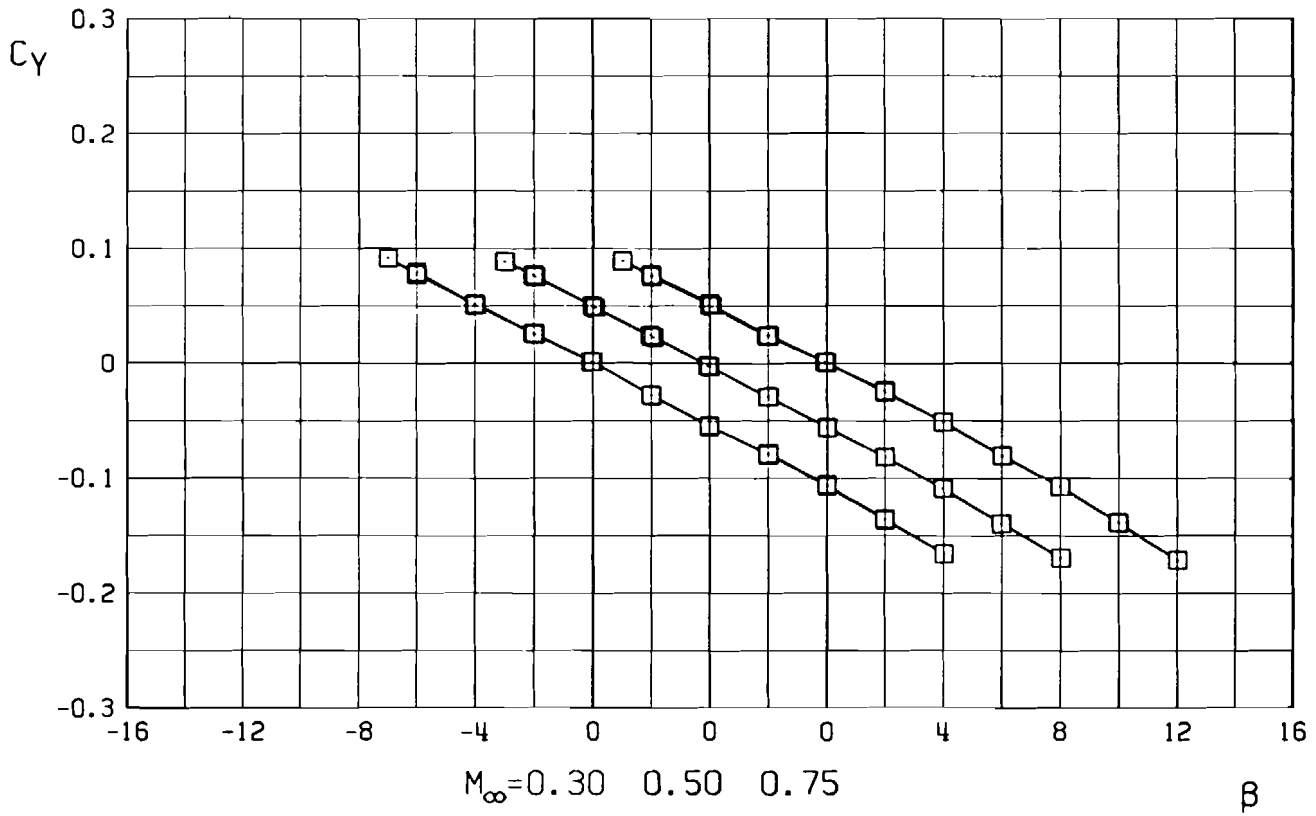

a. Side-force coefficient, α = 0

Figure 7. Lateral-directional characteristics of the A-10 model.

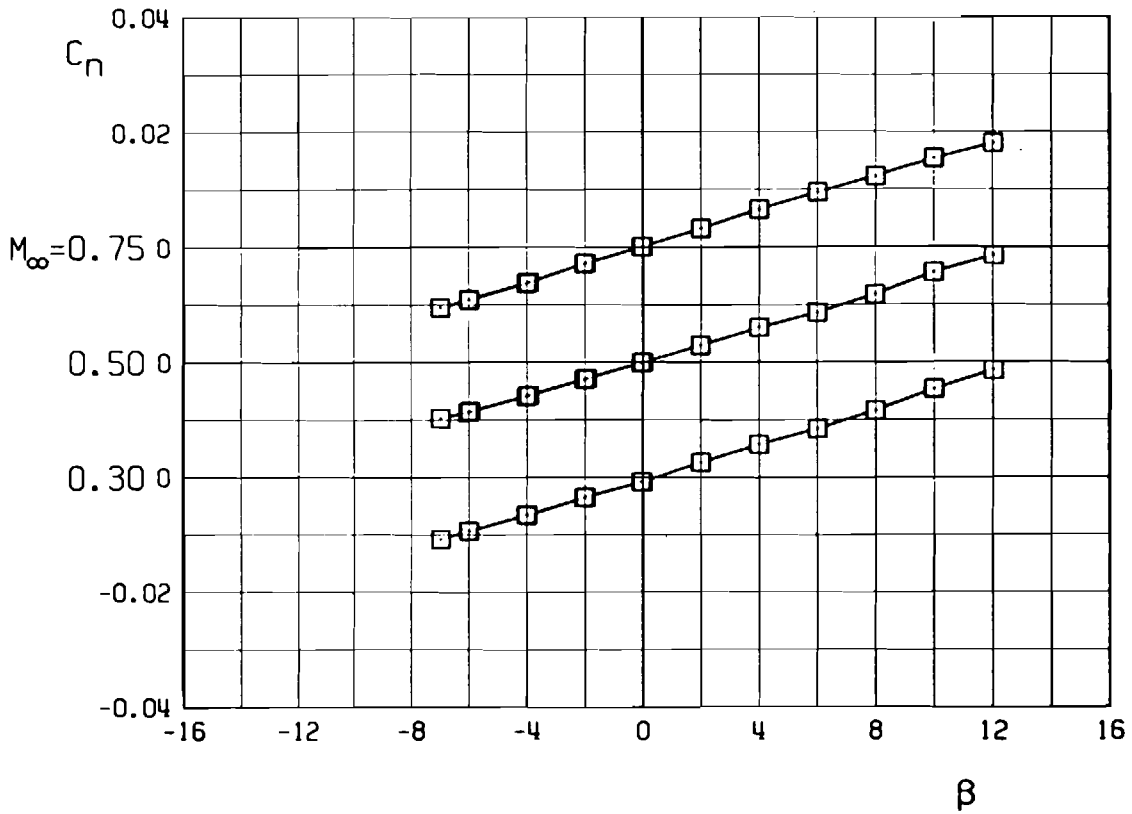

b. Yawing-moment coefficient, α = 0
Figure 7. Continued.

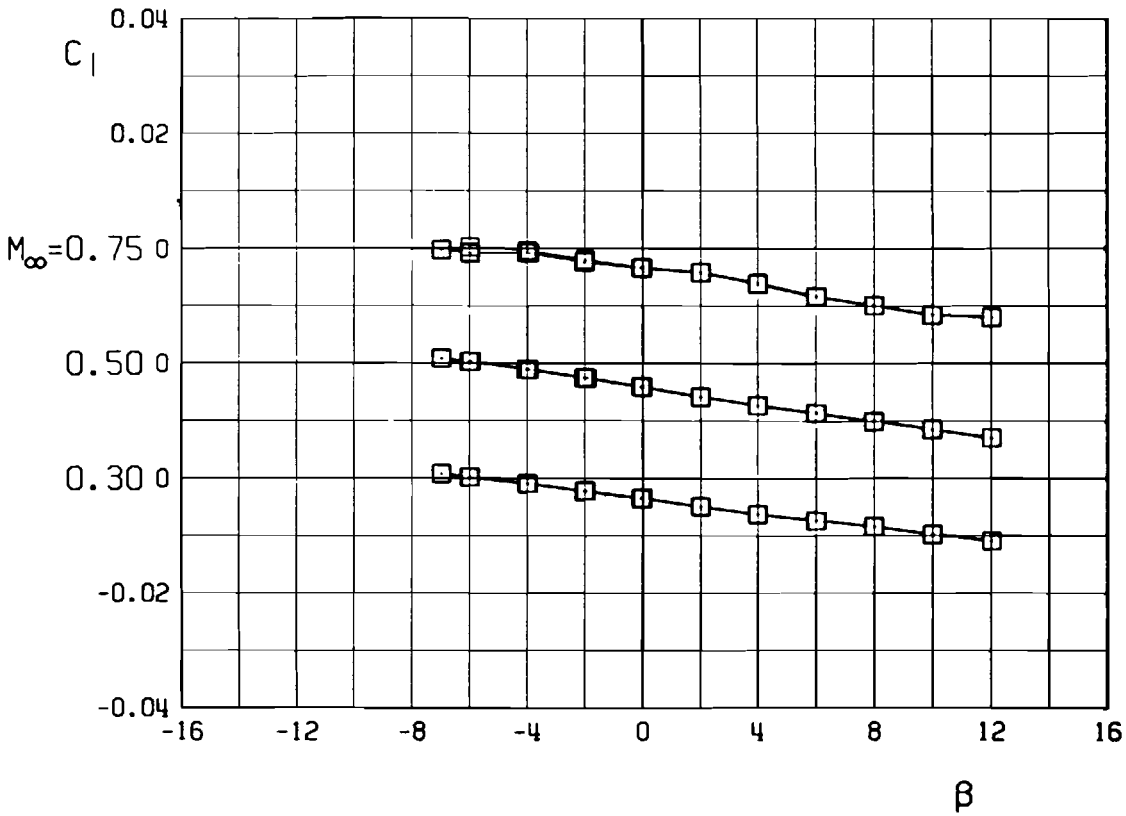

c. Rolling-moment coefficient, α = 0

Figure 7. Continued.

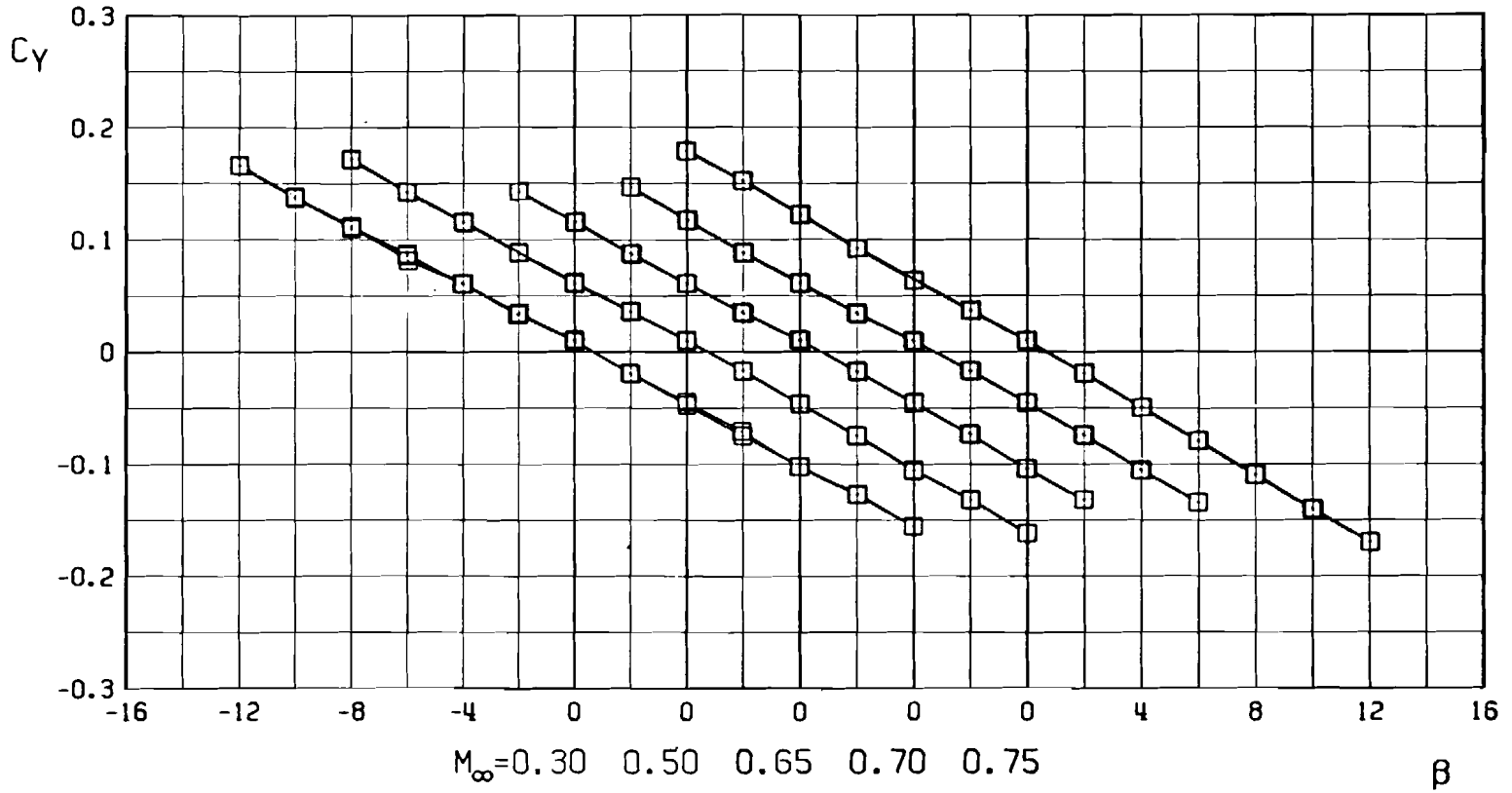

d. Side-force coefficient, α = 5 deg
Figure 7. Continued.

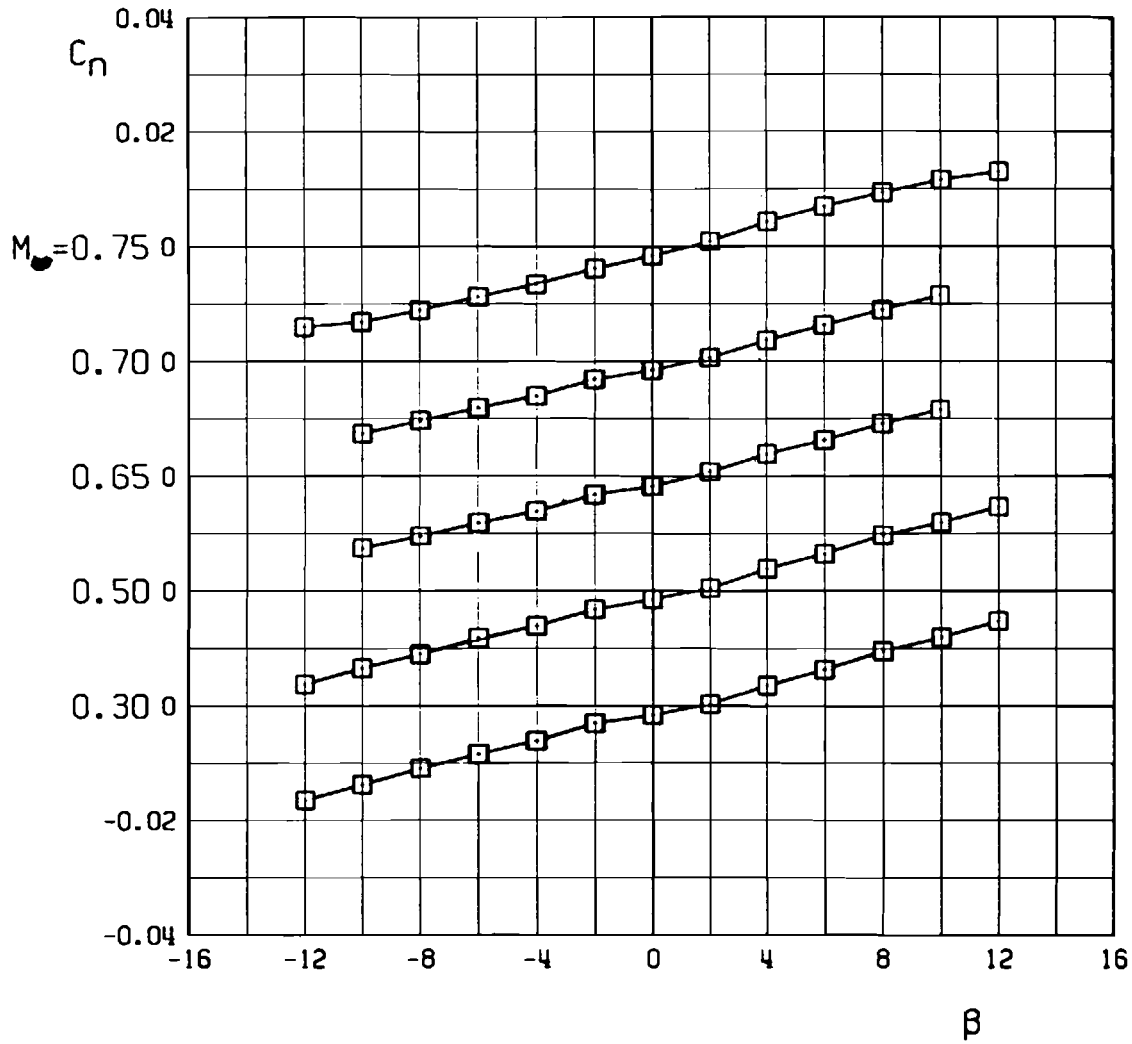

e. Yawing-moment coefficient, α = 5 deg
Figure 7. Continued.

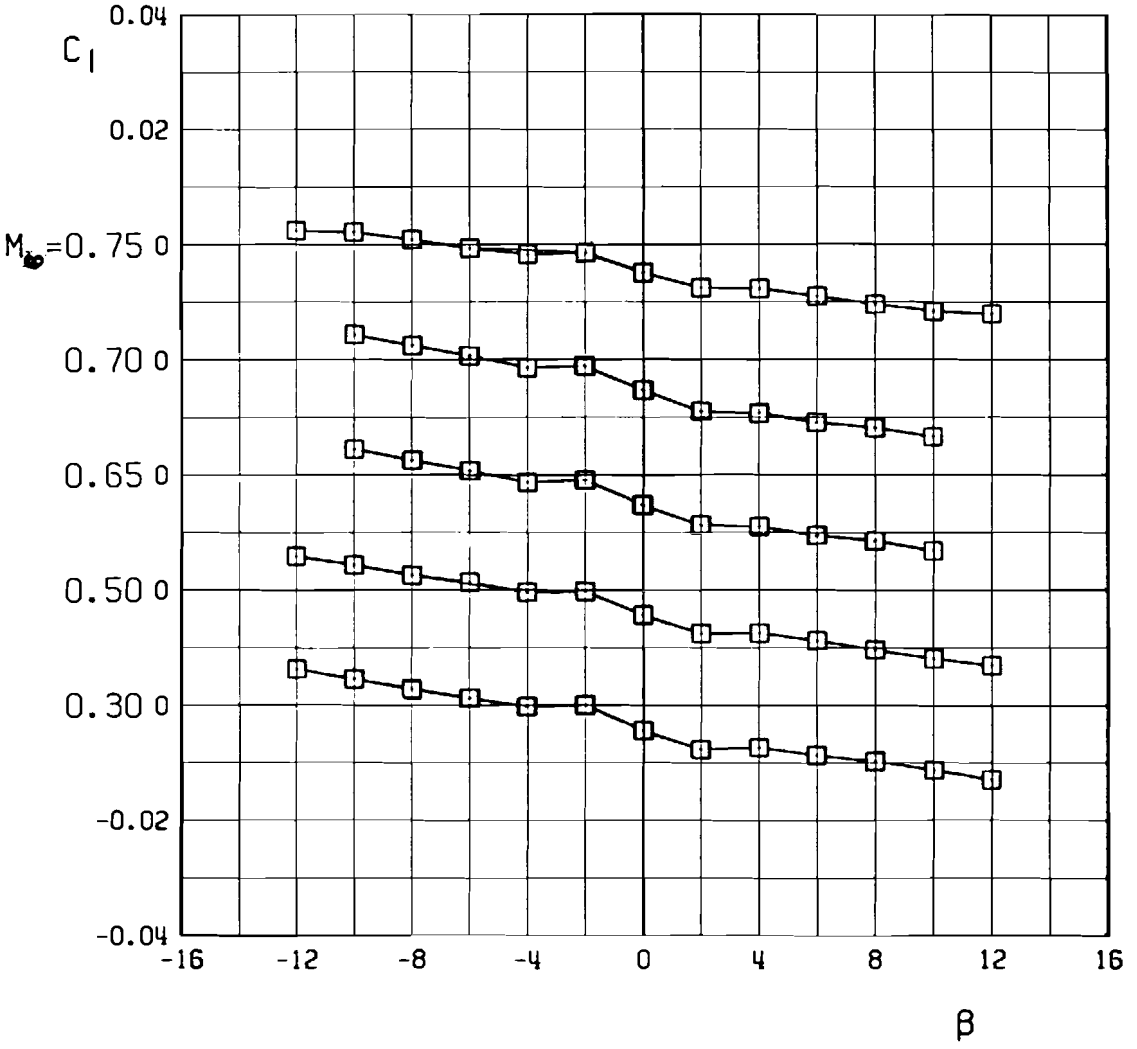

f. Rolling-moment coefficient, α = 5 deg

Figure 7. Continued.

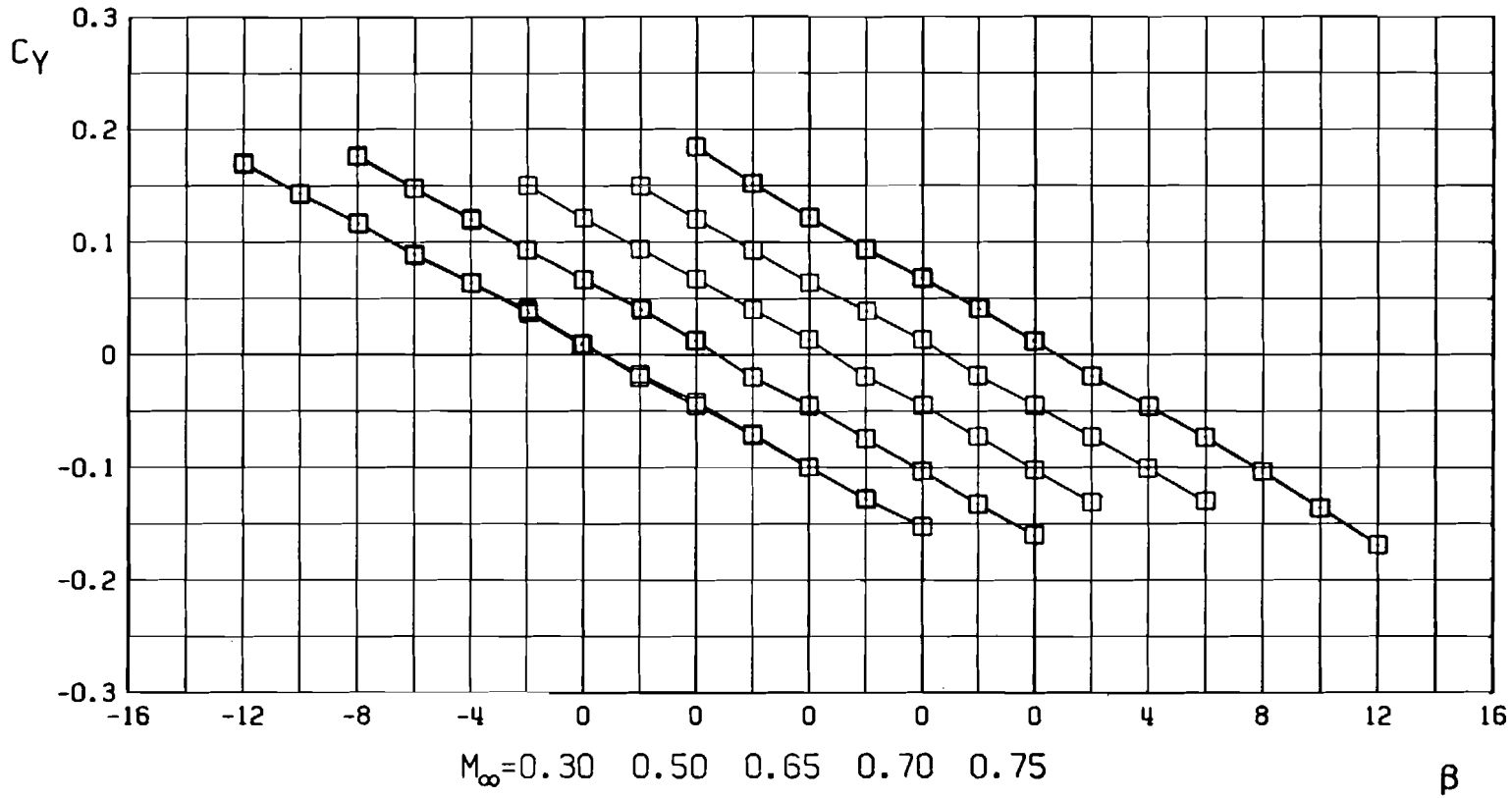

g. Side-force coefficient, α = 10 deg
Figure 7. Continued.

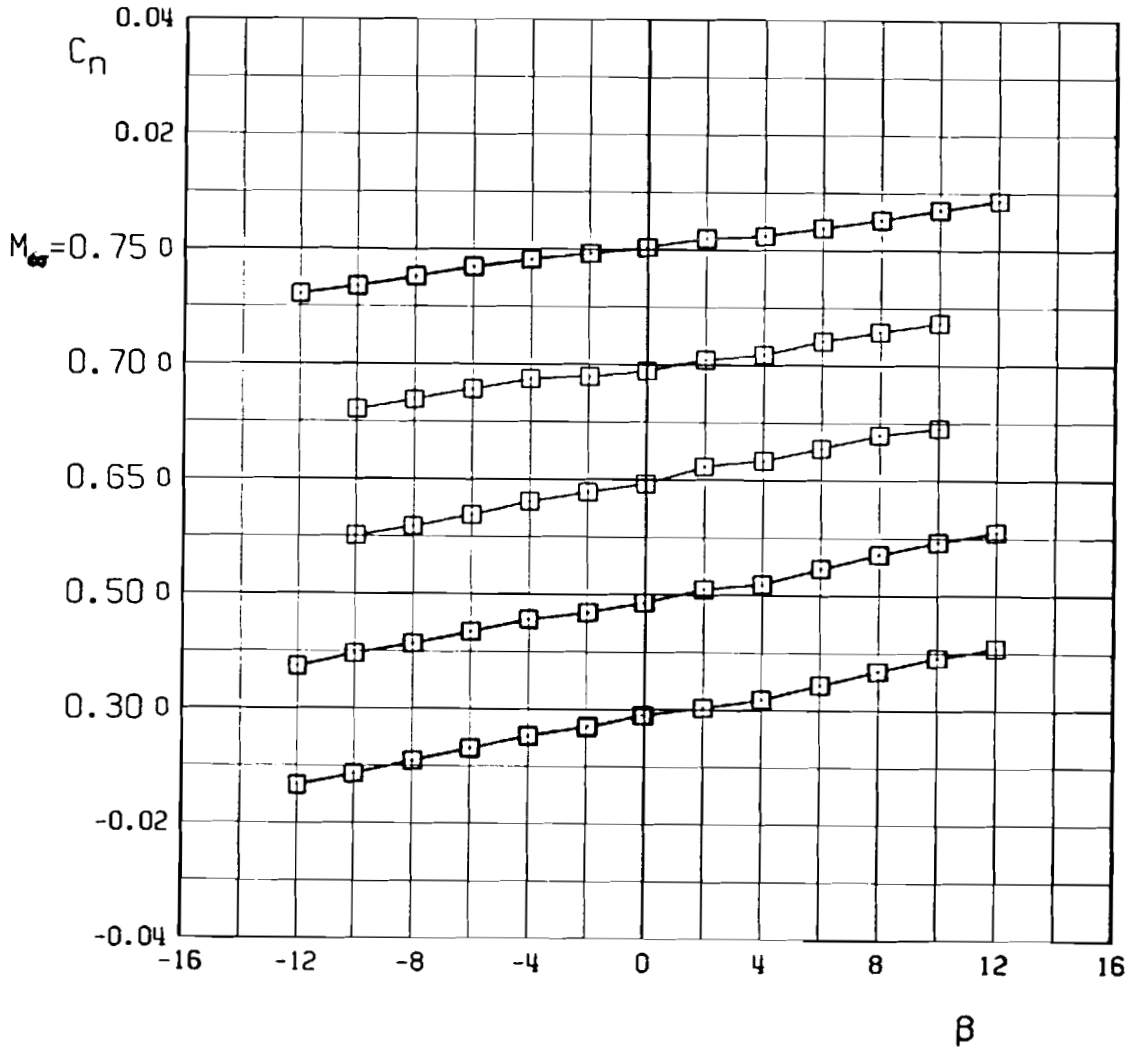

h. Yawing-moment coefficient, α = 10 deg
Figure 7. Continued.

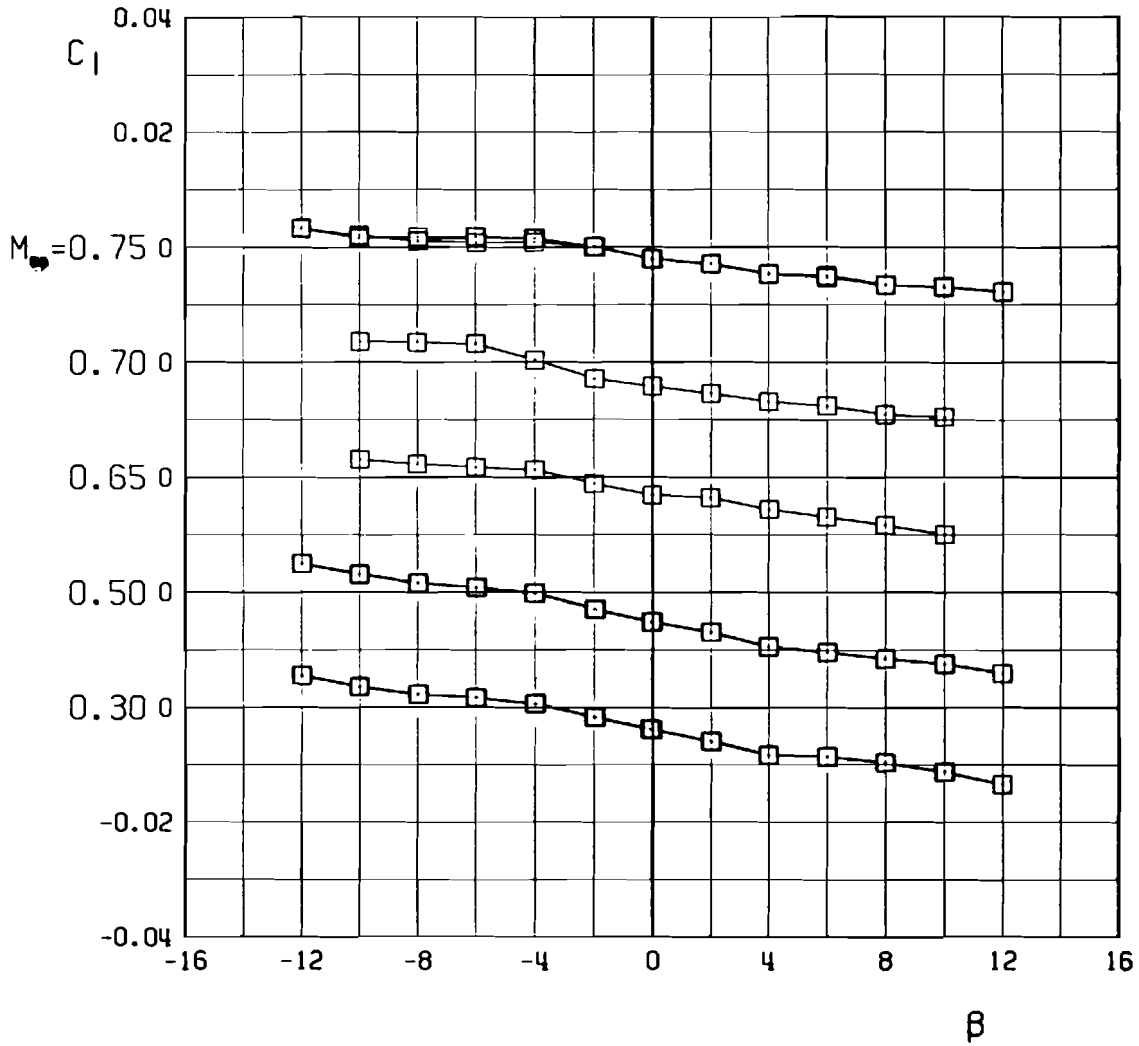

i. Rolling-moment coefficient, α = 10 deg

Figure 7. Continued.

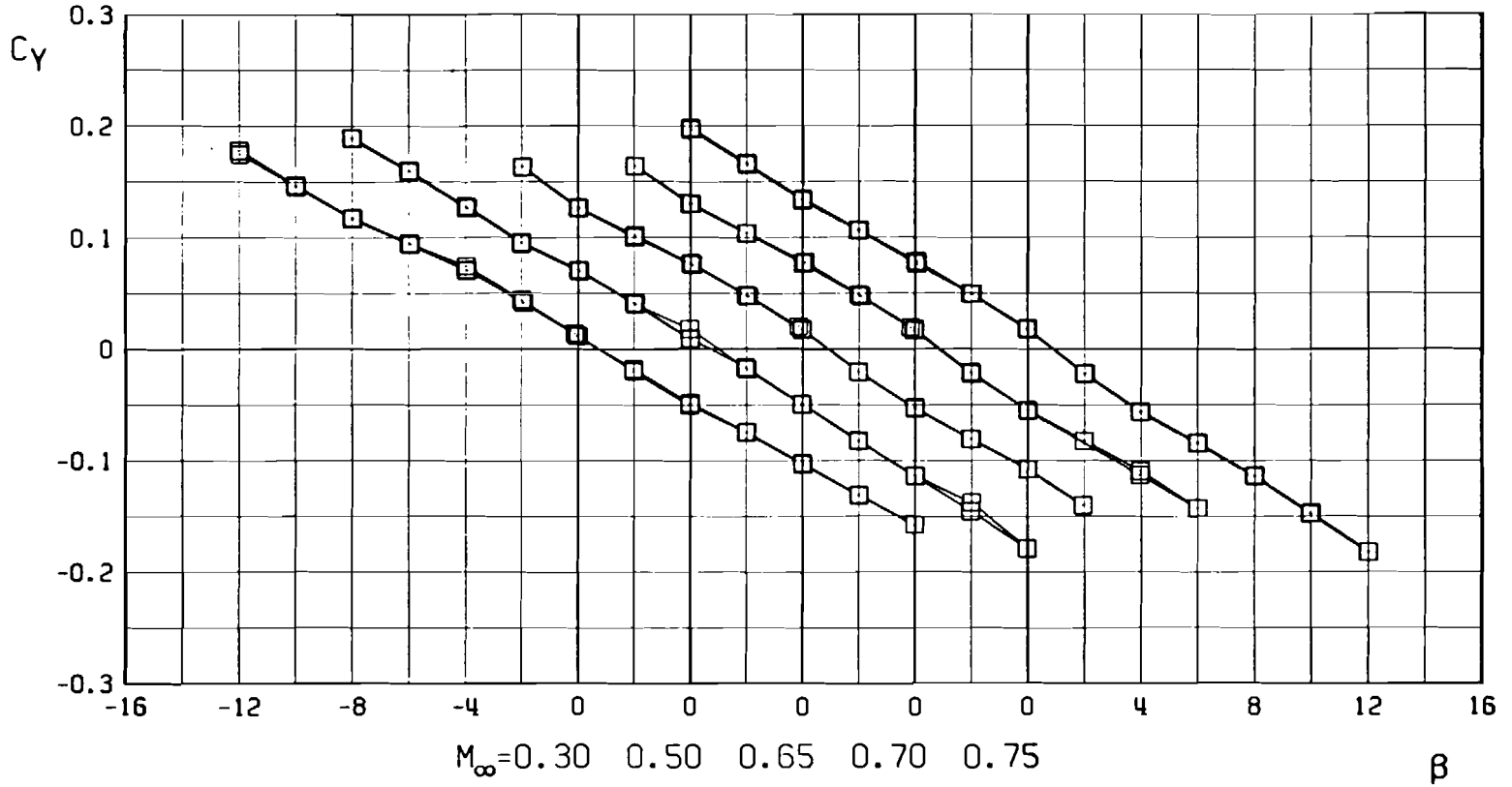

j. Side-force coefficient, α = 15 deg
Figure 7. Continued.

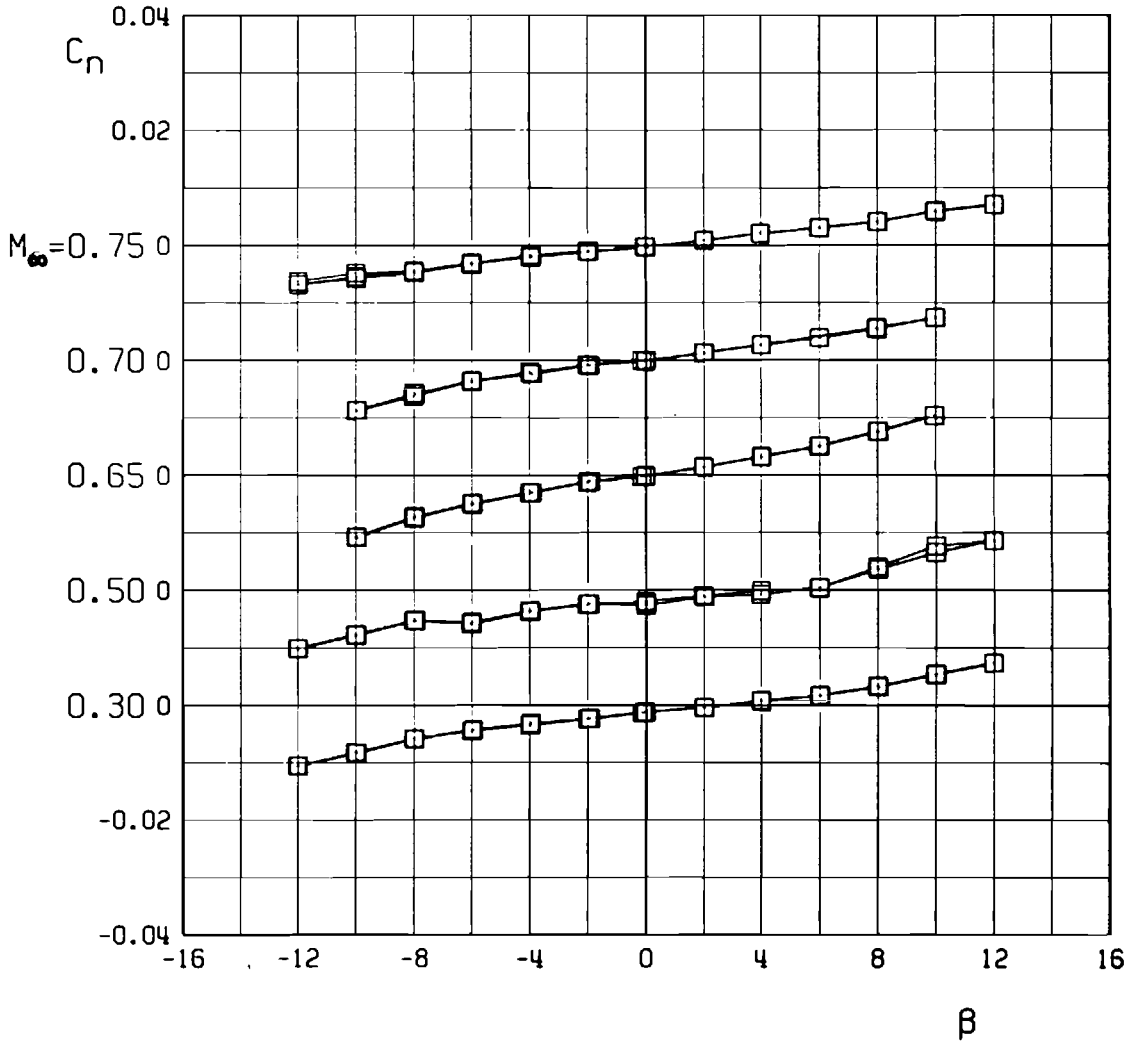

k. Yawing-moment cofficient, α = 15 deg
Figure 7. Continued.

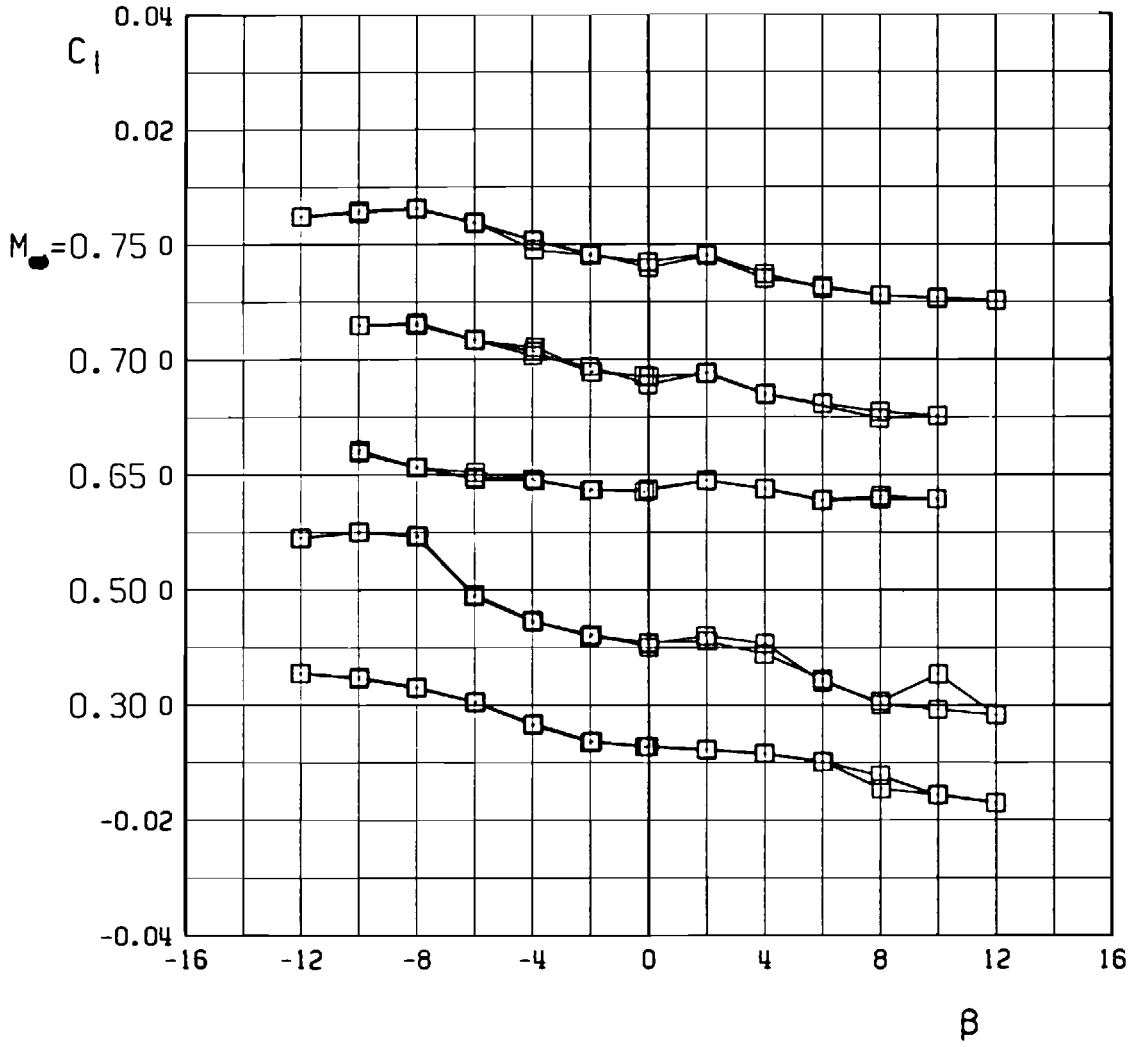

l. Rolling-moment coefficient, α = 15 deg

Figure 7. Continued.

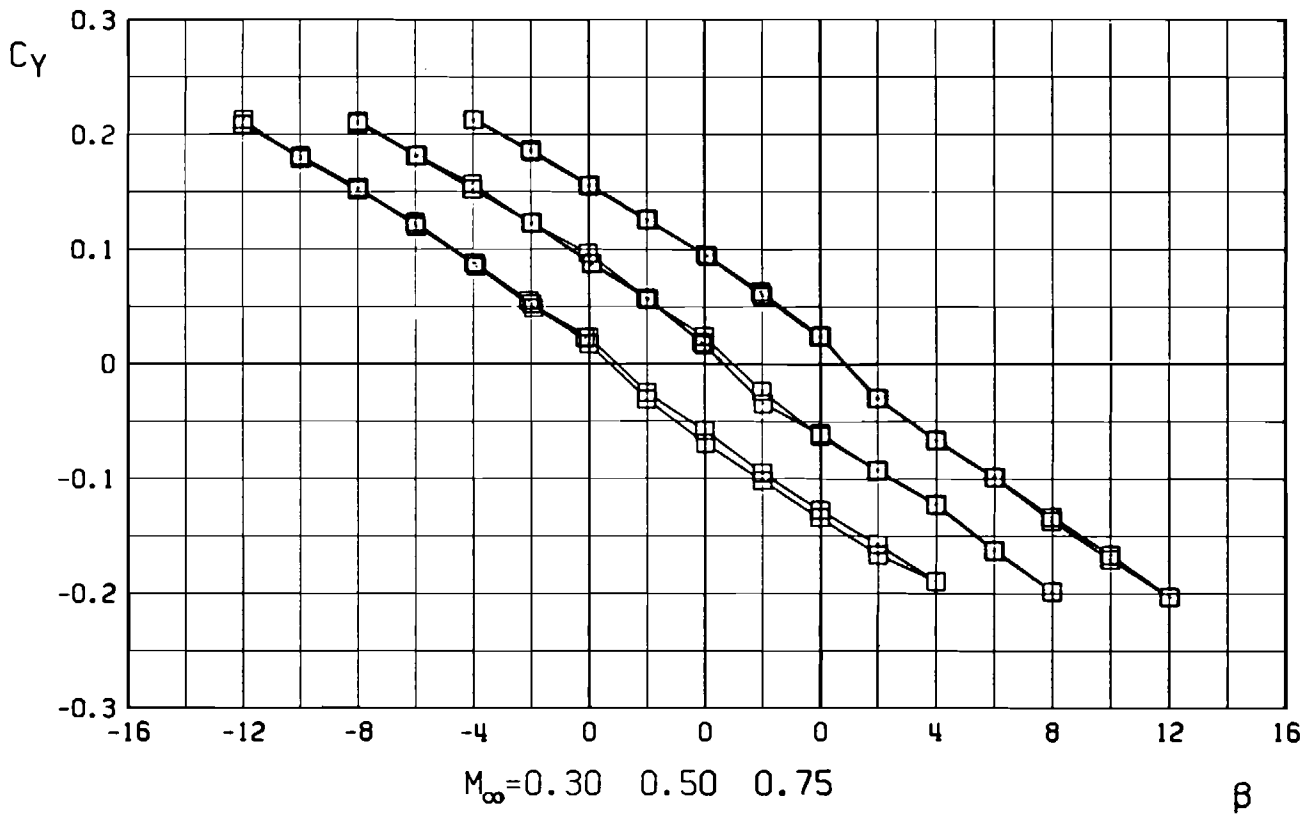

m. Side-force coefficient, α = 20 deg

Figure 7. Continued.

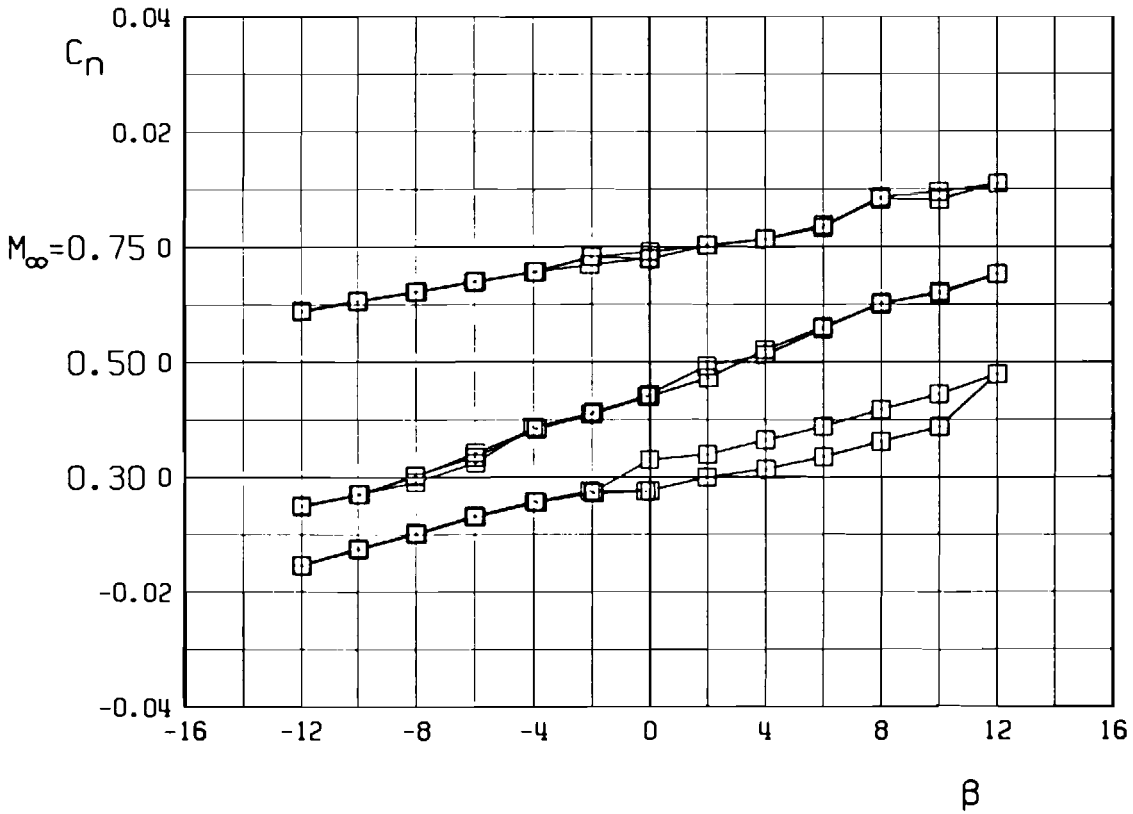

n. Yawing-moment coefficient, α = 20 deg
Figure 7. Continued.

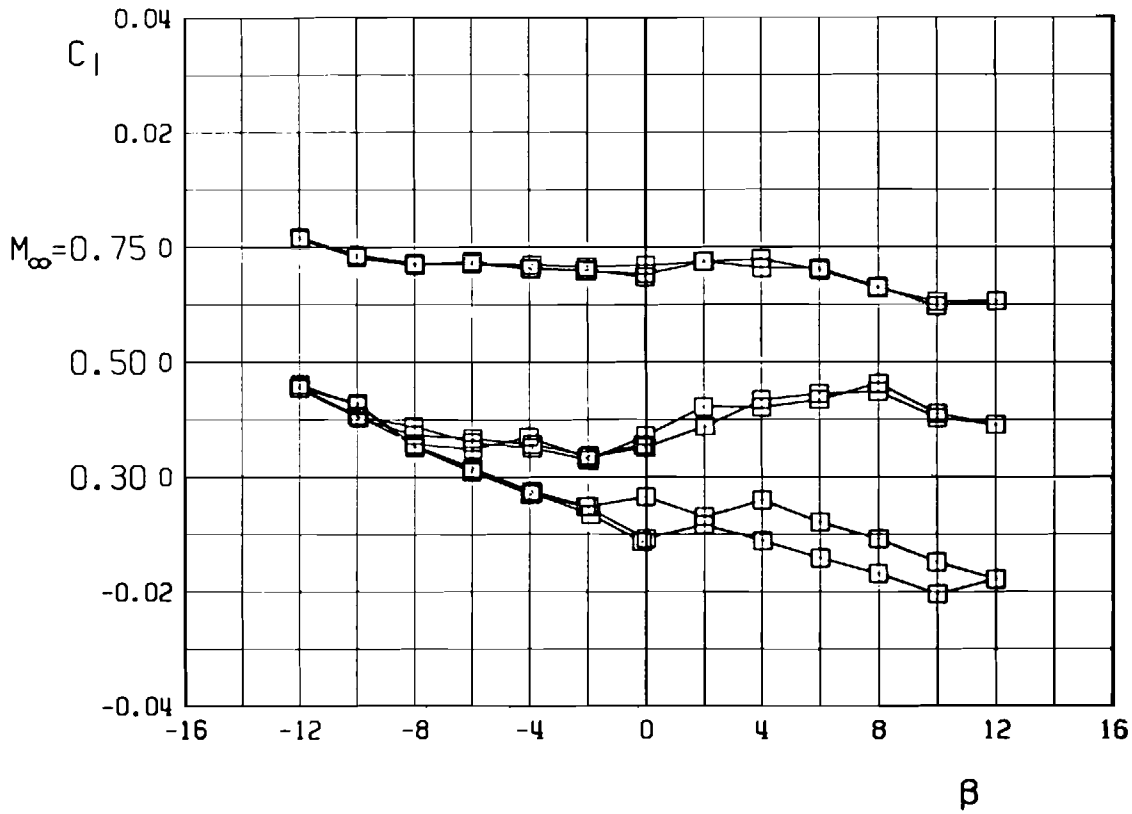

o. Rolling-moment coefficient, α = 20 deg

Figure 7. Concluded.

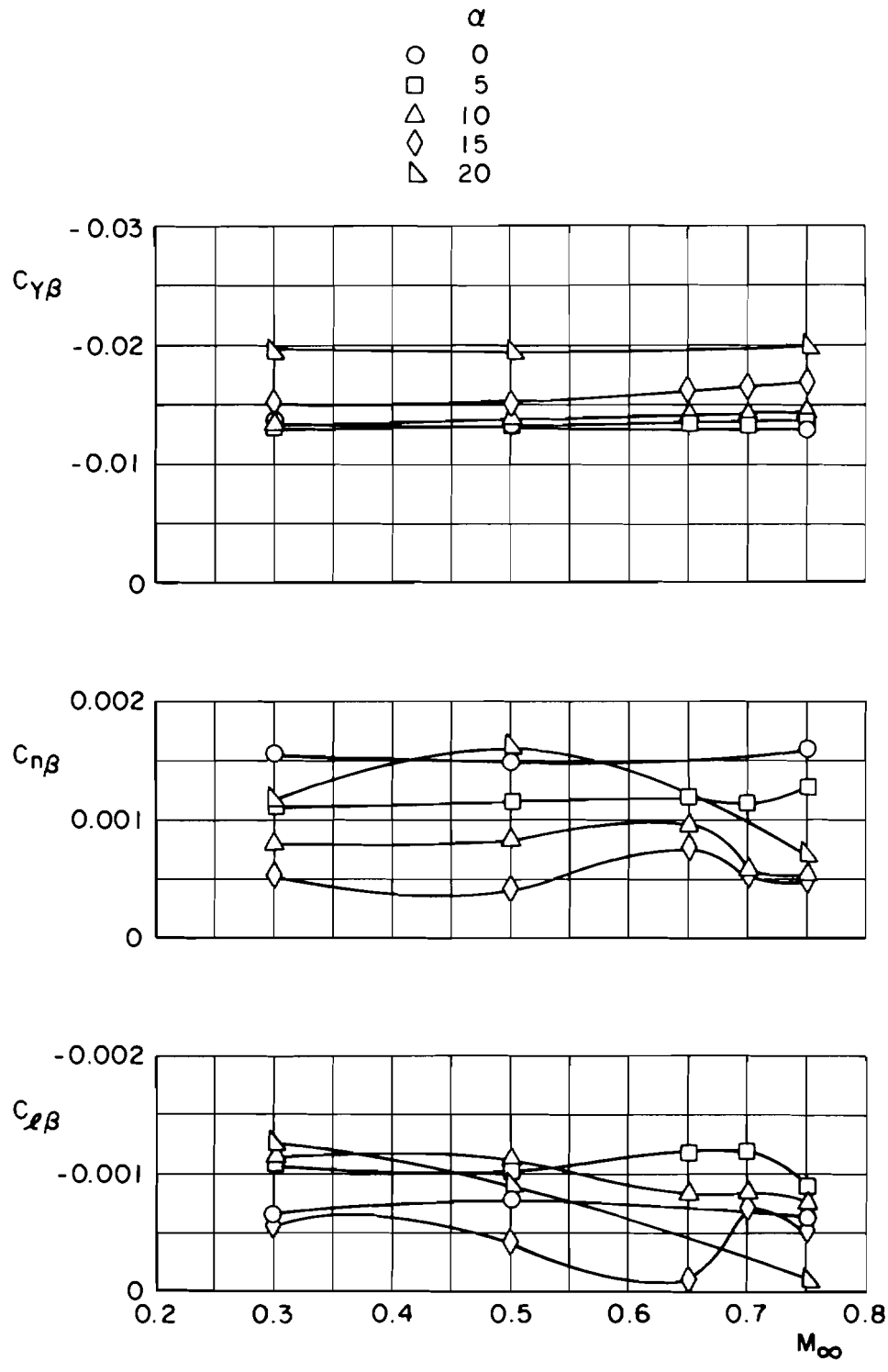

Figure 8. Summary of lateral-directional characteristics.

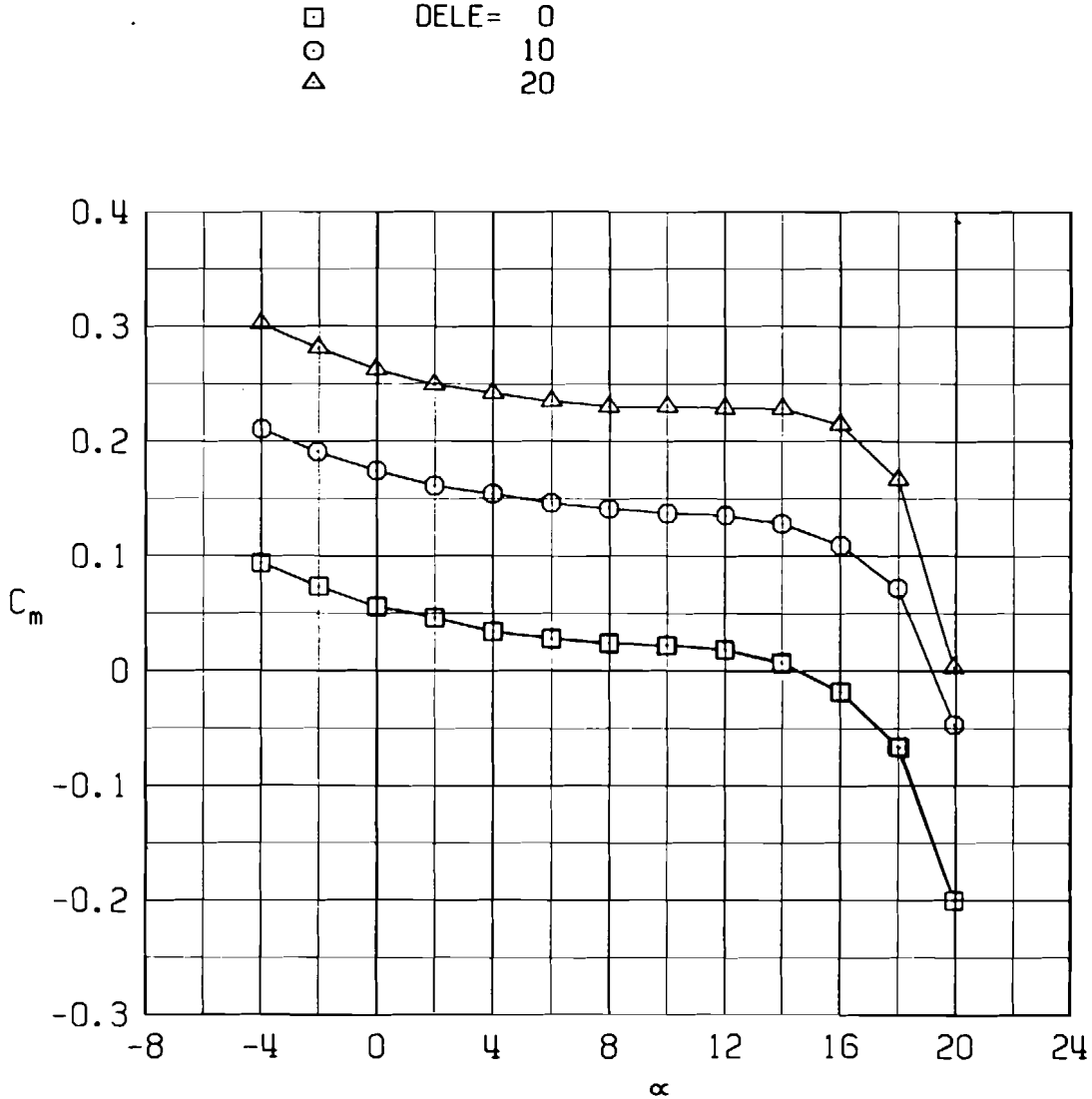

a. Elevator deflection at $M_\infty = 0.30$

Figure 9. Effect of control deflections on the aerodynamic characteristics of the A-10 model, a = 0.

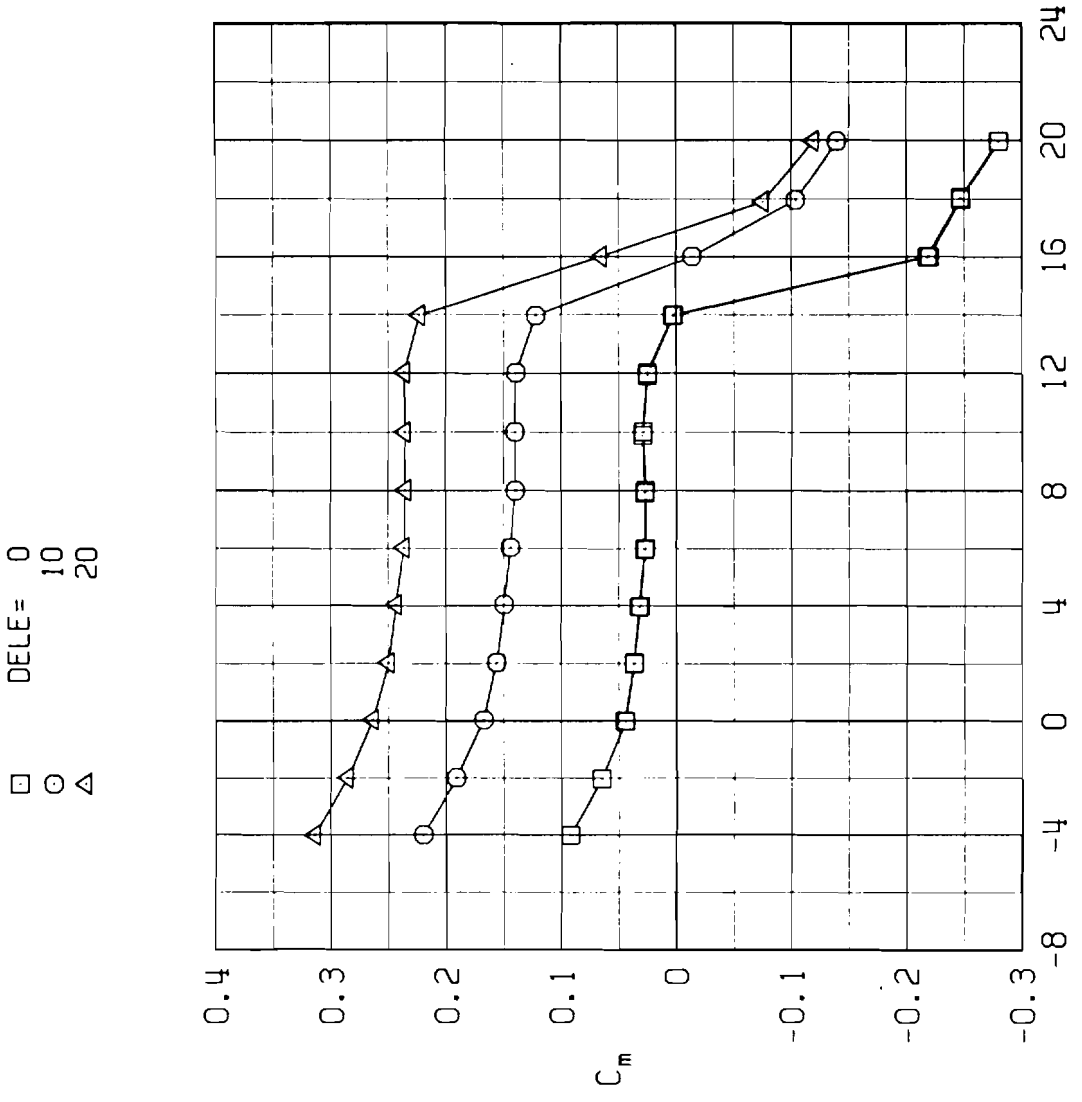

b. Elevator deflection at M_∞ = 0.50
Figure 9. Continued.

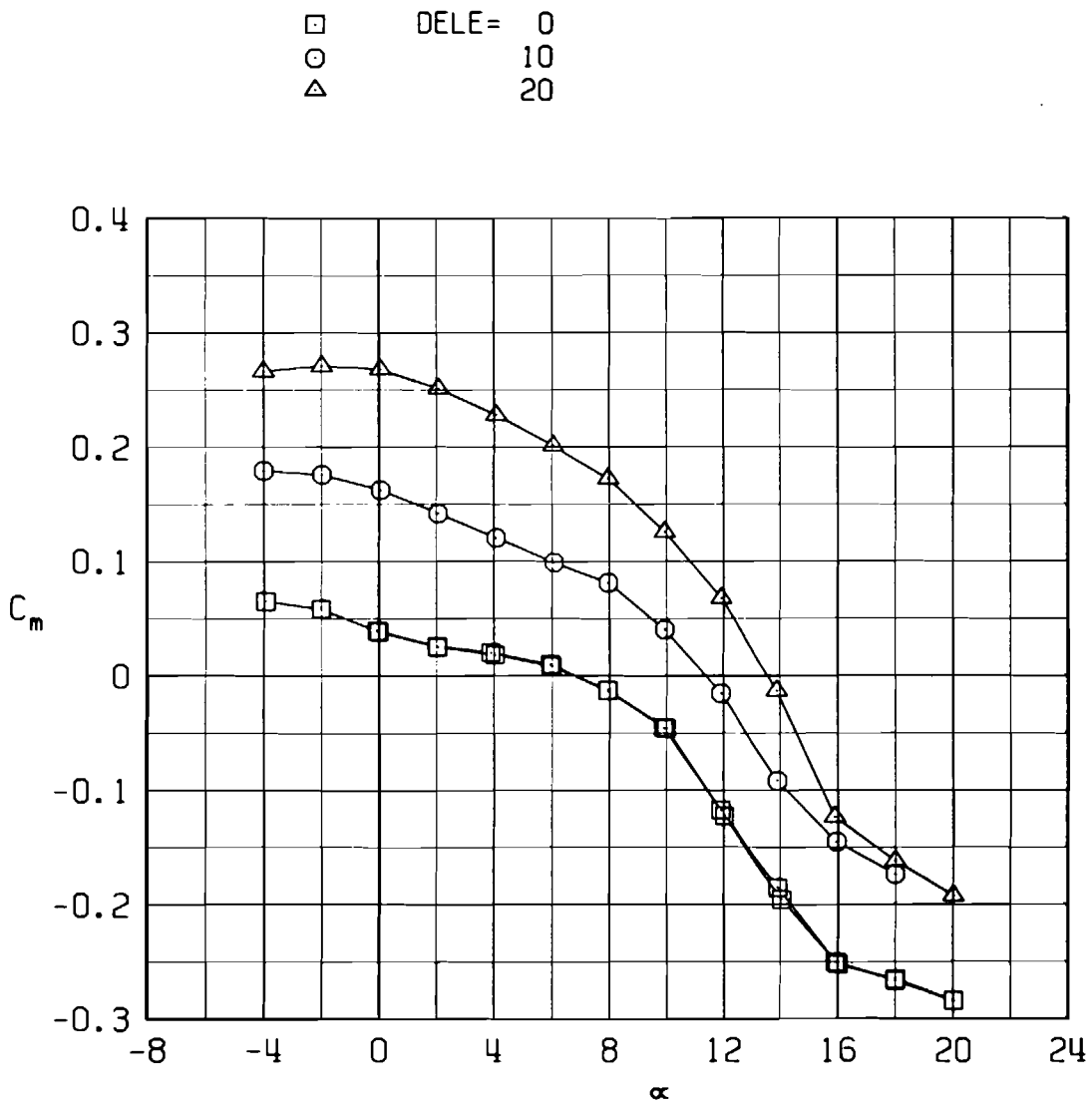

c. Elevator deflection at M_∞ = 0.75

Figure 9. Continued.

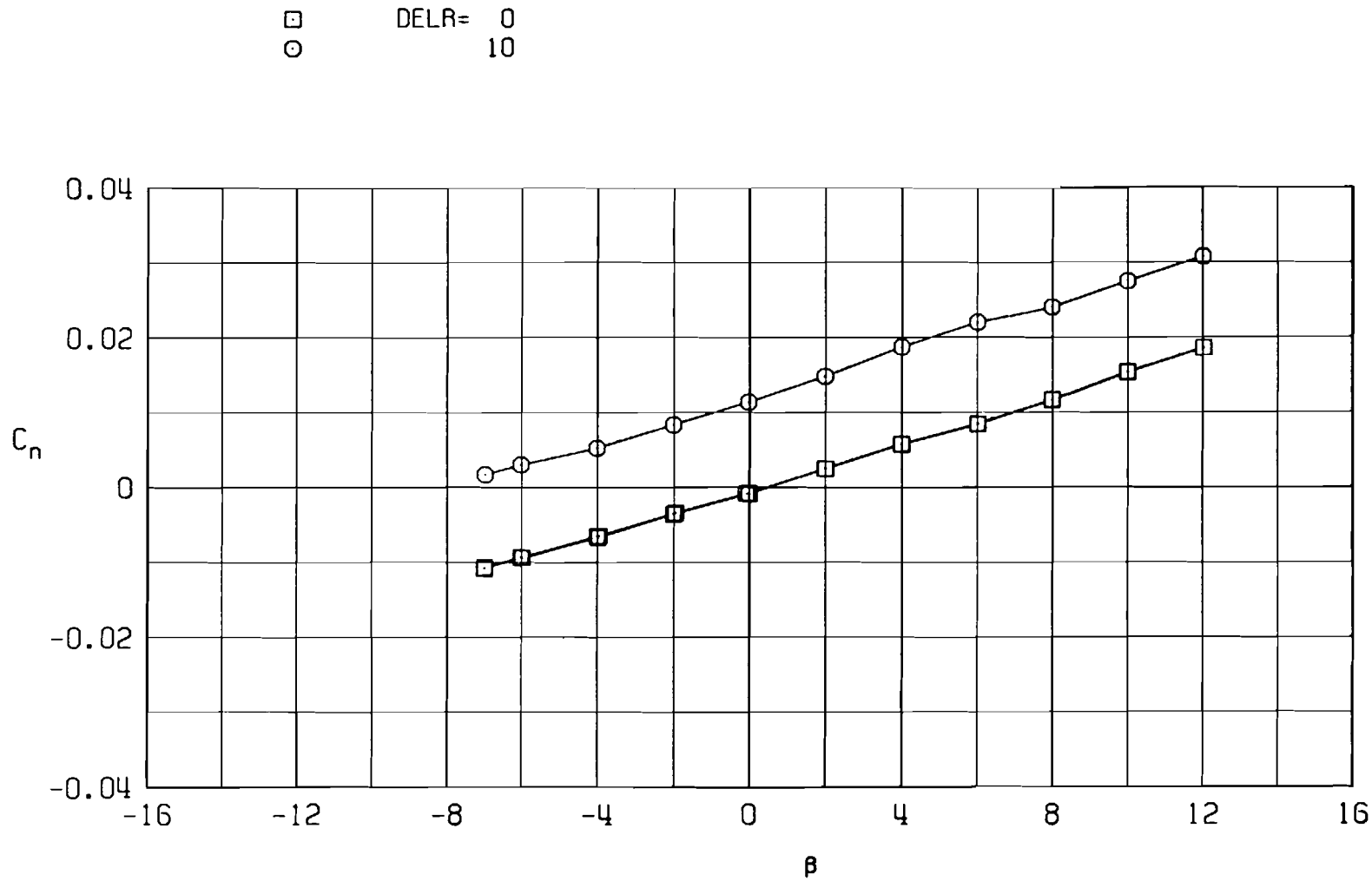

d. Rudder deflection at M_∞ = 0.30

Figure 9. Continued.

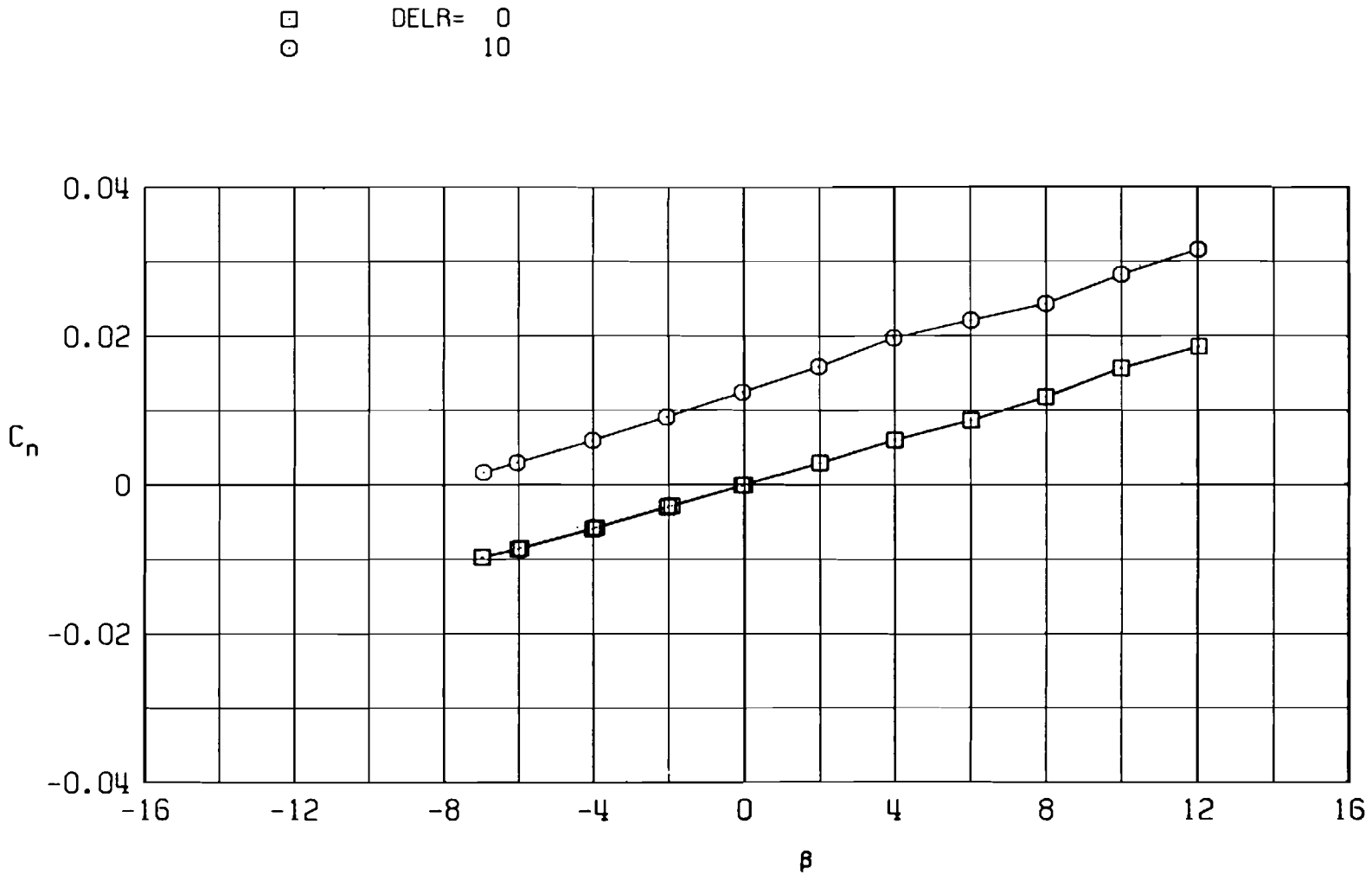

e. Rudder deflection at M_∞ = 0.50
Figure 9. Continued.

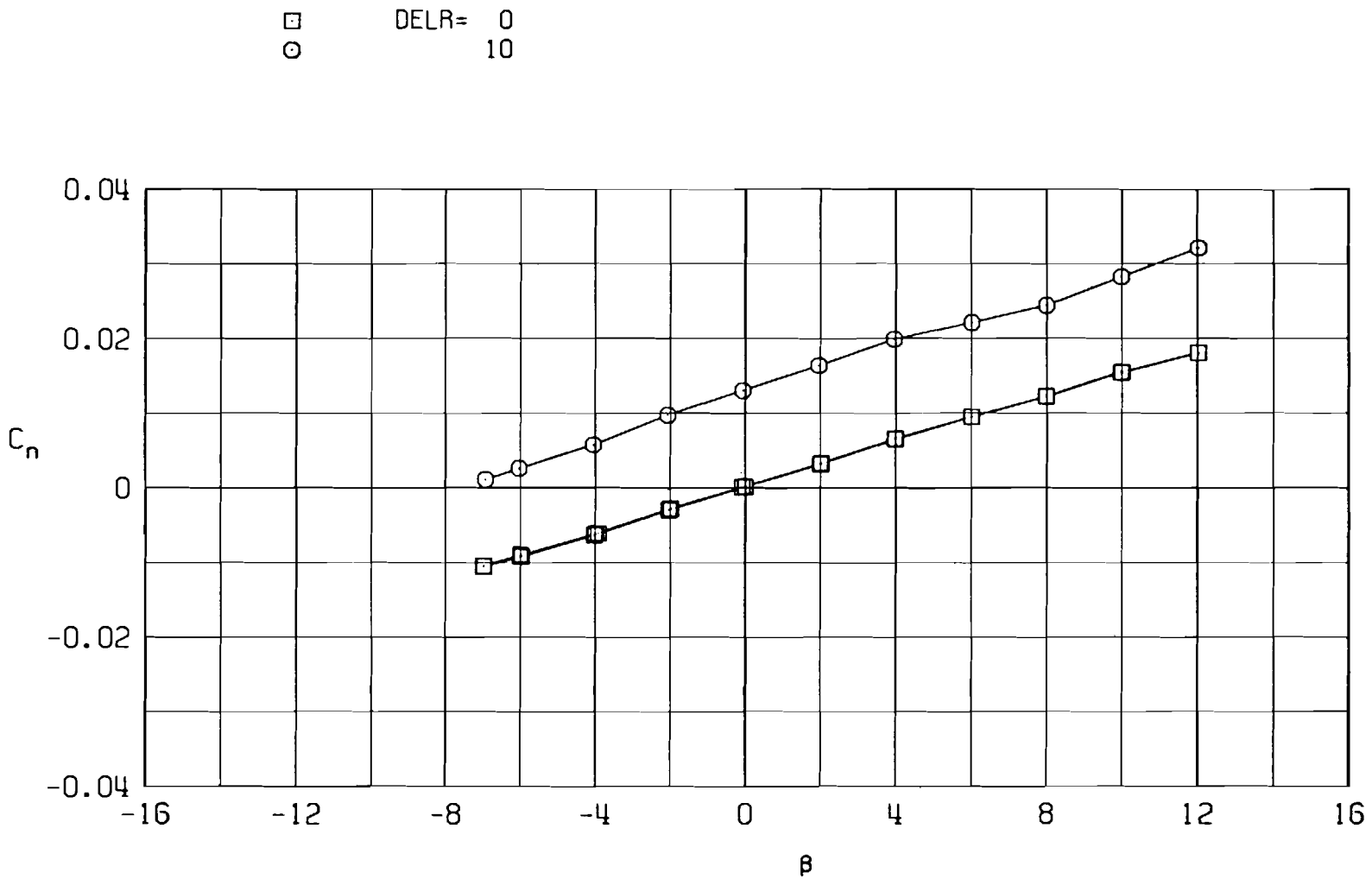

f. Rudder deflection at M_∞ = 0.75
Figure 9. Continued.

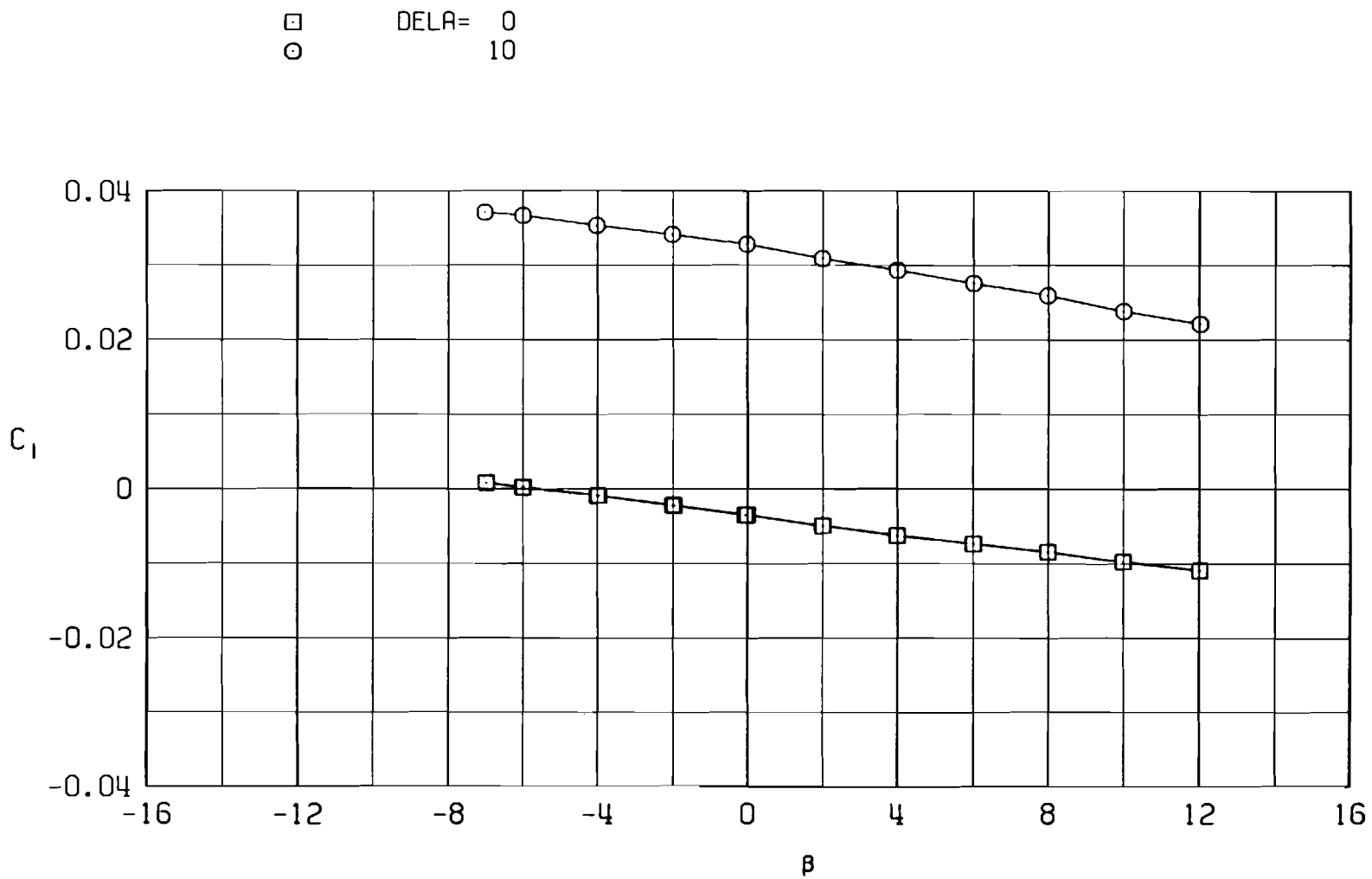

g. Aileron deflection at M_∞ = 0.30
Figure 9. Continued.

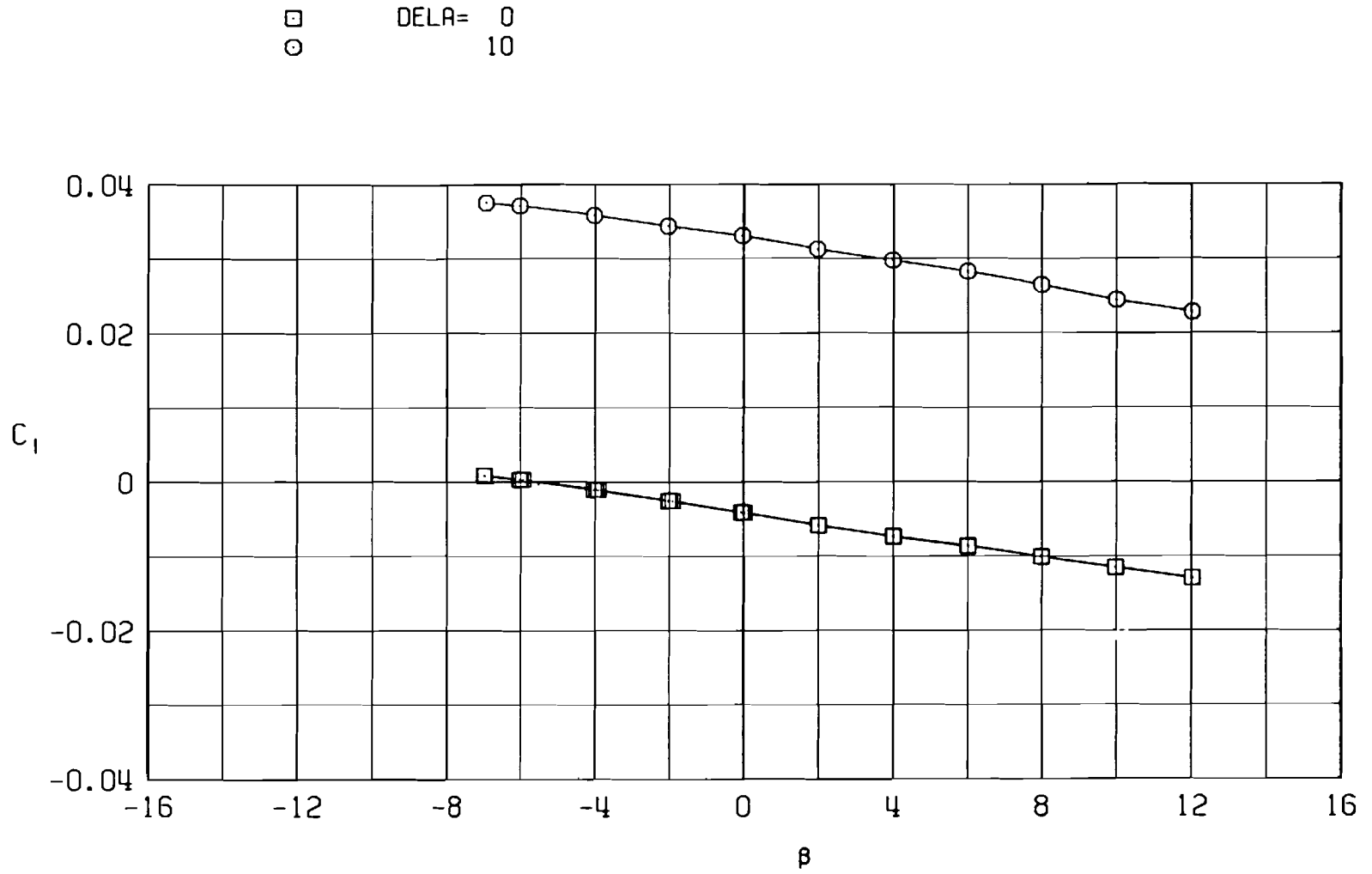

h. Aileron deflection at M_∞ = 0.50

Figure 9. Continued.

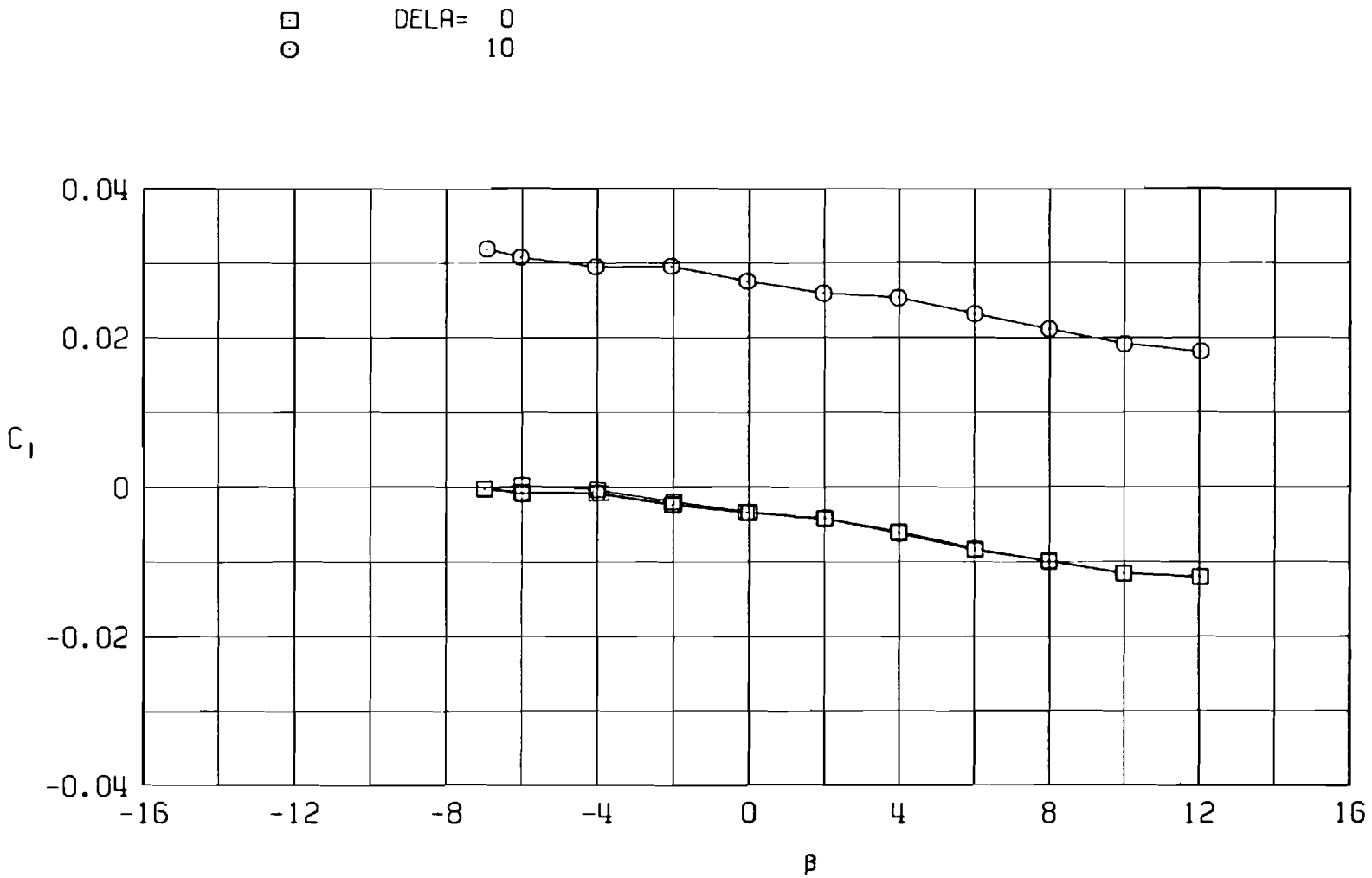

i. Aileron deflection at $M_\infty = 0.75$

Figure 9. Concluded.

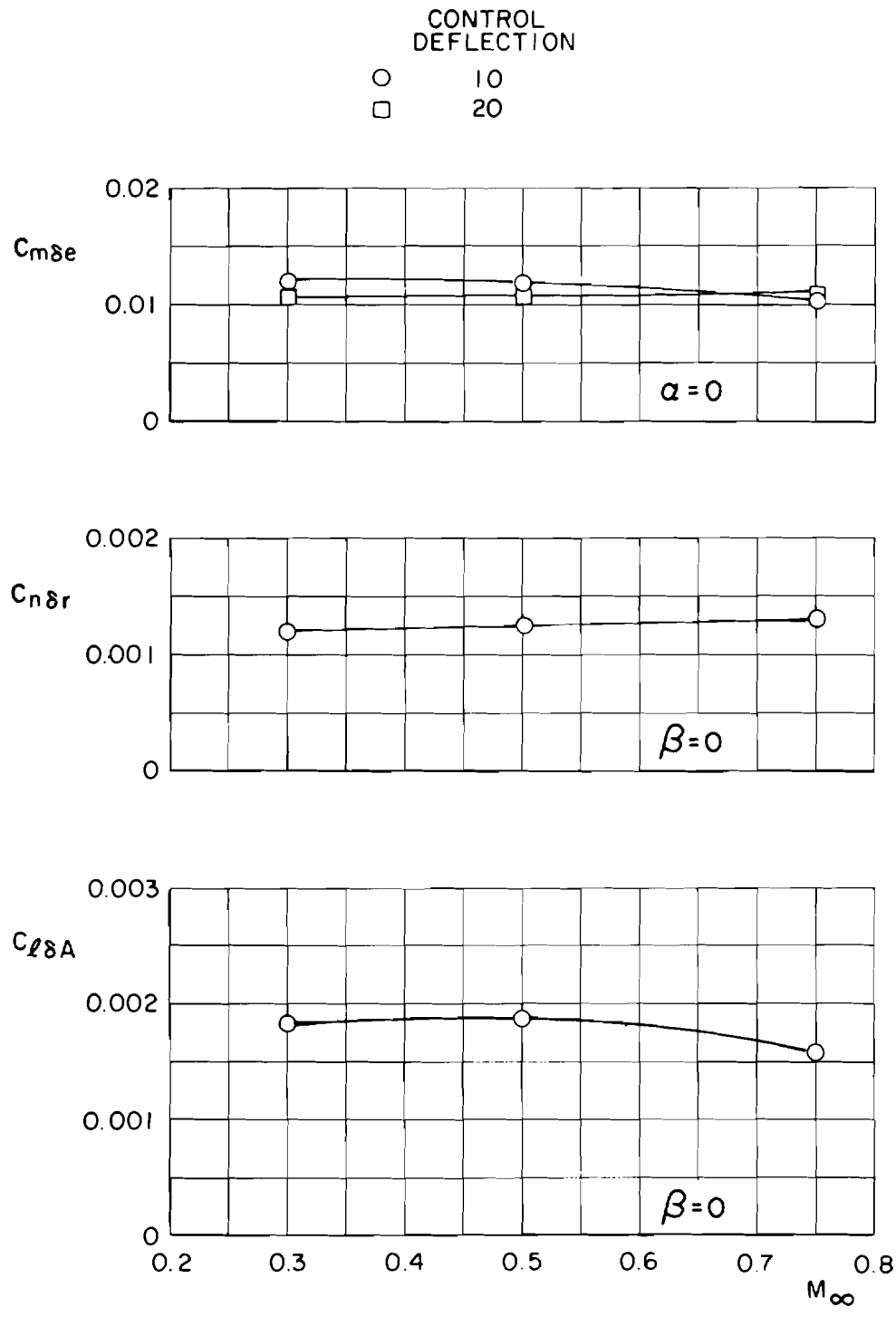

Figure 10. Variation of control effectiveness with Mach number.

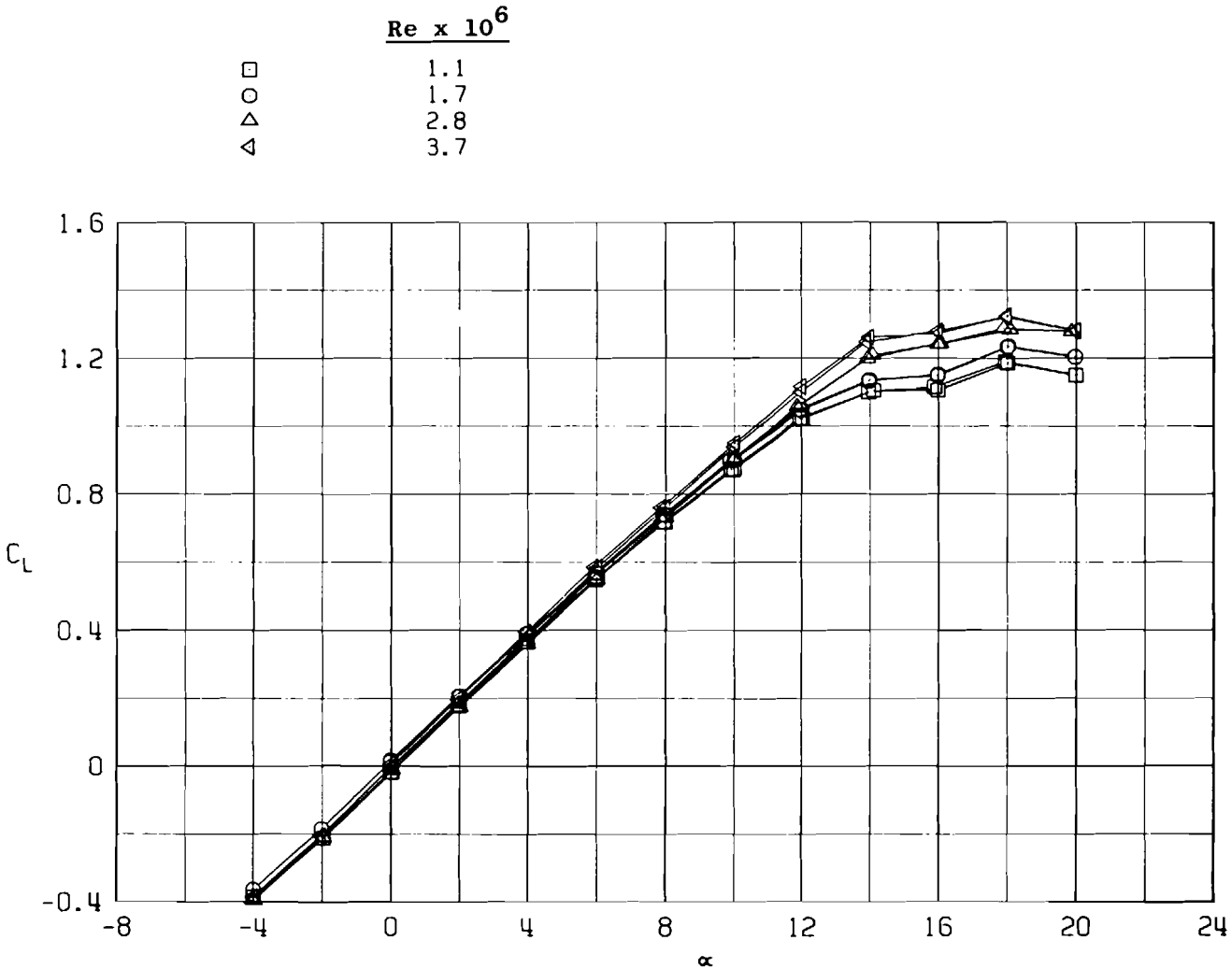

a. Lift coefficient

Figure 11. Effect of Reynolds number on the aerodynamic characteristics of the A-10 model, M_∞ = 0.50.

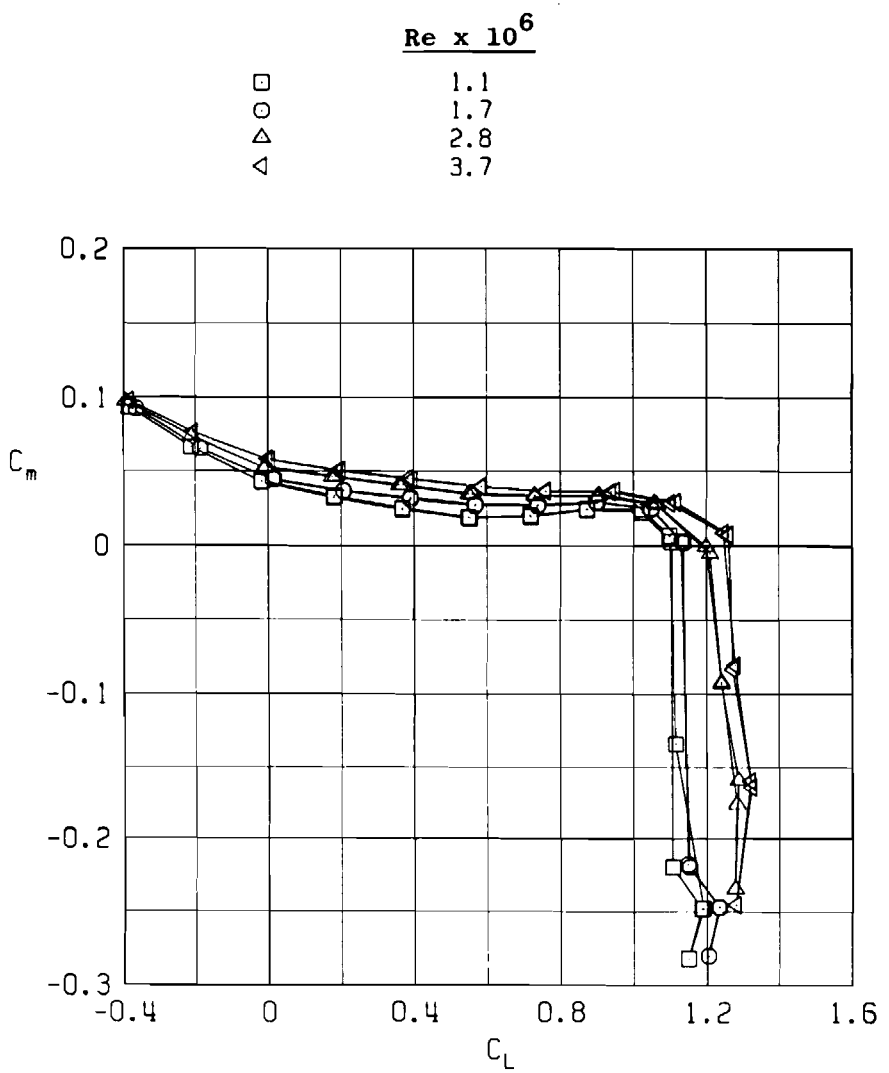

b. Pitching-moment coefficient
Figure 11. Continued.

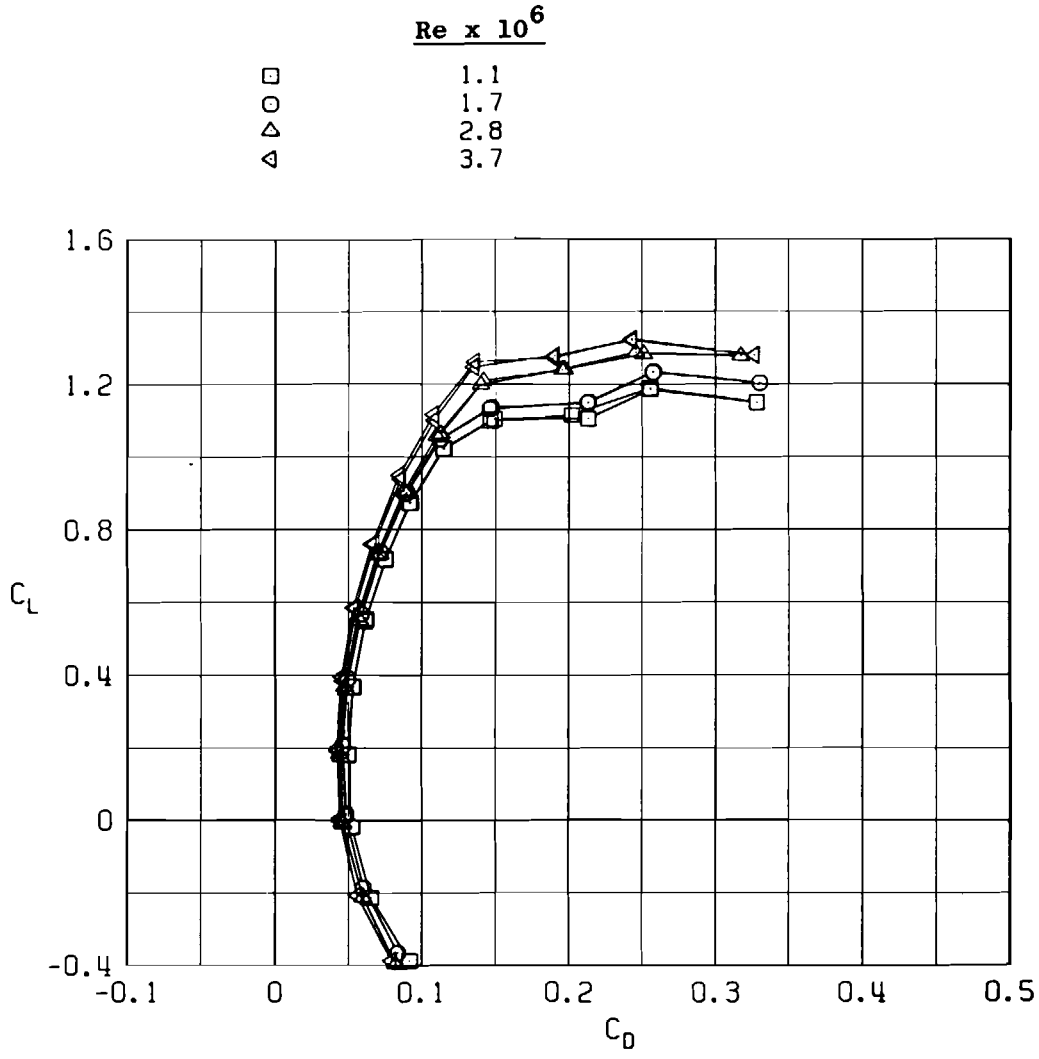

c. Drag coefficient

Figure 11. Continued.

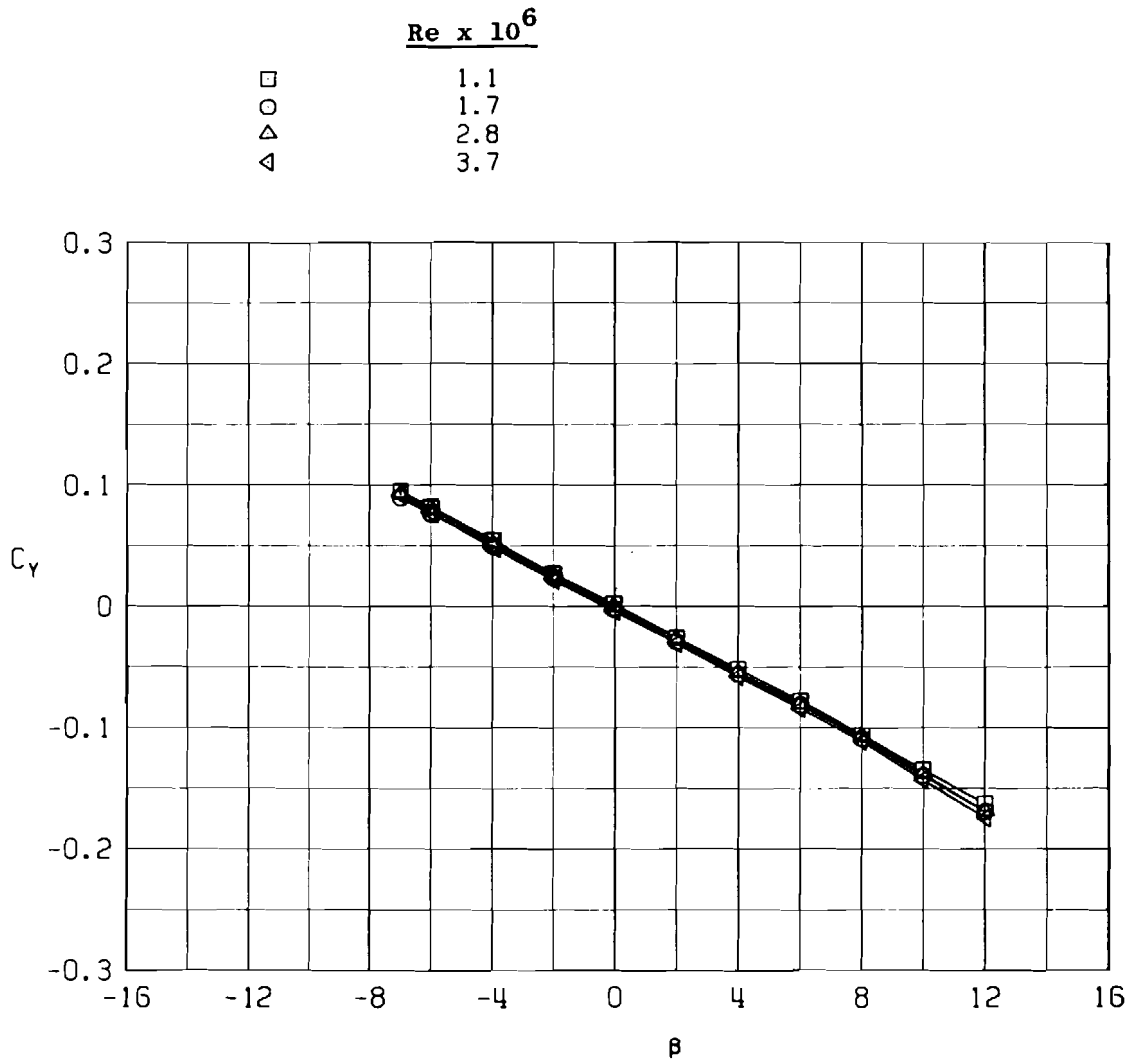

d. Side-force coefficient, α = 0

Figure 11. Continued.

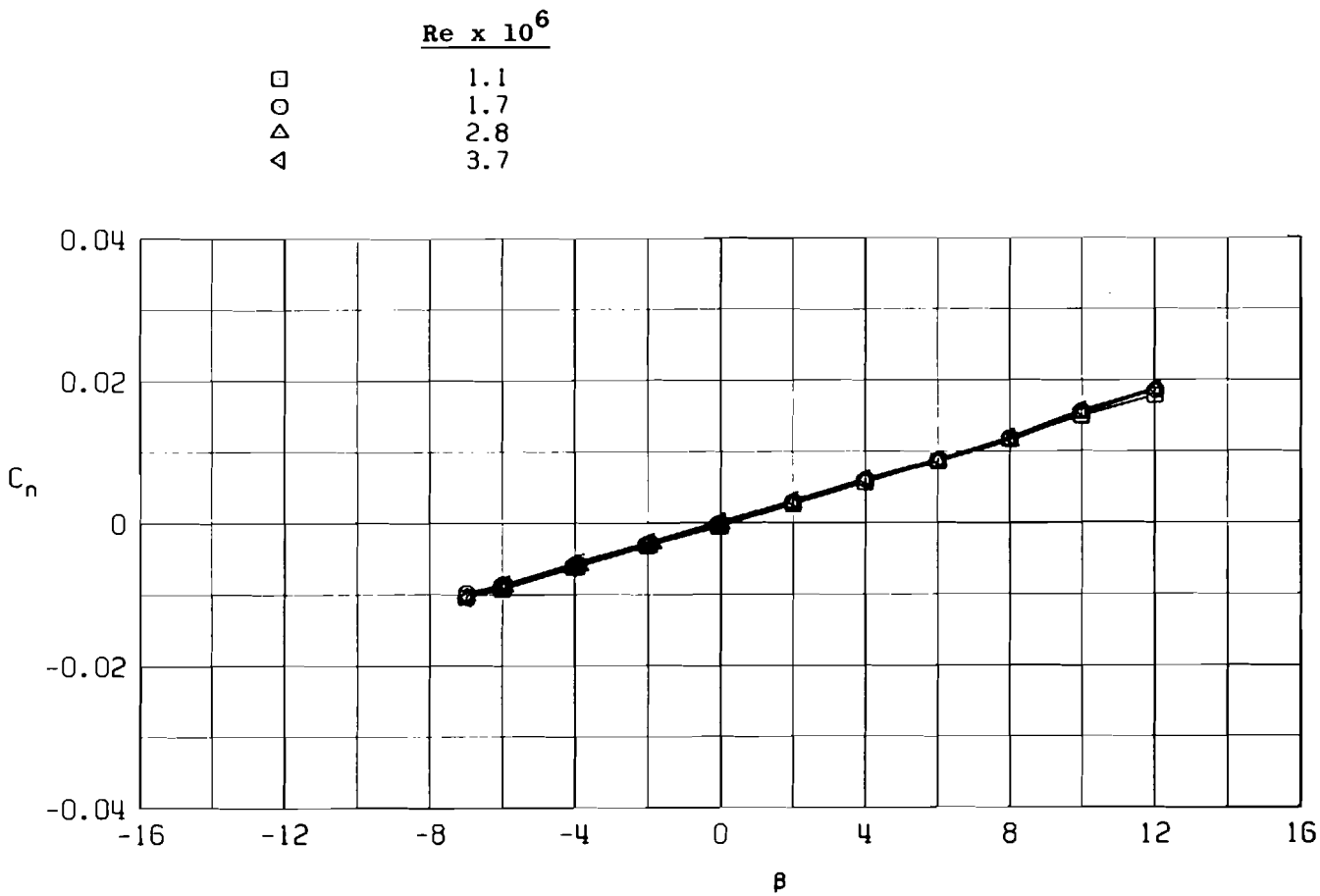

e. Yawing-moment coefficient, α = 0

Figure 11. Continued.

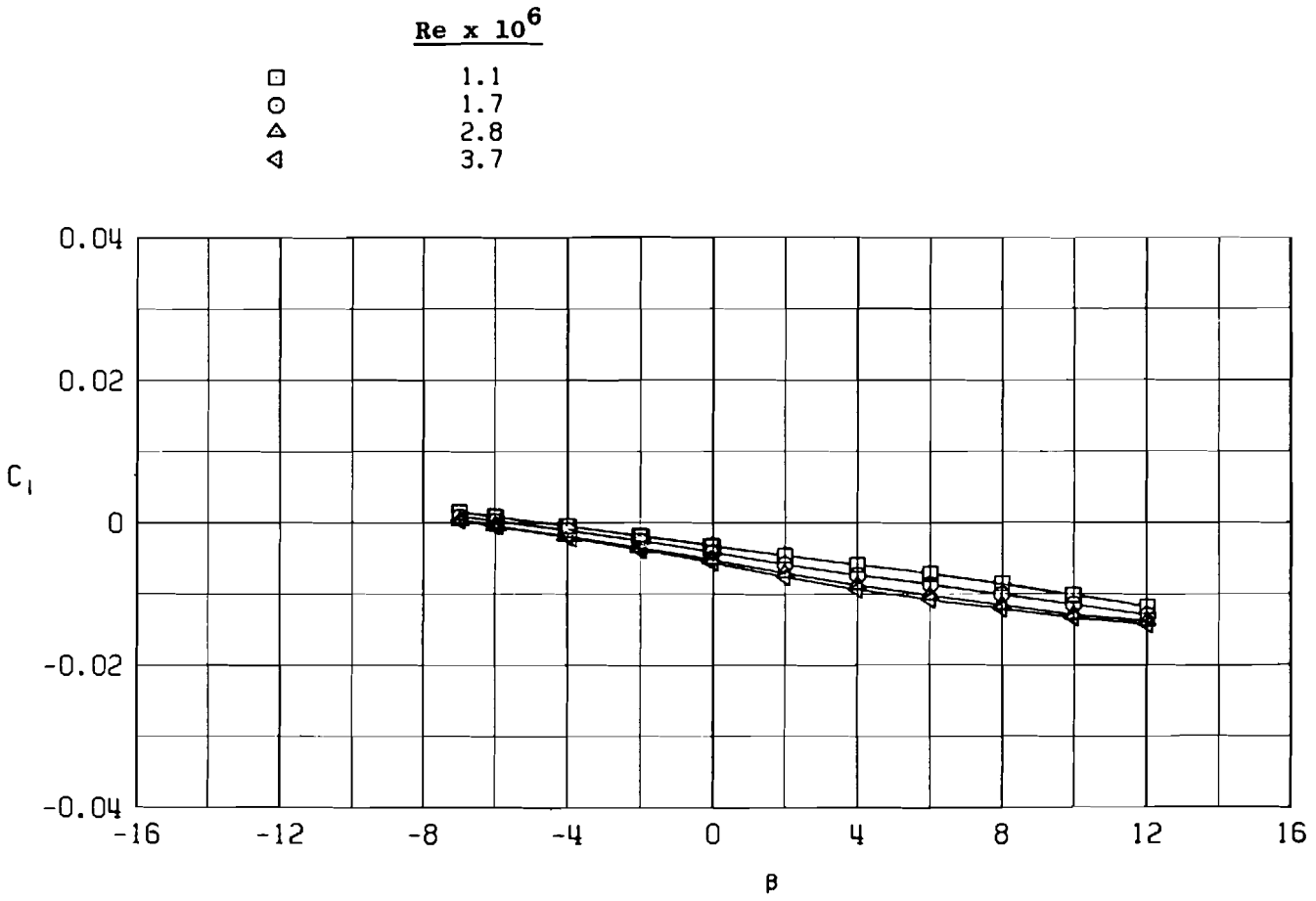

f. Rolling-moment coefficient, α = 0

Figure 11. Concluded.

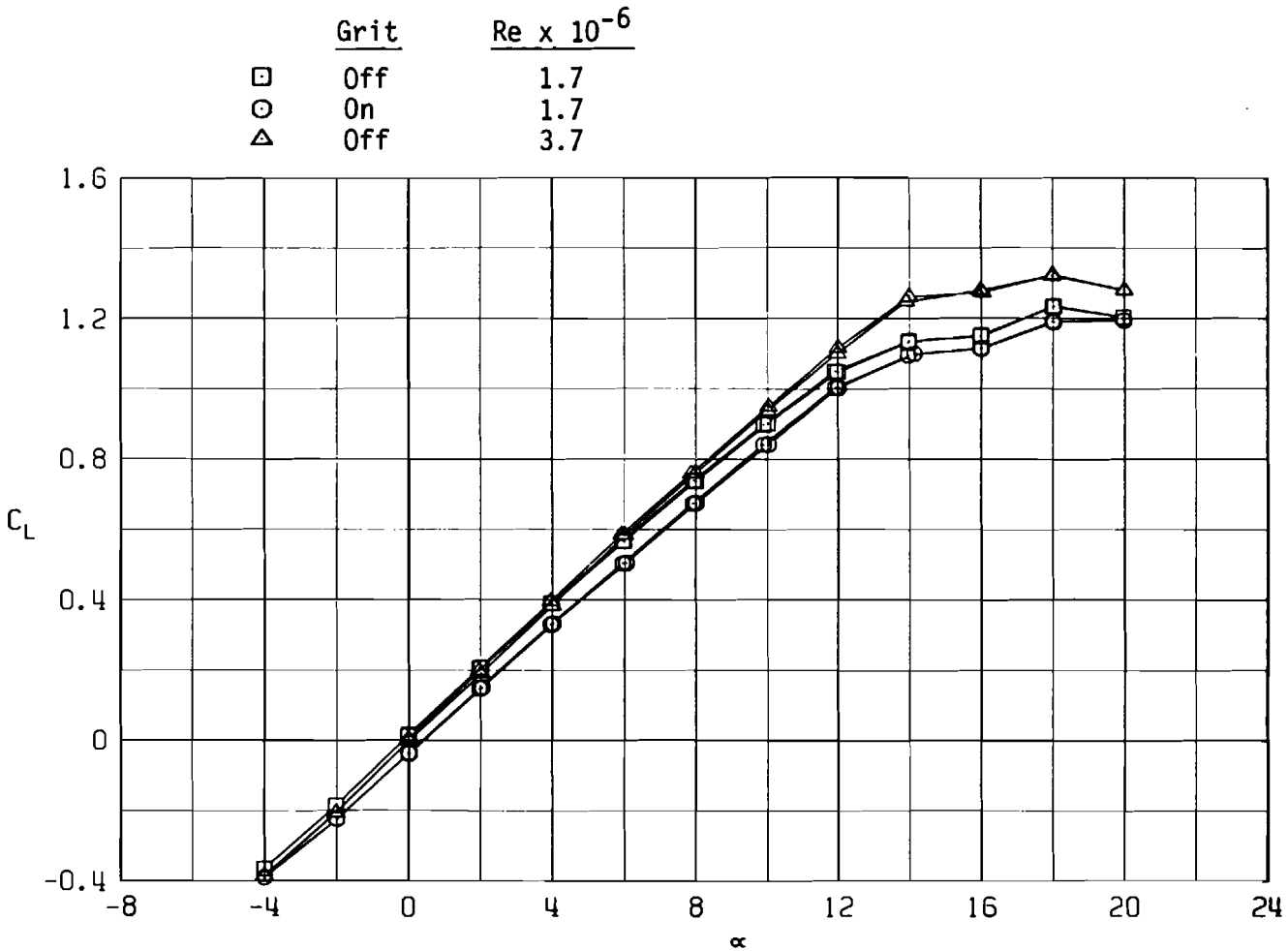

a. Lift coefficient

Figure 12. Effect of boundary-layer transition grit on the aerodynamic characteristics of the A-10 model, M_∞ = 0.50.

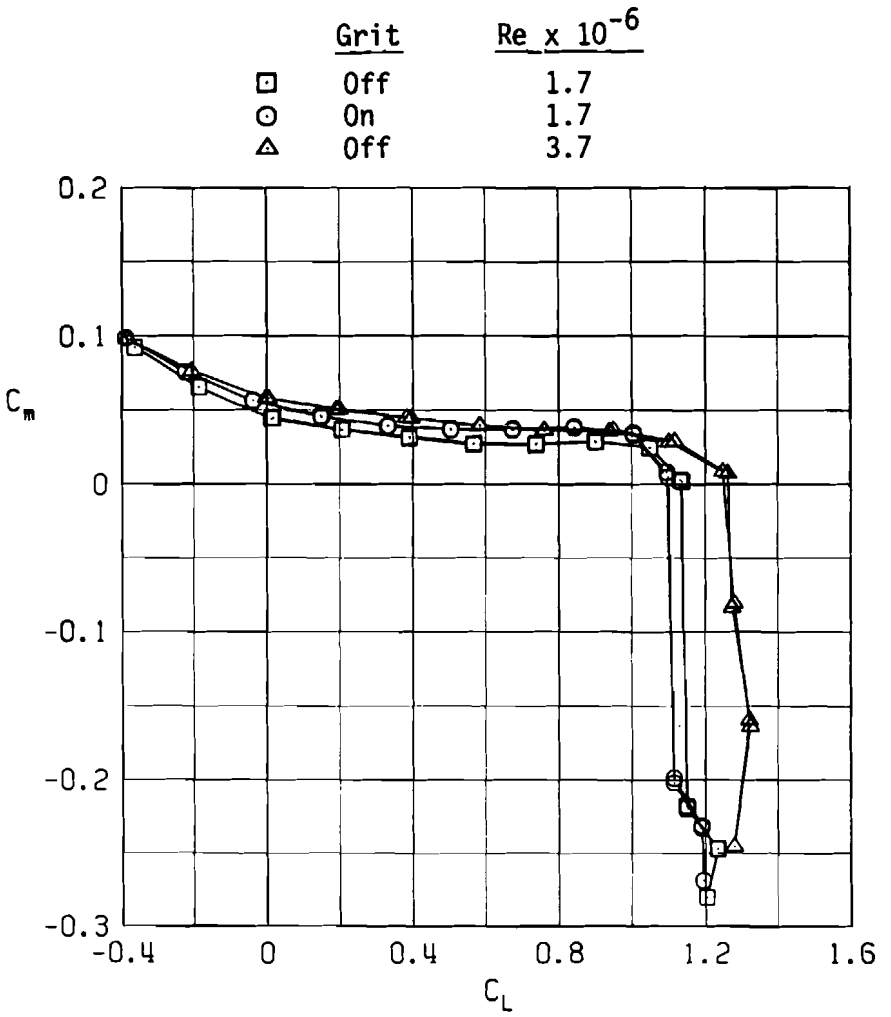

b. Pitching-moment coefficient

Figure 12. Continued.

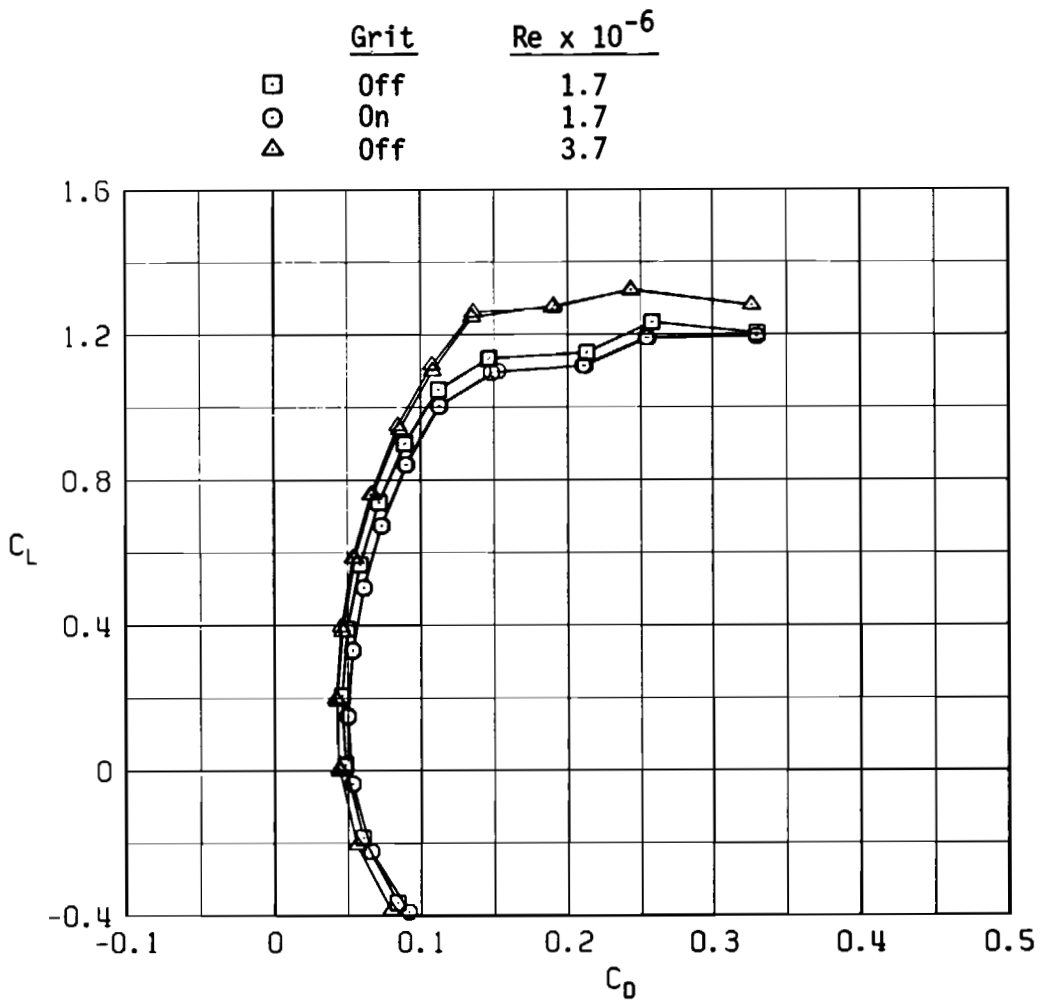

c. Drag coefficient
Figure 12. Continued.

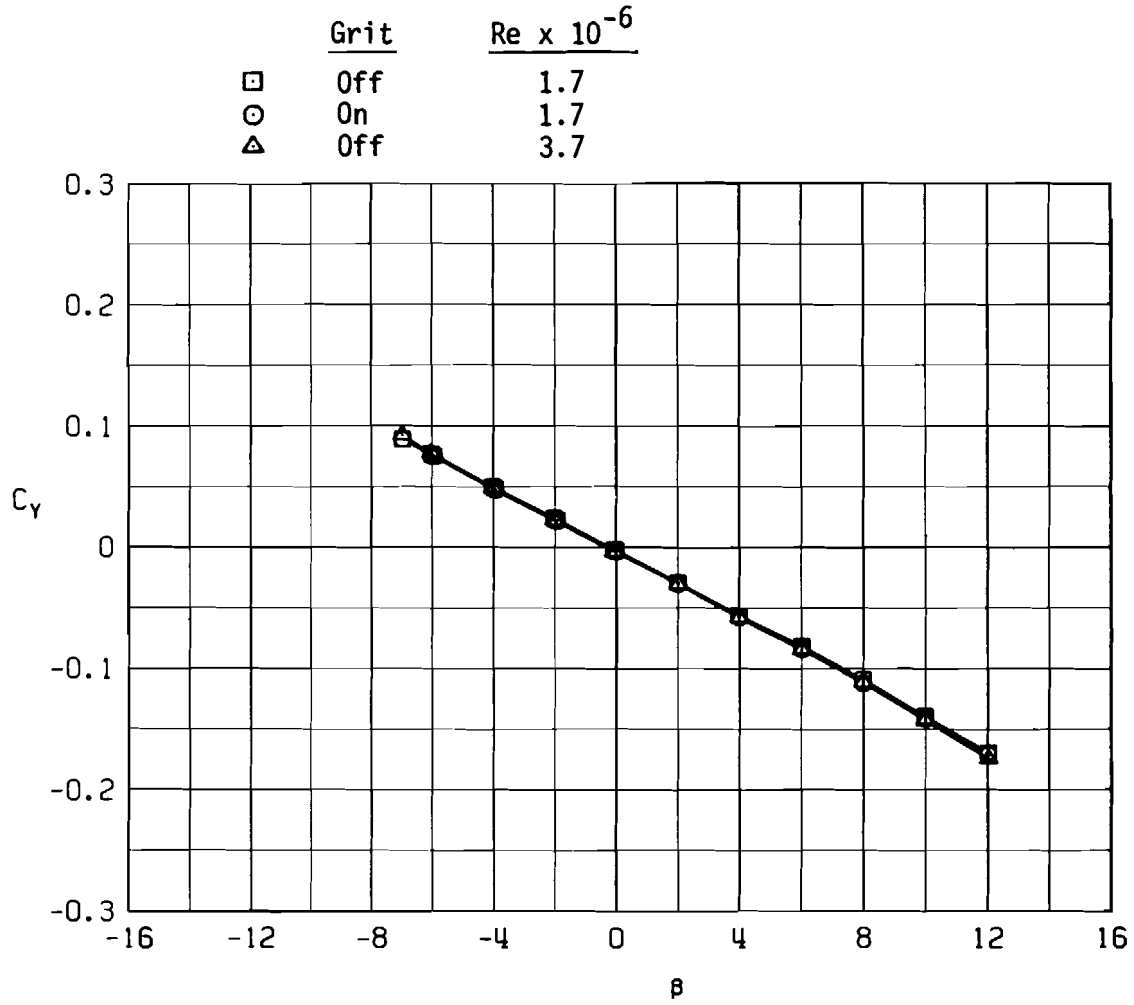

d. Side-force coefficient, $\alpha = 0$

Figure 12. Continued.

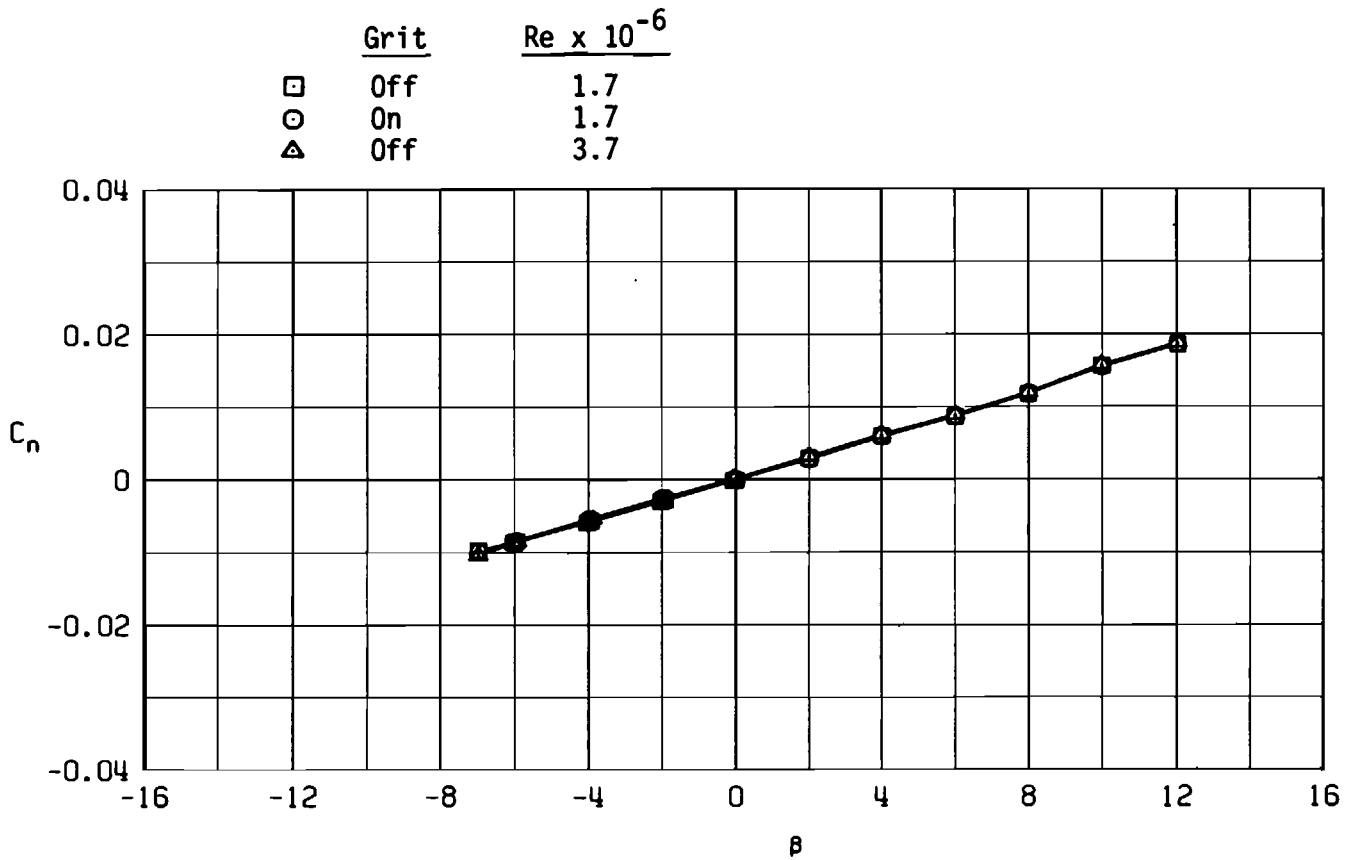

e. Yawing-moment coefficient, α = 0
Figure 12. Continued.

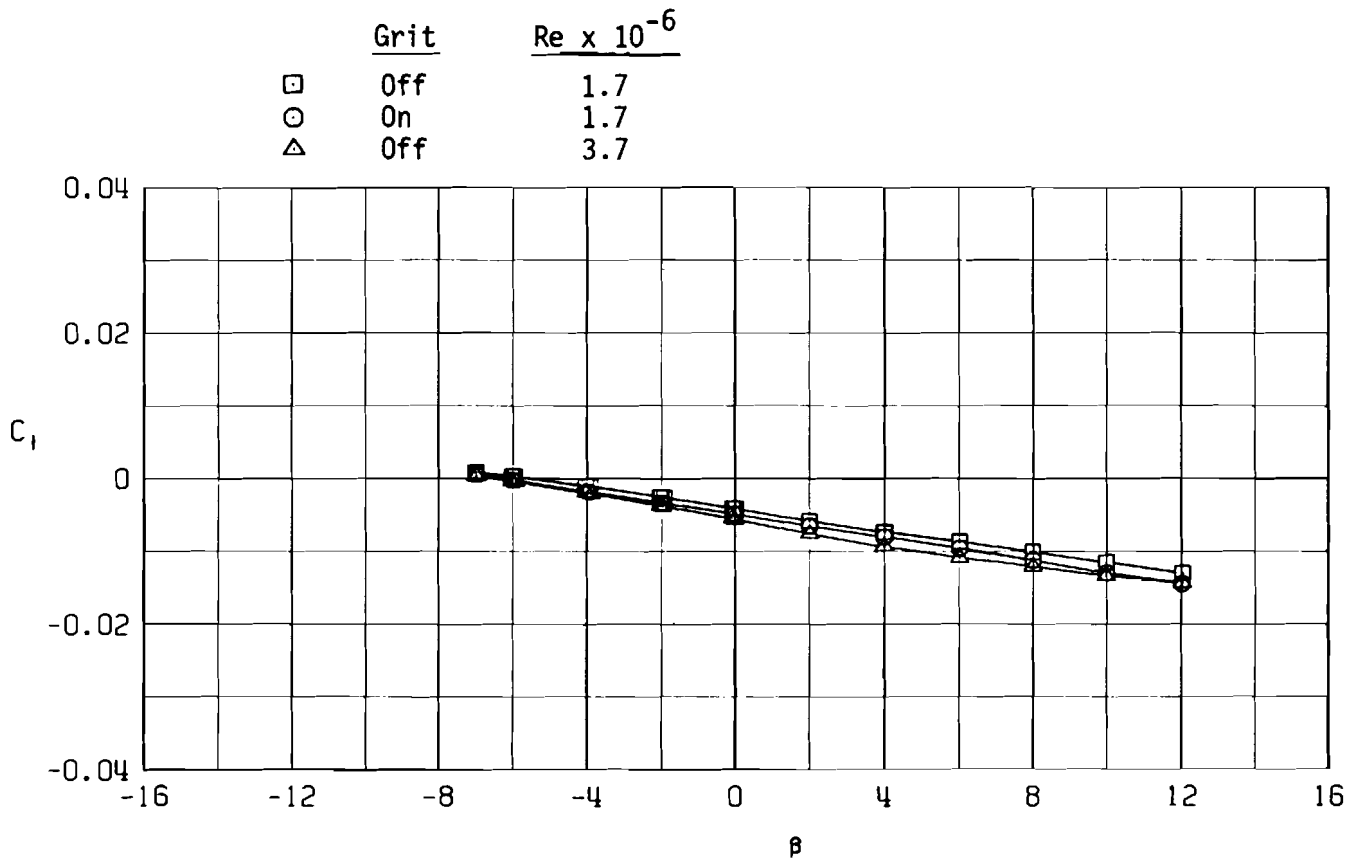

f. Rolling-moment coefficient, α = 0
Figure 12. Concluded.

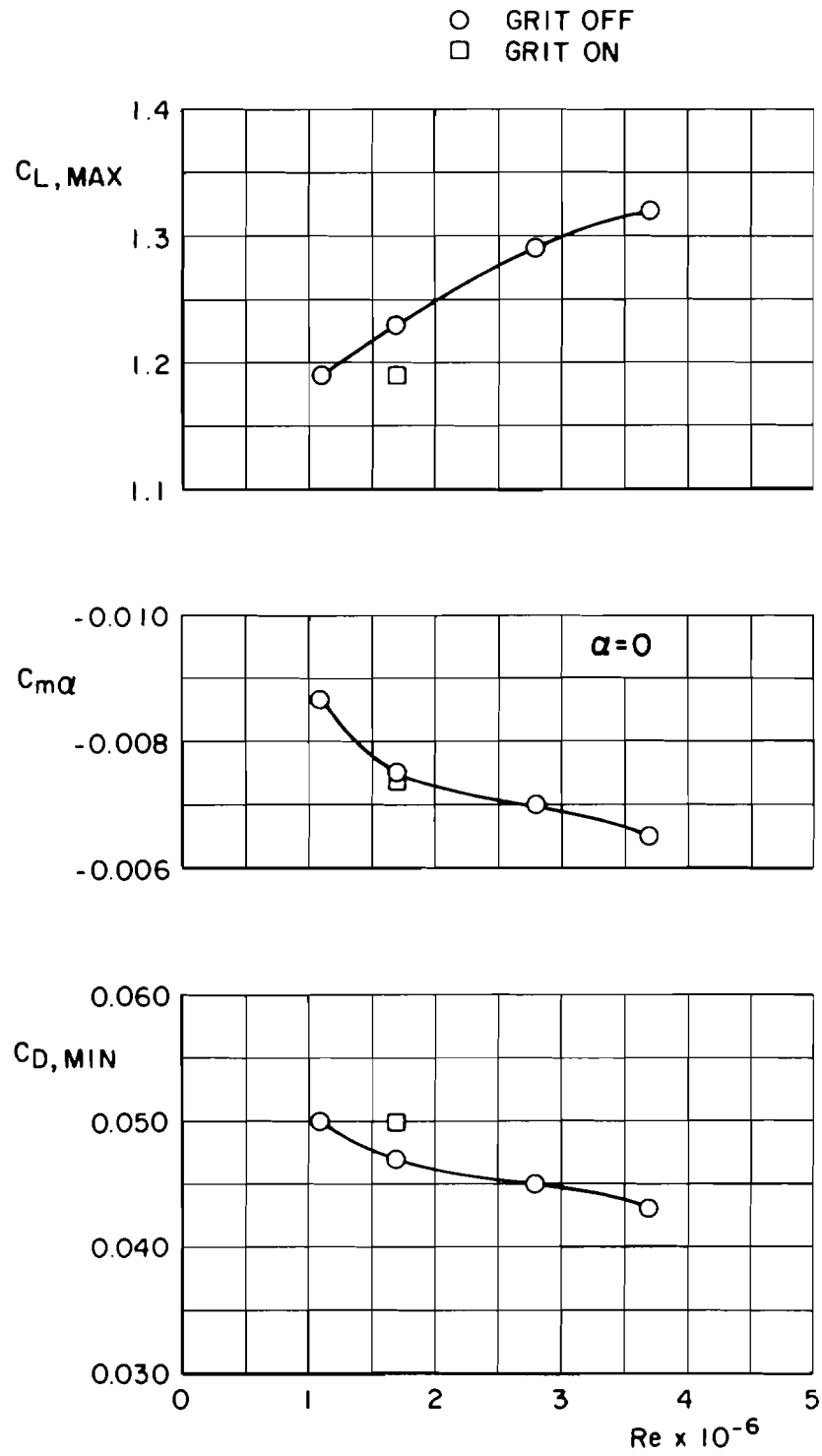

Figure 13. Summary of Reynolds number and grit effects.

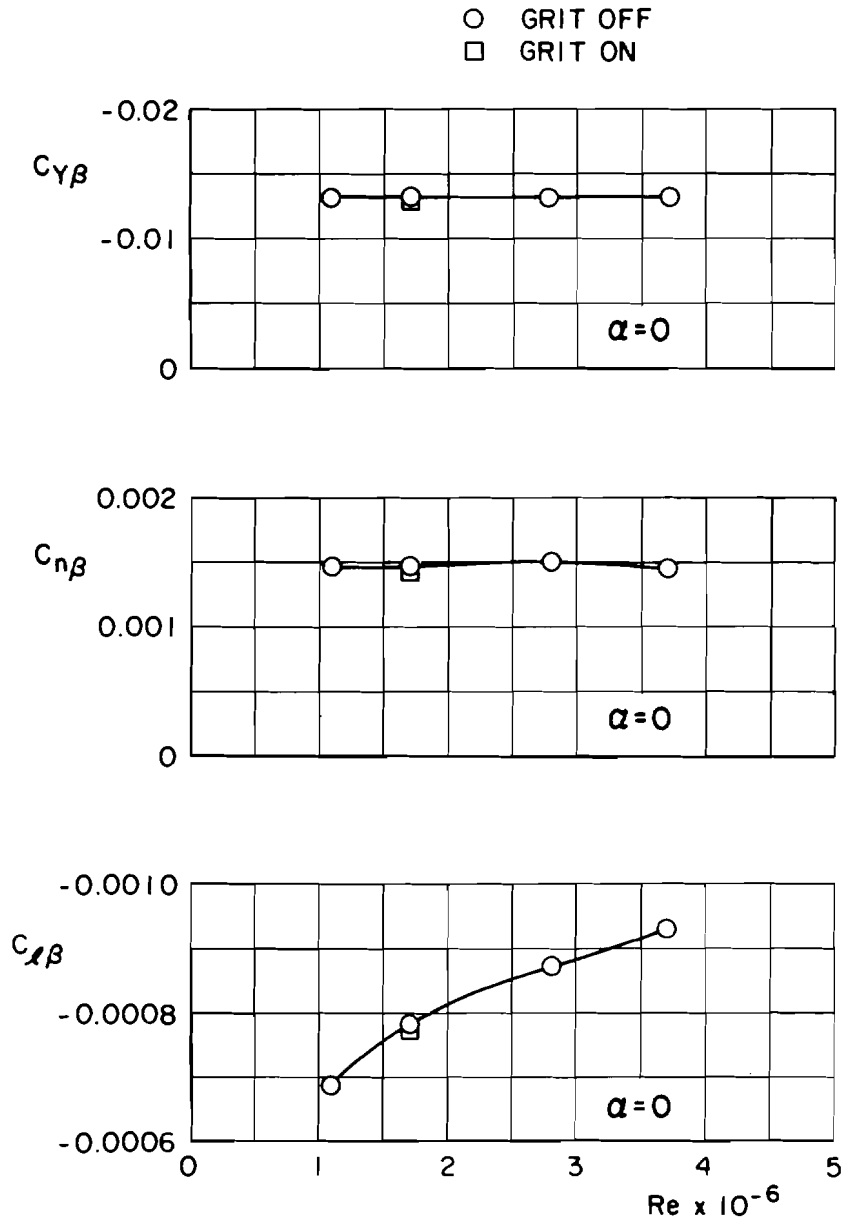

Figure 13. Concluded.

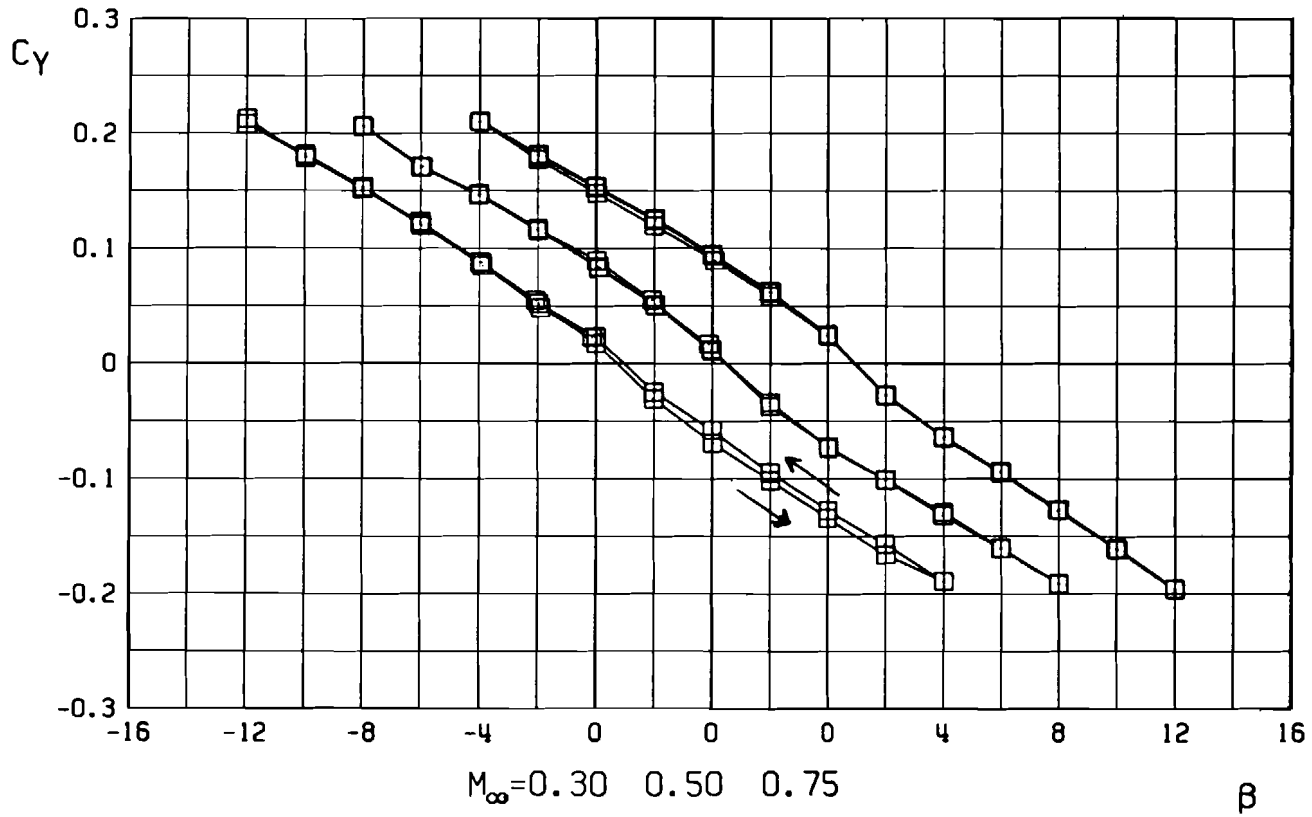

a. Side-force coefficient

Figure 14. Hystersis characteristics in A-10 aerodynamic data, α = 20 deg.

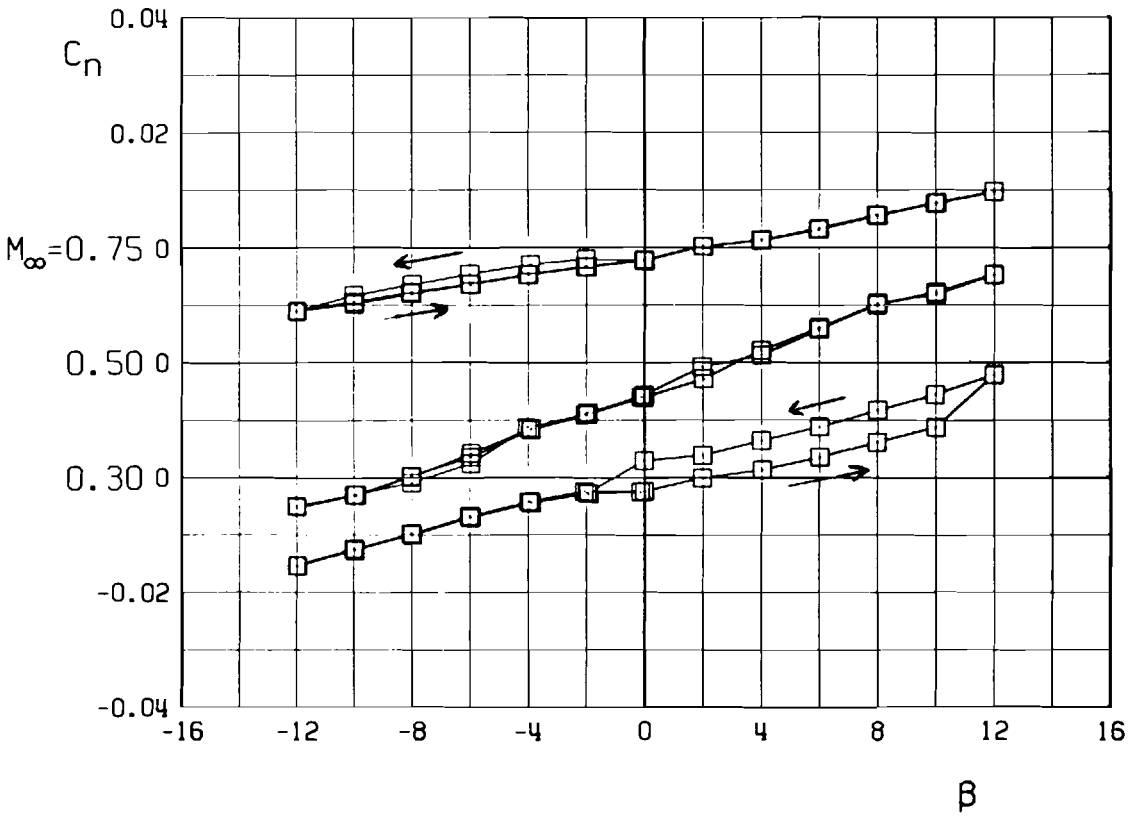

b. Yawing-moment coefficient
Figure 14. Continued.

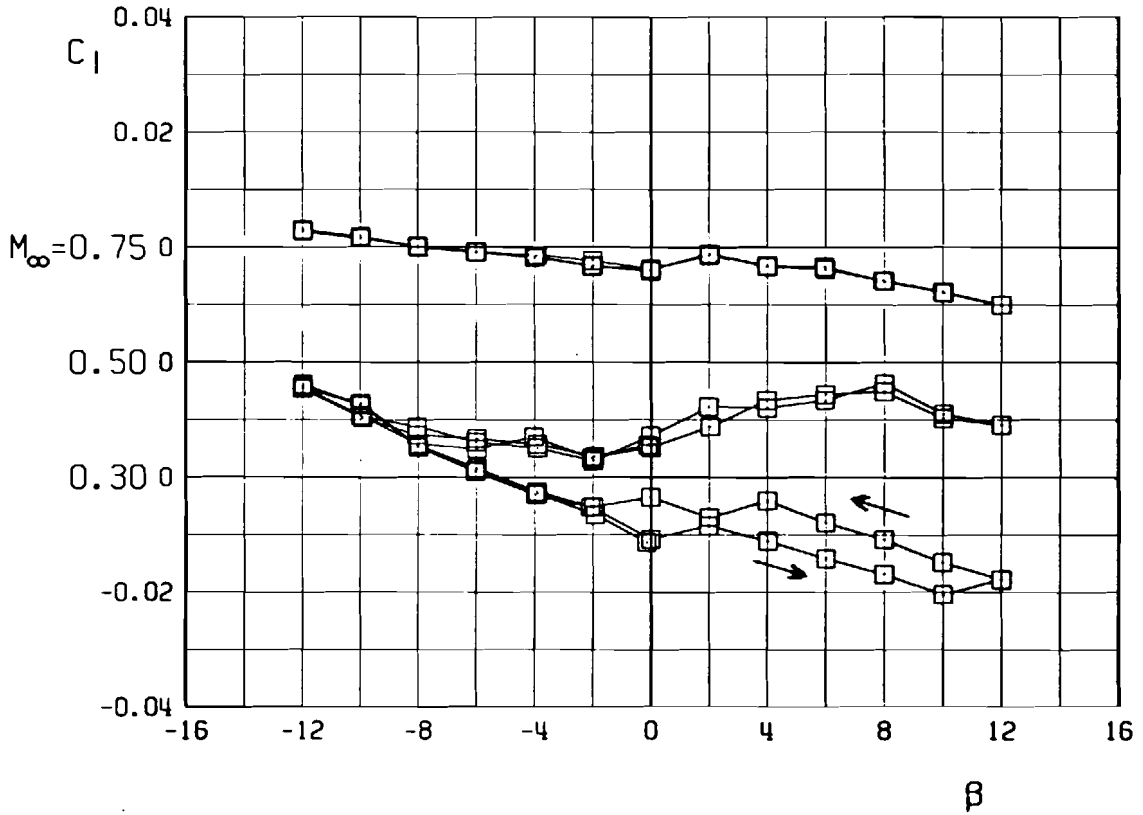

c. Rolling-moment coefficient
Figure 14. Continued.

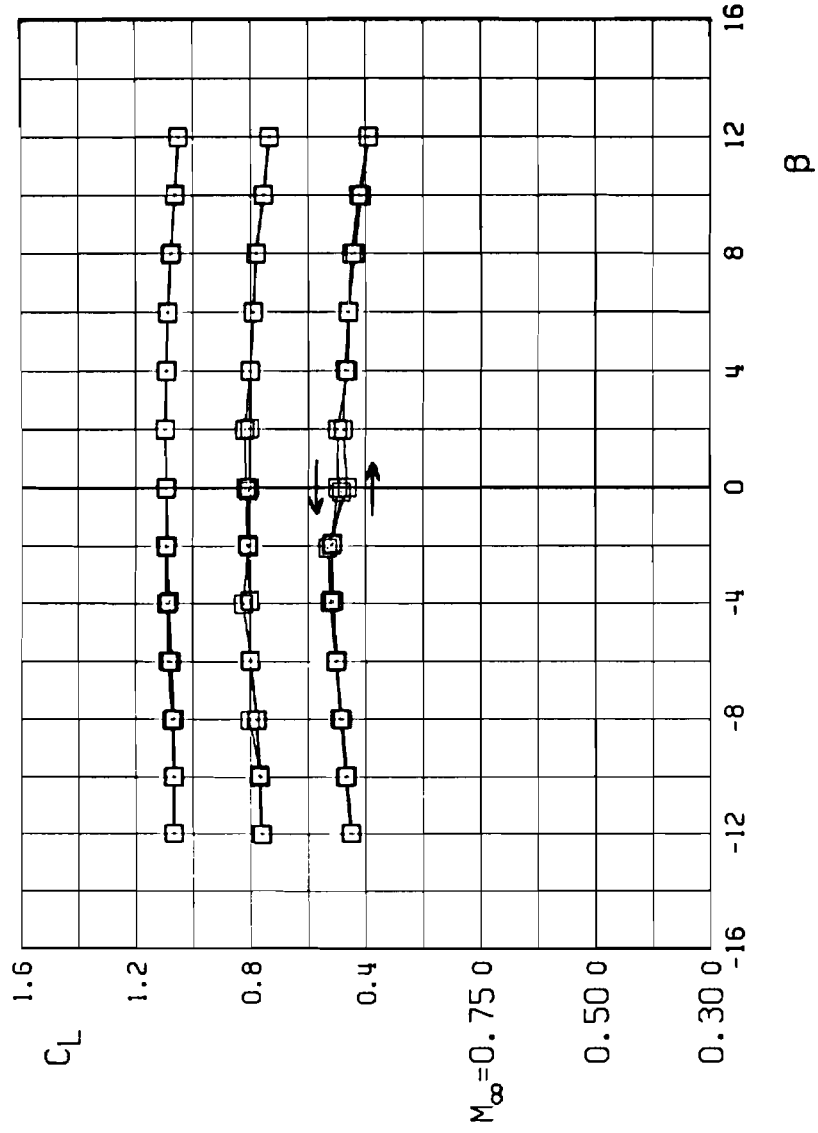

d. Lift coefficient
Figure 14. Continued.

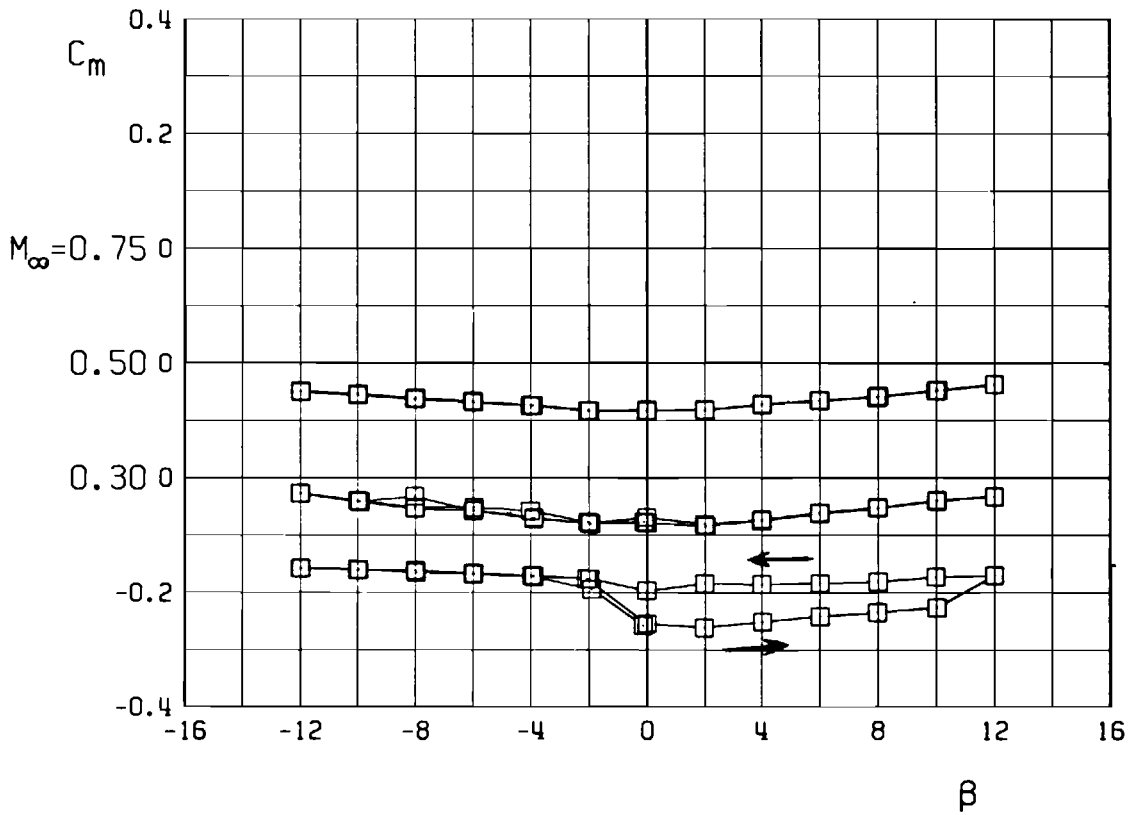

e. Pitching-moment coefficient
Figure 14. Continued.

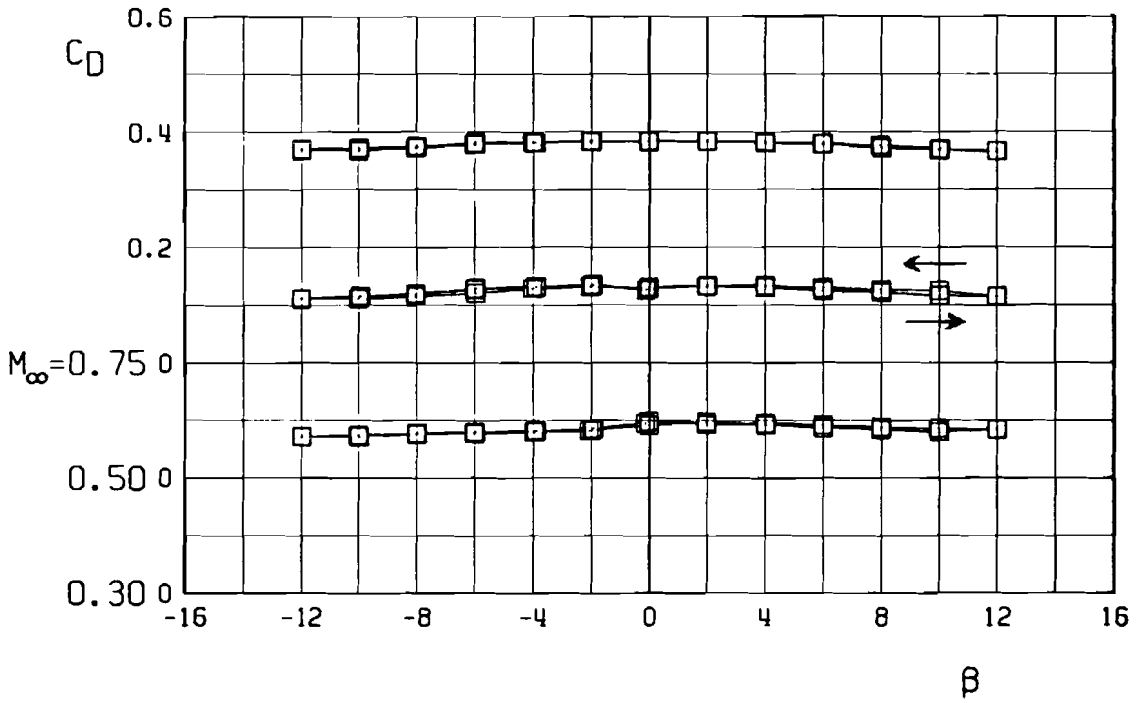

f. Drag coefficient
Figure 14. Concluded.

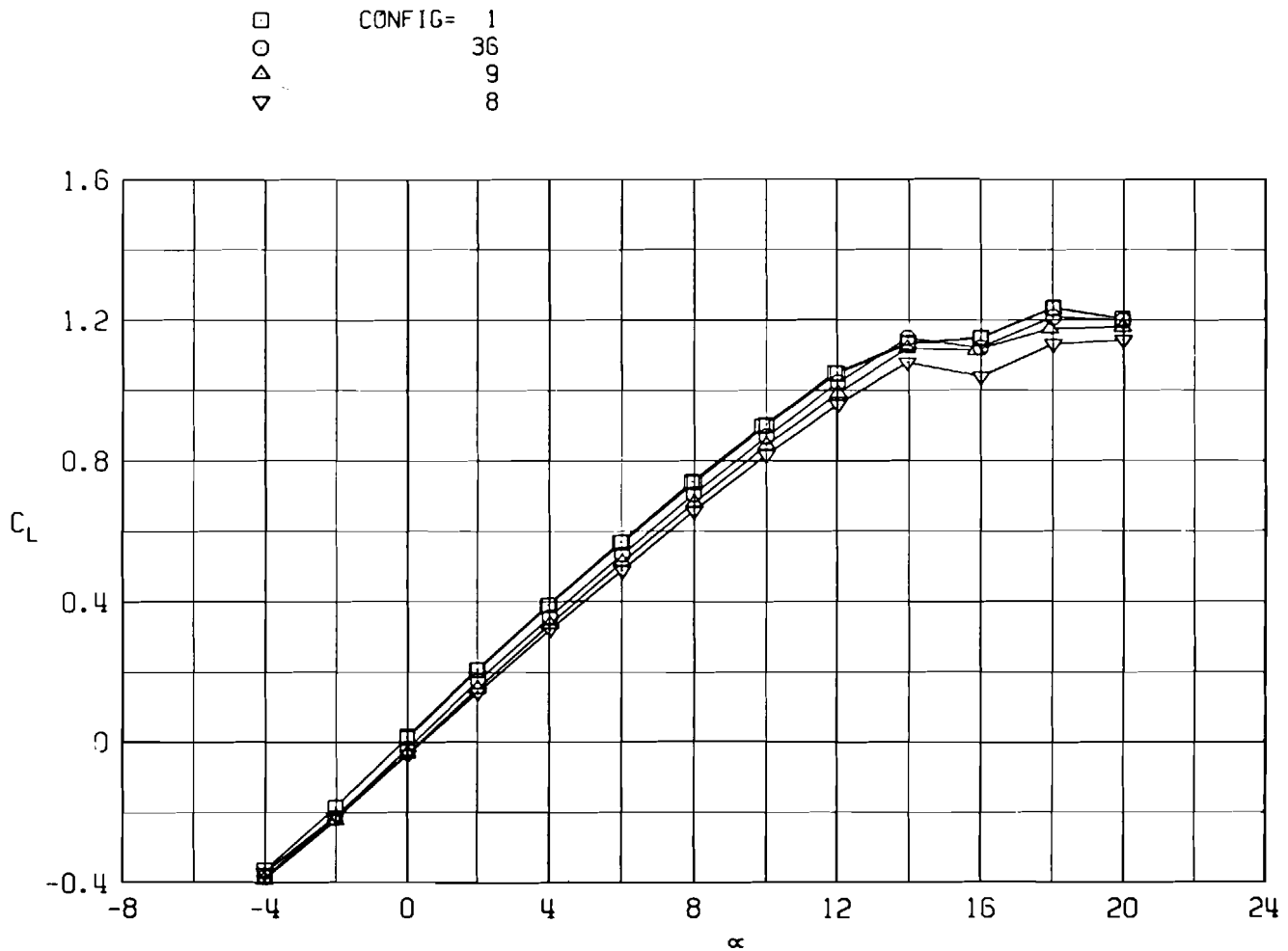

a. Lift coefficient at $M_\infty = 0.50$

Figure 15. Effect of external stores on the aerodynamic characteristics of the A-10 model.

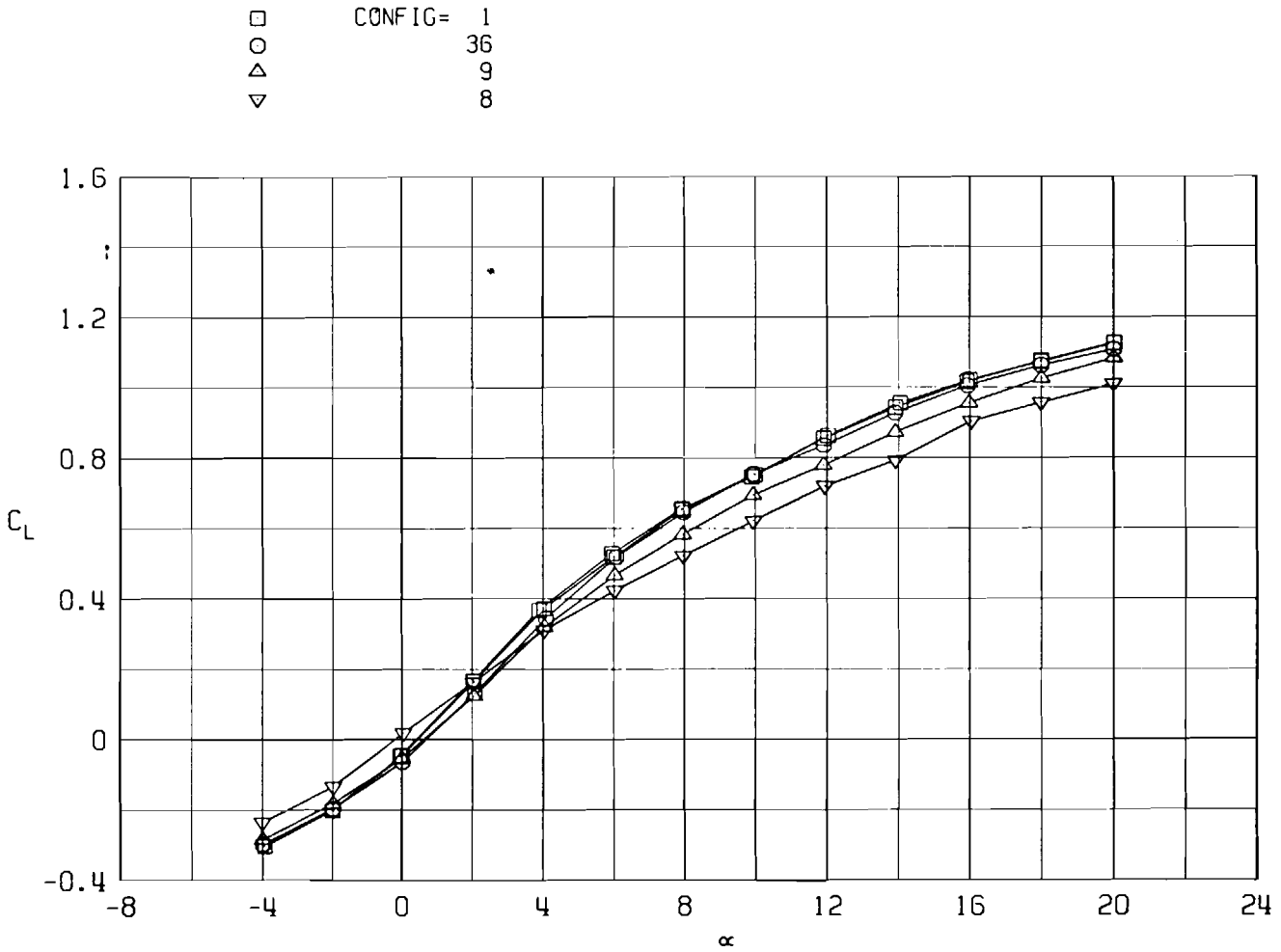

b. Lift coefficient at M_∞ = 0.75

Figure 15. Continued.

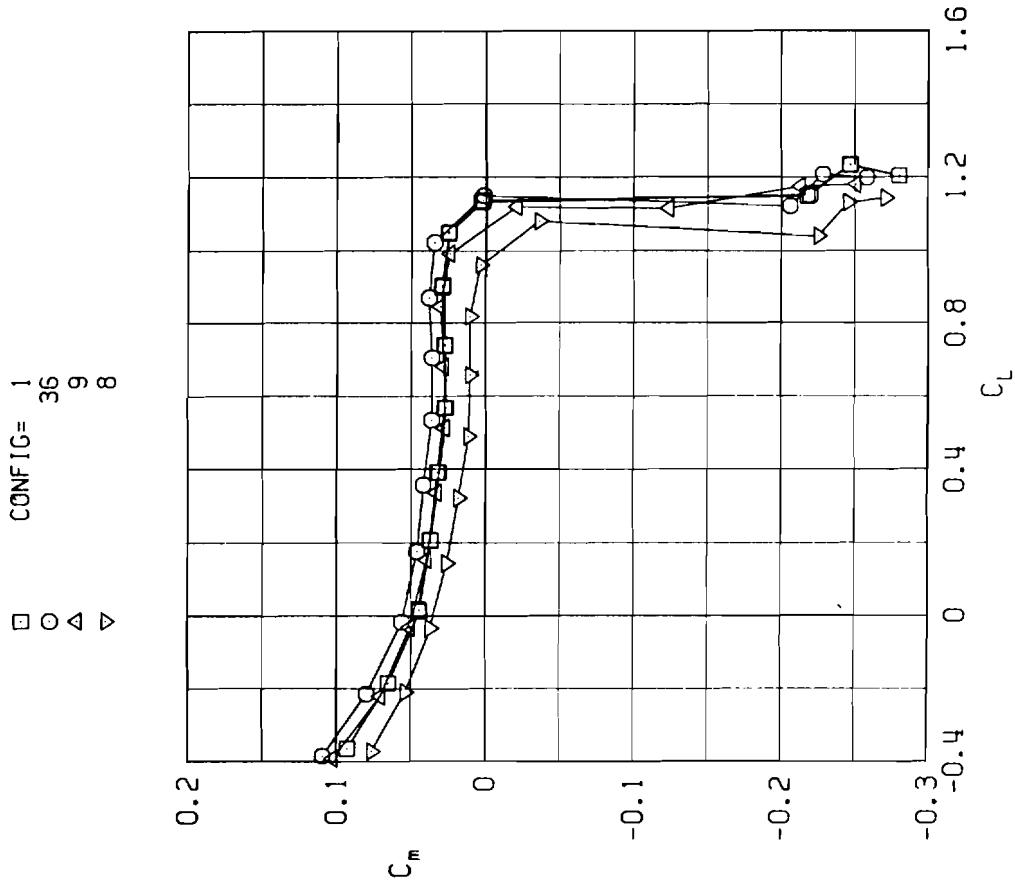

c. Pitching-moment coefficient at M_∞ = 0.50
Figure 15. Continued.

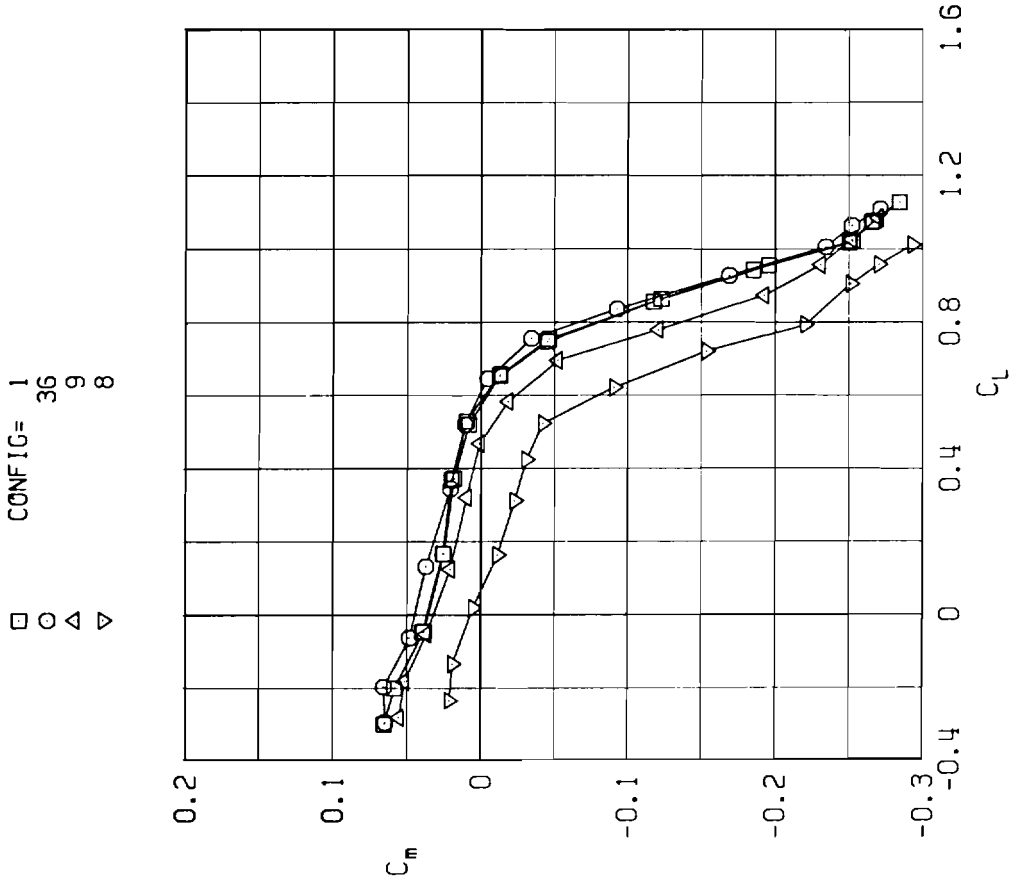

d. Pitching-moment coefficient at M_∞ = 0.75

Figure 15. Continued.

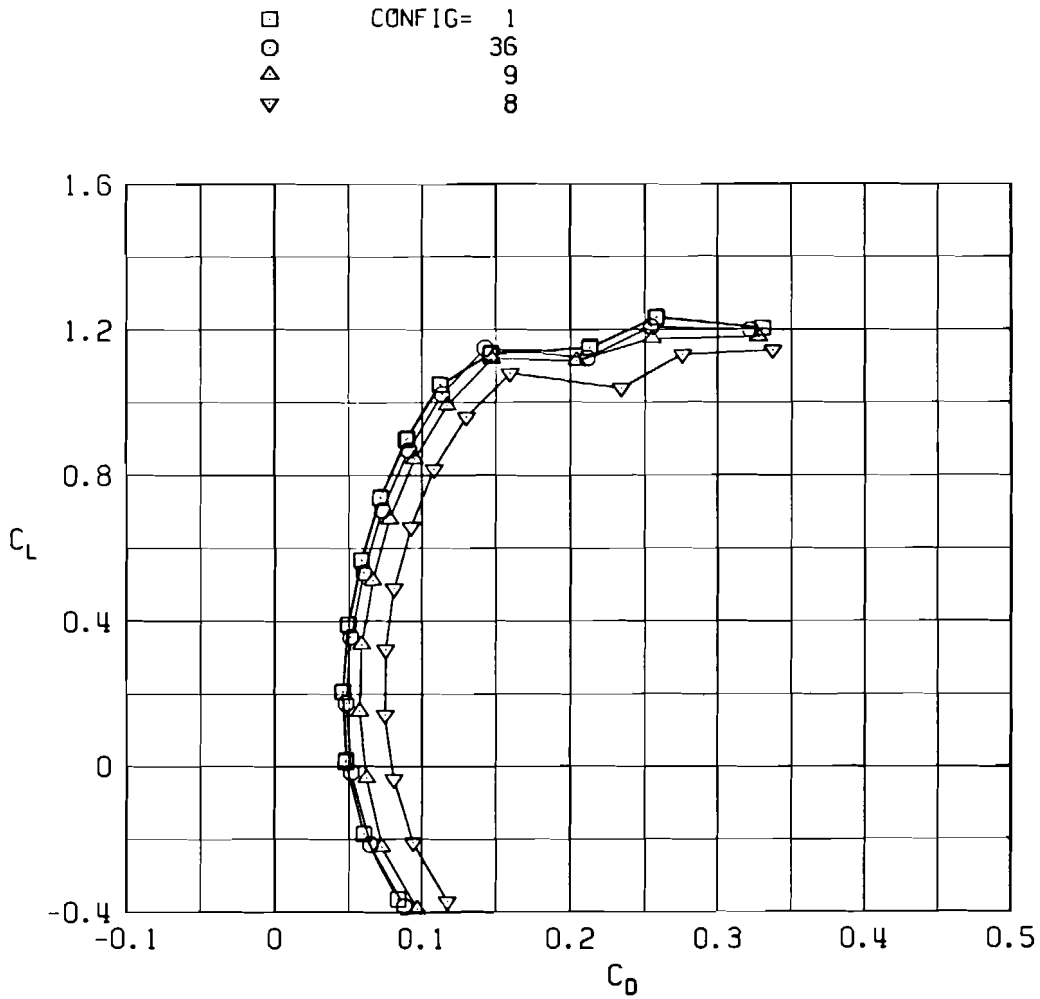

e. Drag coefficient at $M_\infty = 0.50$

Figure 15. Continued.

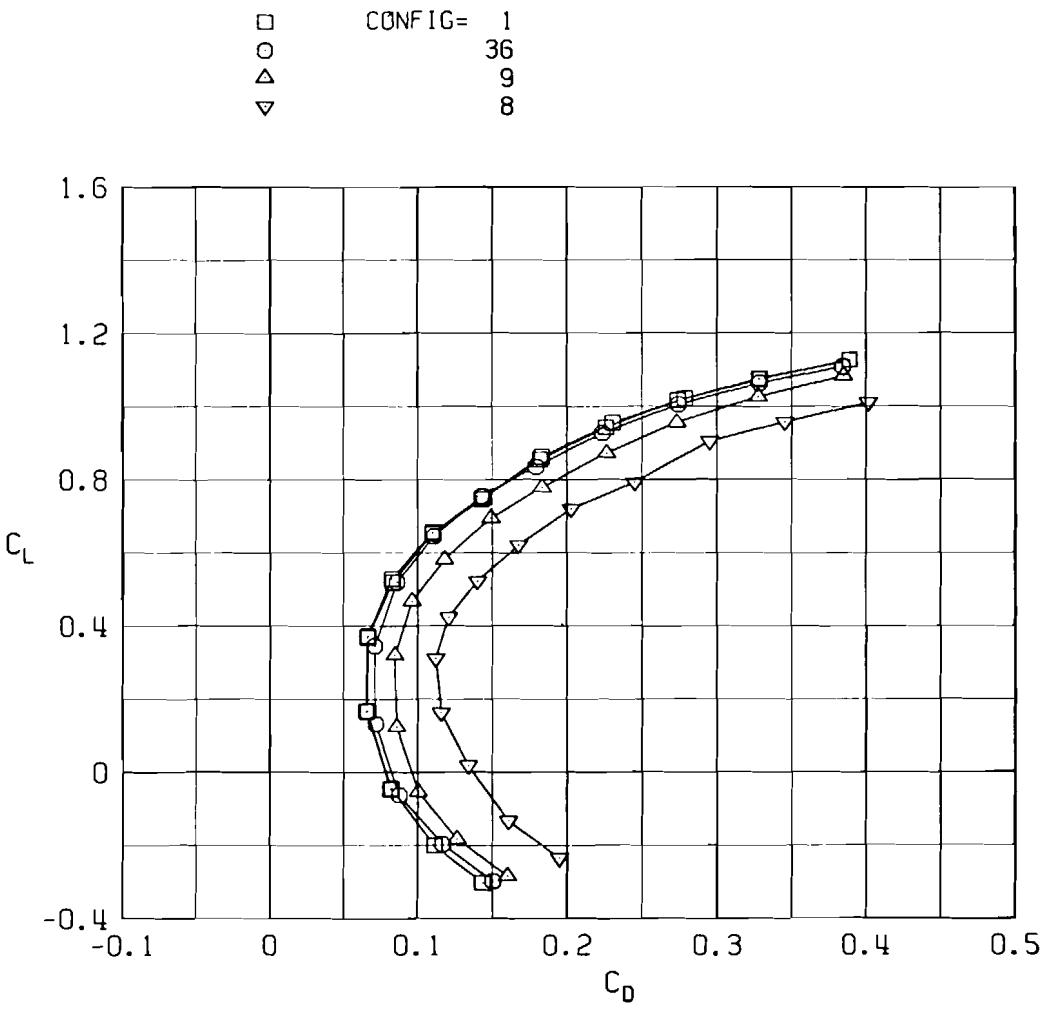

f. Drag coefficient at M_∞ = 0.75

Figure 15. Continued.

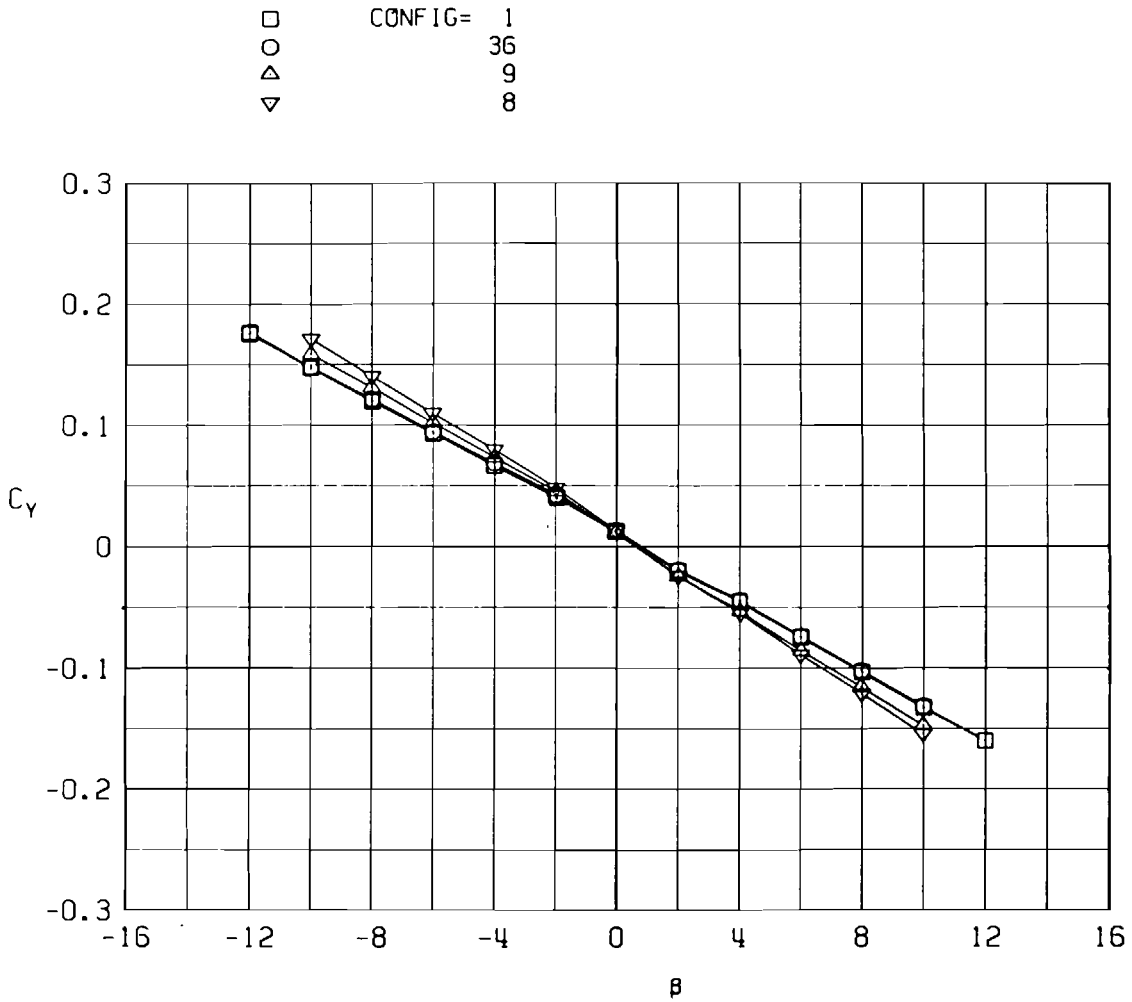

g. Side-force coefficient at M_∞ = 0.50, α = 10 deg

Figure 15. Continued.

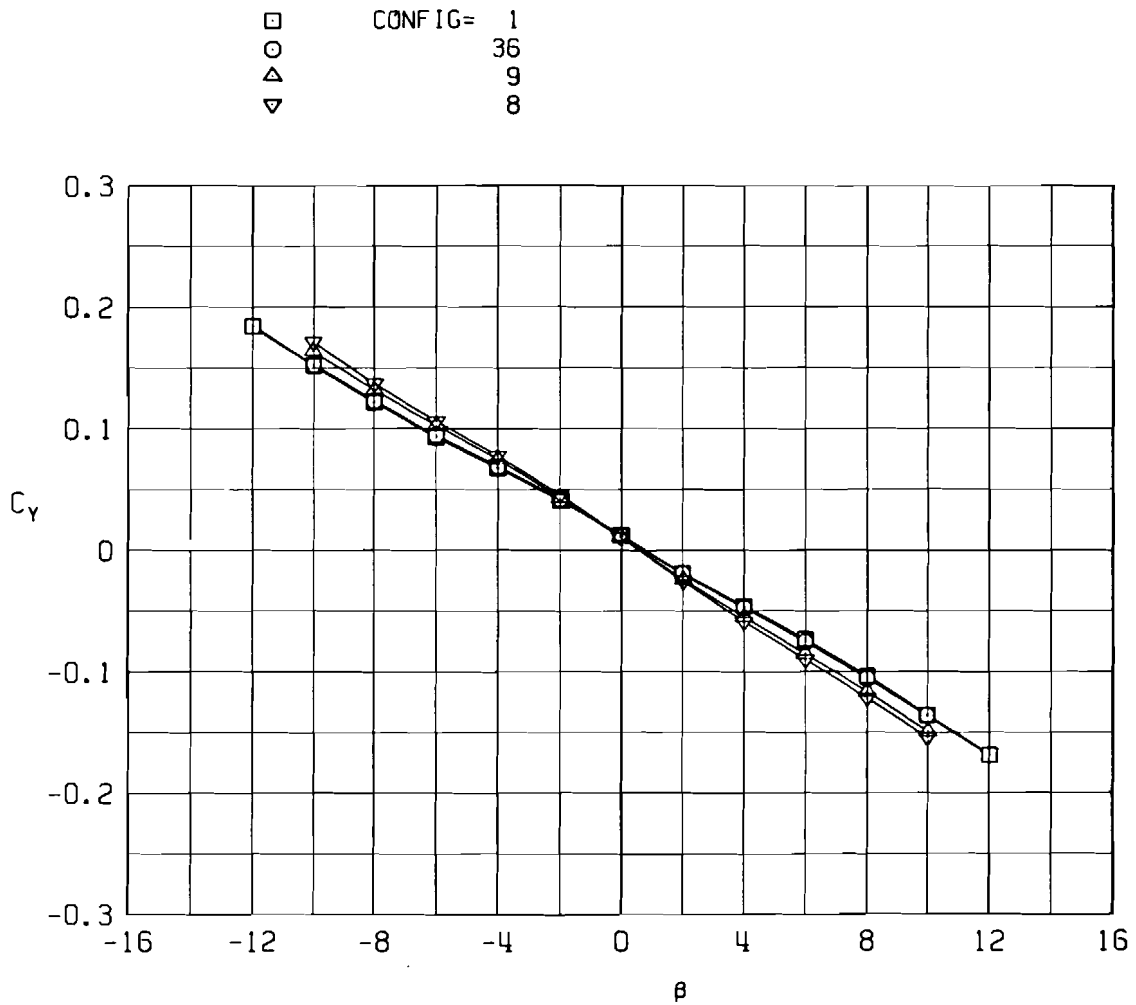

h. Side-force coefficient at M_∞ = 0.75, α = 10 deg
Figure 15. Continued.

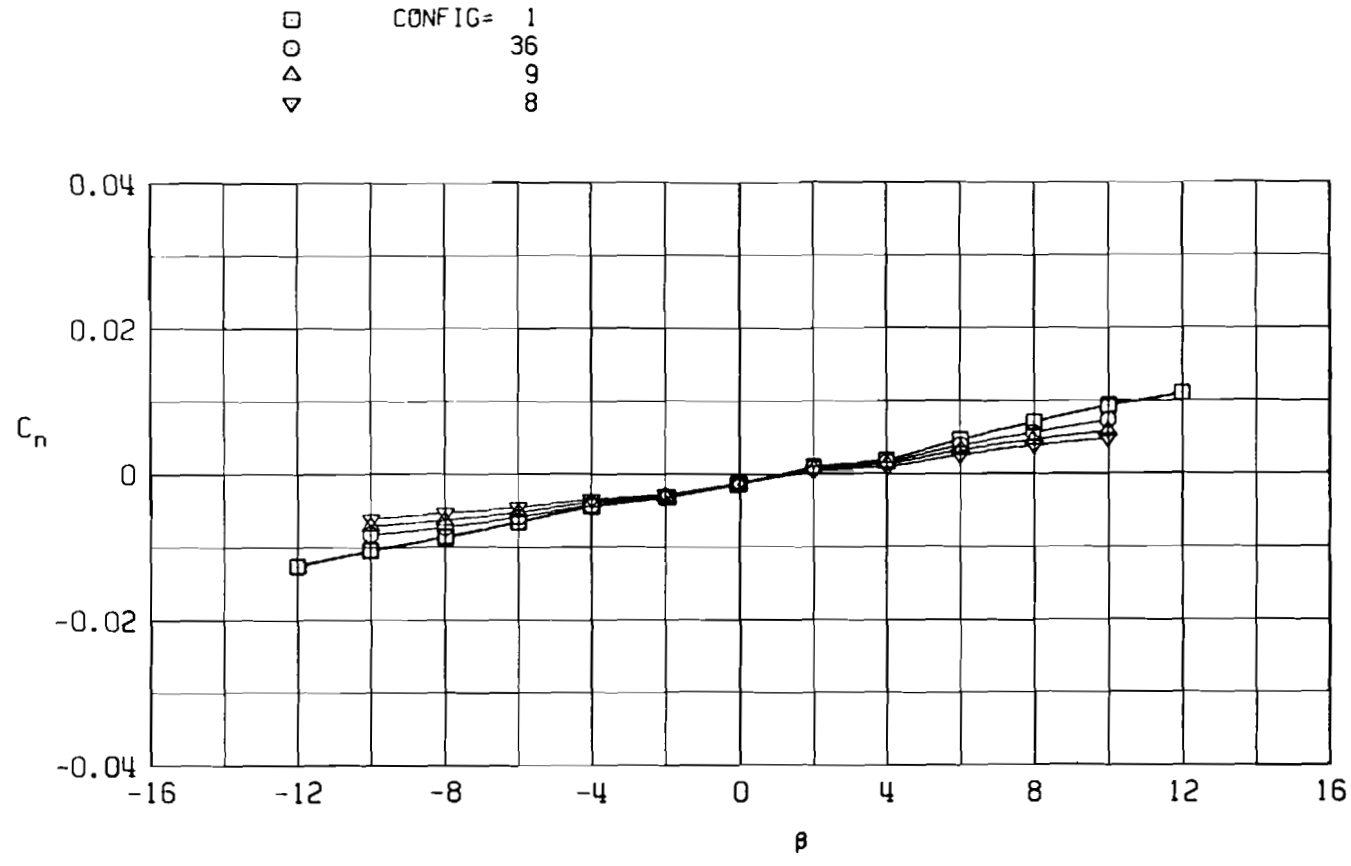

i. Yawing-moment coefficient at M_∞ = 0.50, α = 10 deg

Figure 15. Continued.

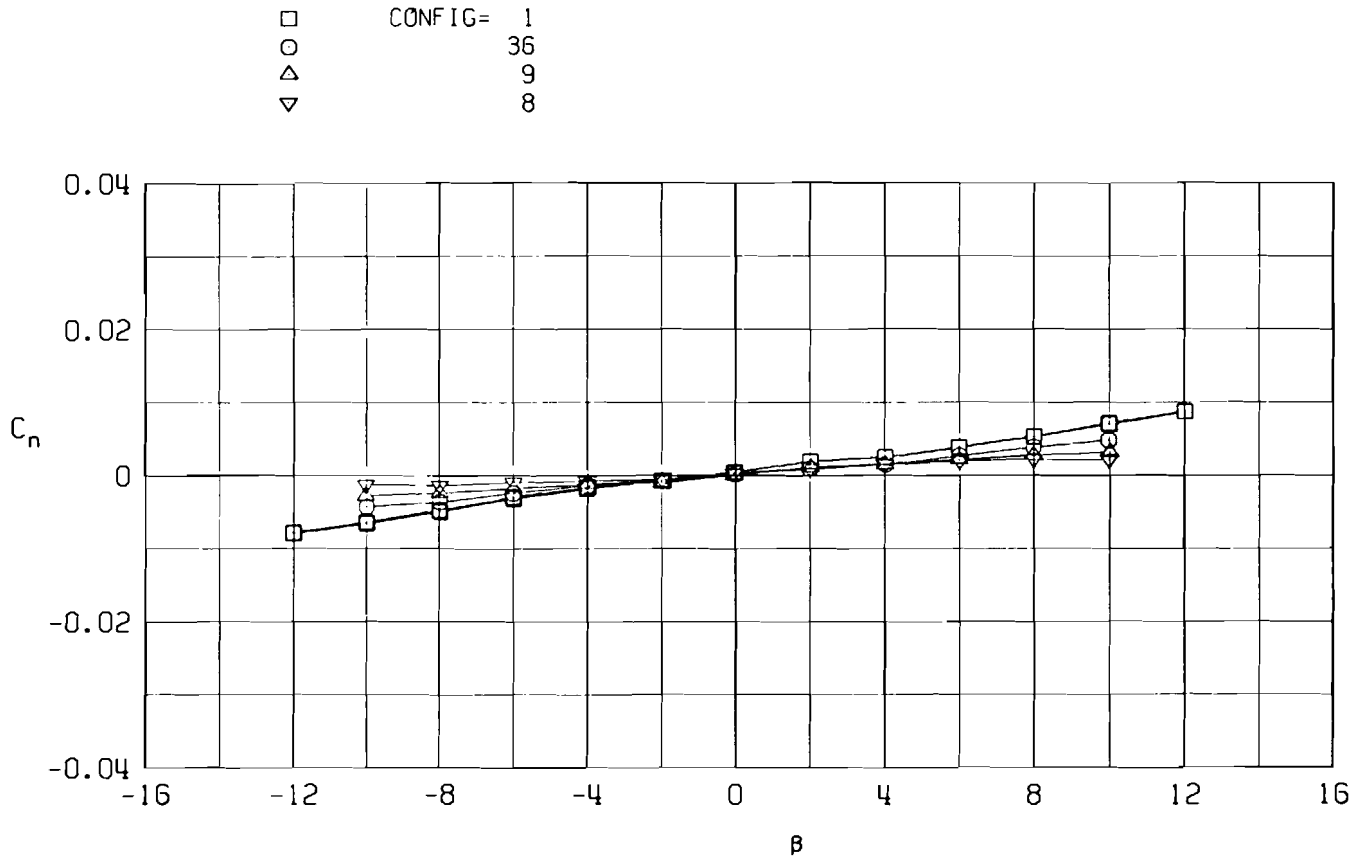

j. Yawing-moment coefficient at M_∞ = 0.75, α = 10 deg

Figure 15. Continued.

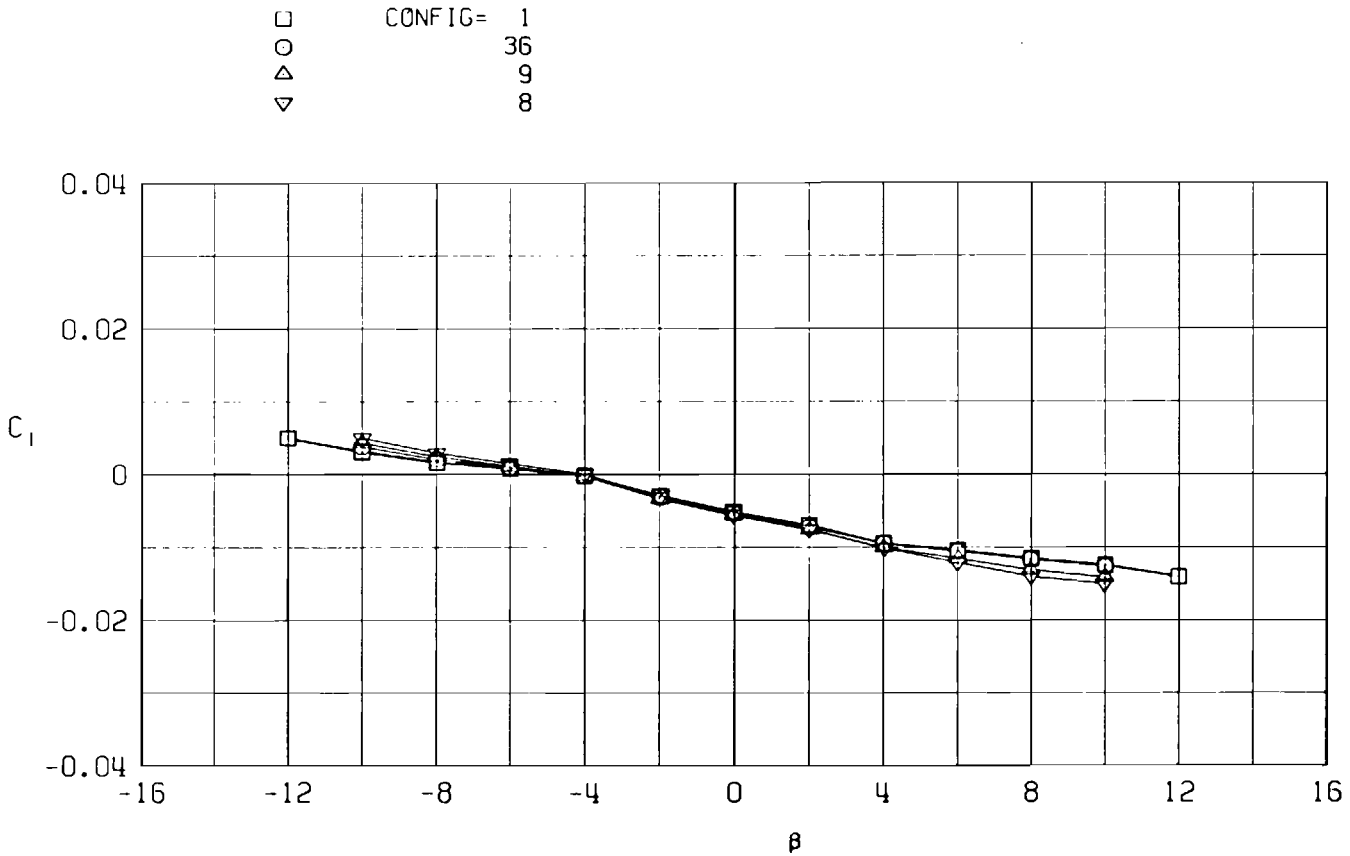

k. Rolling-moment coefficient at M_∞ = 0.50, α = 10 deg

Figure 15. Continued.

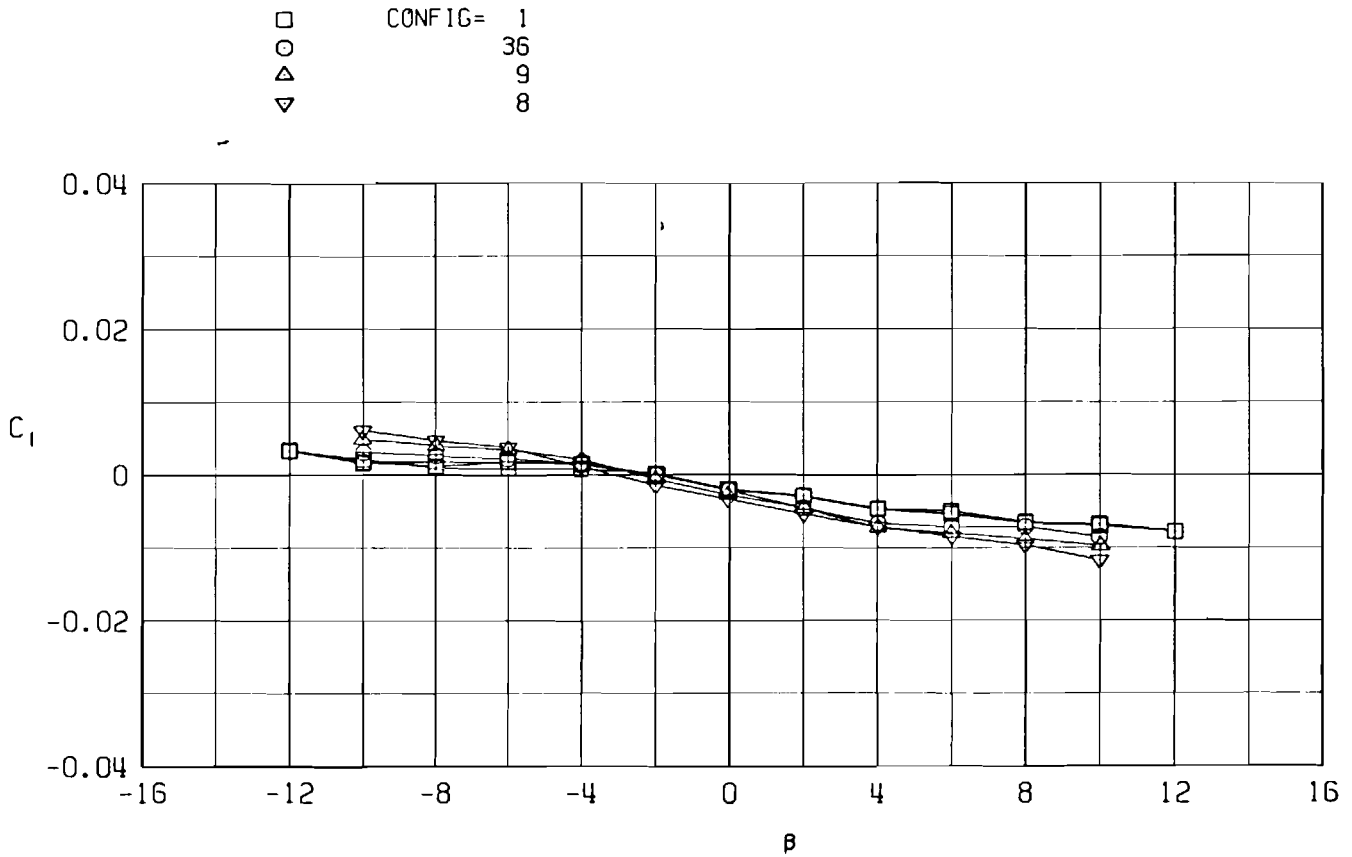

l. Rolling-moment coefficient at M_∞ = 0.75, α = 10 deg

Figure 15. Concluded.

Table 1. Identification of Store Configurations

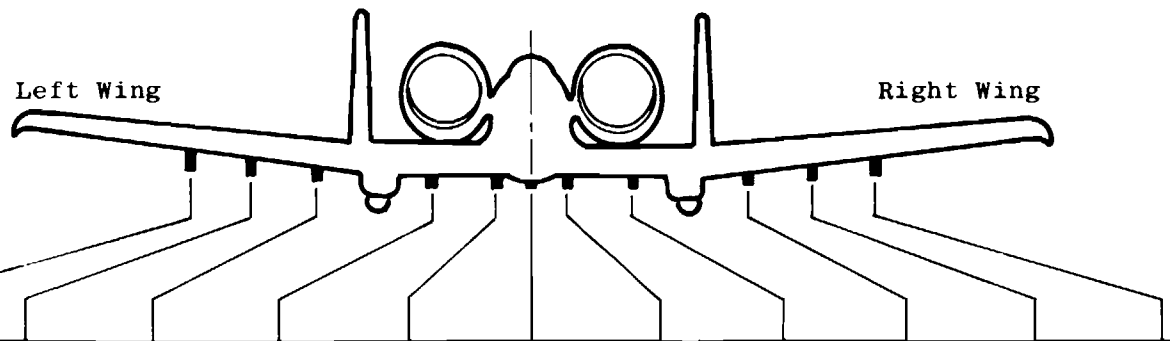

Config No.	Pylon 1	Pylon 2	Pylon 3	Pylon 4	Pylon 5	Pylon 6	Pylon 7	Pylon 8	Pylon 9	Pylon 10	Pylon 11
1	Empty	Empty	Empty	Empty	Empty	Empty	Empty	Empty	Empty	Empty	Empty
36				▽ Empty TER				▽ Empty TER			
9		MK-82	MK-82	MK-82	MK-82		MK-82	MK-82	MK-82	MK-82	
8		SUU-30	SUU-30	SUU-30	SUU-30		SUU-30	SUU-30	SUU-30	SUU-30	Empty

Table 2. Summary of Nominal Test Conditions

M_∞	P_T, psfa	Re x 10^{-6}, 1/ft	Q, psf
0.30	800	0.7	47
0.30	1,200	1.1	70
0.30	2,000	1.8	120
0.30	2,800	2.5	165
0.50	800	1.1	120
0.50	1,200	1.7	175
0.50	2,000	2.8	295
0.50	2,800	3.7	415
0.65	1,200	2.1	265
0.70	1,200	2.2	295
0.75	800	1.5	220
0.75	1,200	2.2	325
0.75	2,000	3.7	540
0.75	2,800	4.9	755

Table 3. Data Uncertainies

	Mach Number				
	0.30	0.50	0.65	0.70	0.75
C_N	± 0.083	± 0.028	± 0.015	± 0.012	± 0.010
C_m	± 0.014	± 0.006	± 0.004	± 0.004	± 0.003
C_Y	± 0.015	± 0.006	± 0.004	± 0.003	± 0.003
C_n	± 0.0009	± 0.0004	± 0.0003	± 0.0002	± 0.0002
C_ℓ	± 0.0014	± 0.0005	± 0.0003	± 0.0002	± 0.0002
CA	± 0.014	± 0.005	± 0.003	± 0.002	± 0.002
C_L	± 0.081	± 0.027	± 0.014	± 0.012	± 0.010
C_D	± 0.025	± 0.009	± 0.005	± 0.004	± 0.003

NOMENCLATURE

A_{BASE}	Balance cavity area used for calculating the base axial-force coefficient, 0.01517 ft^2
ALFA, α	Model wind axis system angle of attack measured relative to aircraft waterline, deg
BETA, β	Model wind axis system angle of sideslip measured relative to aircraft longitudinal axis, deg
BL	Model buttline, in.
b	Model reference span, 1.874 ft
$\bar{c}$	Model reference chord, 0.4772 ft
C_D	Total measured drag coefficient, total measured drag/QS
$C_{D,MIN}$	Minimum measured value of C_D within a given polar
C_L	Lift coefficient, total measured lift force/QS
$C_{L,MAX}$	Maximum measured value of C_L within a given polar
$C_{L\alpha}$	Slope of a linear least square curve fit of C_L versus α ($-4 \leq \alpha \leq 4$ deg)
C_ℓ	Body axis rolling-moment coefficient, body axis rolling moment/QSb
$C_{\ell\beta}$	Slope of a linear least square curve fit of C_ℓ versus β ($-4 \leq \beta \leq 4$ deg)

$C_{\ell\delta A}$	Aileron control effectiveness parameter, $\Delta C_\ell / \Delta \delta A$
C_m	Pitching-moment coefficient, total measured pitching moment/$QS\bar{c}$
$C_{m\alpha}$	Slope of a linear least square curve fit of C_m versus α ($-4 \leq \alpha \leq 4$ deg)
$C_{m\delta e}$	Elevator control effectiveness parameter, $\Delta C_m / \Delta \delta_e$
C_N	Normal-force coefficient, total measured normal force/QS
$C_{N\alpha}$	Slope of a linear least square curve fit of C_N versus α ($-4 \leq \alpha \leq 4$ deg)
C_n	Yawing-moment coefficient, total measured yawing moment/QSb
$C_{n\beta}$	Slope of a linear least square curve fit of C_n versus β ($-4 \leq \beta \leq 4$ deg)
$C_{n\delta r}$	Rudder control effectiveness parameter, $\Delta C_n / \Delta \delta r$
CONFIG	A unique number assigned to each model configuration tested identifying that configuration (see Table 1)
C_Y	Side-force coefficient, total measured side force/QS
$C_{Y\beta}$	Slope of linear least square curve fit of C_Y versus β ($-4 \leq \beta \leq 4$ deg)

DELA, δA	Deflection angle of model ailerons, positive deflections produce positive rolling moments, deg
DELE, δe	Deflection angle of model elevator, positive for elevator trailing edge up, deg
DELR, δr	Deflection angle of model rudder, positive for rudder trailing edge right, deg
M_∞	Free-stream Mach number
MRP	Model moment reference point, 27 percent of the mean aerodynamic chord, MS/21.615, WL/5.0, BL/0.0
MS	Model station, in.
P	Free-stream static pressure, psfa
PART	Numerical index identifying a particular data polar
P_{BASE}	Measured base pressure, psfa
PHIA	Model roll angle, positive right wing down, deg
POINT	Unique number associated with a particular data point within a data polar
P_T	Free-stream total pressure, psfa
Q	Free-stream dynamic pressure, psf
Re	Free-stream unit Reynolds number, ft^{-1}
S	Model reference area, 1.2650 ft^2

SM	Slope of a linear least square curve fit of C_m versus C_L for $-4 \leq \alpha \leq 4$ deg, fraction of $\bar{c}$; positive when center of pressure is forward of the moment reference point
STA-XX	Armament pylon station numbers 1 through 11; pylon stations are numbered from left wingtip to right wingtip
TEST	Test number associated with a particular test entry
TT	Free-stream total temperature, °F
WL	Model waterline, in.
Z_B	Distance between the centroid of area of the base and the MRP measured normal to the balance X-axis, positive when the centroid of the base area is below the MRP, 0.0108 ft